Curriculum Vitae

Umut Aypar
Radiation Oncology Research Laboratories
University of Maryland School of Medicine
655 West Baltimore Street, BRB 7-010
Baltimore, MD 21201
(410) 706-1572 (phone)
(410) 706-6138 (fax)

Degree and Date to be Conferred: Ph.D., 2011

Collegiate Institutions Attended:

2005–Present	University of Maryland, School of Medicine, Baltimore, MD Ph.D., Molecular Medicine Program Human Genetics and Genomic Medicine track
2001–2005	Ohio Wesleyan University, Delaware, OH Bachelor of Arts Botany/Microbiology with concentration in Microbiology Zoology with concentration in Genetics

Professional Publications:

1. Miller JH, Jin S, Morgan WF, Yang A, Wan Y, **Aypar U**, Peters JS, Springer DL. Profiling mitochondrial proteins in radiation-induced genome-unstable cell lines with persistent oxidative stress by mass spectrometry. *Radiation Research* 169(6):700-6 (2008).

2. **Aypar U**, Morgan WF, Baulch JE. Radiation-Induced Genomic Instability: Are Epigenetic Mechanisms the Missing Link? *International Journal of Radiation Biology* Epub ahead of print (2010).

3. **Aypar U**, Morgan WF, Baulch JE. Radiation-induced epigenetic alterations after low and high LET irradiations. *Mutation Research* Epub ahead of print (2010).

4. **Aypar U**, Morgan WF, Baulch JE. Epigenetic alterations in radiation-induced genomically unstable clones. *Cancer Research* In preparation (2011).

Professional Positions Held:

2005–Present	**Graduate Research Assistant** William F. Morgan, Ph.D., D.Sc., mentor Radiation Oncology Research Laboratories University of Maryland School of Medicine, Baltimore, MD
6/2004–8/2004	**GEBS Summer Scholars Program** Mark D. Noble, Ph.D., advisor "In search of new markers for the study of glial restricted precursors" University of Rochester School of Medicine and Dentistry, Rochester, NY
1/2004–12/2004	**Independent Study Course Research** Gerald Goldstein, Ph.D., advisor "Evolutionary differences in the keratinase gene sequence of *Bacillus licheniformis* at different geographical areas" Ohio Wesleyan University, Delaware, OH
8/2003–12/2003	**Independent Study Course Research** Laura Tuhela-Reuning, Ph.D., advisor "Effects of bacteria in the dental flora exposed to different conditions" Ohio Wesleyan University, Delaware, OH
6/2003–8/2003	**Internship & Research Experience** Nicosia State Hospital Laboratories & Thalassemia Center Nicosia, CYPRUS
1/2002–5/2002	**Honors Research Tutorial** Edward H. Burtt, Jr., Ph.D. laboratory "Bacteria, Birds and Degradation of Feathers" Ohio Wesleyan University, Delaware, OH

Honors and Awards:

10/2009	**EMS Student and New Investigator Travel Award** 40th Annual Meeting of the Environmental Mutagen Society St. Louis, MO
9/2008	**Scholars in Training (SIT) Award** 54th Annual Meeting of the Radiation Research Society Boston, MA

7/2008	**Poster Award** Student Poster Competition 19th Annual NASA Space Radiation Investigators' Workshop Philadelphia, PA
6/2008	**Travel Award** 19th Annual NASA Space Radiation Investigators' Workshop Philadelphia, PA
9/2007	**Doctoral Scholarship** Ministry of Education, Nicosia, CYPRUS
6/2007	**NASA Space Radiation Summer School Scholar** U. S. Department of Energy's Brookhaven National Laboratory, Upton, NY
5/2005	**Burns-Shirling Award** Botany and Microbiology Department, Ohio Wesleyan University, Delaware, OH
6/2004	**GEBS Summer Research Scholar** University of Rochester School of Medicine and Dentistry, Rochester, NY
1/2005; 1/2004	**The Collegiate All-American Scholar Award nomination**
2002–2005	**The National Dean's List** and **The Dean's List**
2001–2005	**Honors Student** Ohio Wesleyan University, Delaware, OH
2001–2005	**Faculty Scholar Scholarship** Ohio Wesleyan University, Delaware, OH
8/2000	**DISTINCTION in IGCSE Exams** Cambridge International Examinations University of Cambridge, Cambridge, U.K.
5/2000	**Fulbright Scholarship** Seeds of Peace International Camp Otisfield, ME
1998–2001	**Academic Scholarship** Eastern Mediterranean College Famagusta, CYPRUS

Abstracts:

1. **Aypar U**, Tuhela-Reuning L. Effects on bacteria in the dental flora exposed to different conditions. 113th Annual Meeting Program Abstracts issue of The Ohio Journal of Science (2004) – Poster presentation.

2. Robins AR, **Aypar U**, Costello HM, Goldstein G. Inhibition of T2 virus replication by DON. 2005 Annual Meeting of the Ohio Branch American Society for Microbiology Meeting (2005) – Poster presentation.

3. Dziegielewski J, Baulch JE, Pyles DN, **Aypar U**, Murley JS, Grdina DJ, Morgan WF. Amifostine metabolite WR-1065 protects irradiated cells from genetic instability. Abstracts of 53rd Annual Meeting of the Radiation Research Society (2006) – Poster presentation.

4. Baulch JE, Dziegielewski J, Goetz W, Li YJ, **Aypar U**, Murley JS, Grdina DJ, Morgan WF. Amifostine metabolite WR-1065 mitigates high and low LET radiation-induced genomic instability. Abstracts of 18th Annual NASA Space Radiation Investigators' Workshop (2007) – Poster presentation.

5. Dziegielewski J, Baulch JE, Goetz W, Li YJ, **Aypar U**, Murley JS, Grdina DJ, Morgan WF. Effects of synthetic and nutritional radio-protectors on high and low LET radiation-induced genomic instability. Abstracts of 18th Annual NASA Space Radiation Investigators' Workshop (2007) – Poster presentation.

6. Dziegielewski J, **Aypar U**, Baulch JE, Bachman KE, Morgan WF. In search of new radio-protecting agents. Abstract Book of 13th International Congress of Radiation Research (2007) – Poster presentation.

7. **Aypar U**, Morgan WF, Baulch JE. Epigenetic alterations in radiation induced genomic instability. Abstracts of 19th Annual NASA Space Radiation Investigators' Workshop (2008) – Poster & Platform presentation.

8. **Aypar U**, Malkiel LN, Baulch JE. Effects of high and low LET irradiation on DNA methylation and genomic instability. Abstracts of 54th Annual Meeting of the Radiation Research Society (2008) – Poster presentation.

9. **Aypar U**, Morgan WF, Baulch JE. Epigenetic alterations in radiation induced genomic instability. Abstracts of 54th Annual Meeting of the Radiation Research Society (2008) – Poster presentation.

10. **Aypar U**, Malkiel LN, Baulch JE. Effects of irradiation on DNA methylation and Genomic instability. Abstracts of 39th Annual Meeting of the Environmental Mutagen Society (2008) – Poster presentation.

11. **Aypar U**, Morgan WF, Baulch JE. Epigenetic alterations in high and low LET radiation induced genomic instability. Abstracts of 39th Annual Meeting of the Environmental Mutagen Society (2008) – Poster presentation & Selected for platform presentation in Platform Session III – Mutagenic and Carcinogenic Mechanisms.

12. Goetz W, Corcoran JJ, **Aypar U**, Baulch JE. Effects of high LET irradiation on DNA methylation. Abstracts of 2009 NASA Human Research Program Investigators' Workshop (2009) – Poster presentation.

13. **Aypar U**, Morgan WF, Baulch JE. Epigenetic alterations in high and low LET radiation induced genomic instability. Low Dose Radiation Research Investigators' Workshop VIII (2009) – Poster presentation.

14. **Aypar U**, Morgan WF, Baulch JE. Epigenetic alterations in radiation induced genomic instability. Abstracts of 40th Annual Meeting of the Environmental Mutagen Society (2009) – Poster presentation & Selected for platform presentation in Symposium 10: Assessing the Relative Cancer Risks of Genotoxic and Non-Genotoxic Exposures in Light of Mixed Mexhanisms of Action.

15. **Aypar U**, Morgan WF, Baulch JE. Epigenetic alterations in radiation induced genomic instability. Abstracts of 60th Annual Meeting of The American Society of Human Genetics (2010) – Poster presentation & Selected for platform presentation in Ataxia-Telangiectasia/Genome Instability Satellite Meeting.

Abstract

Title of Dissertation: Epigenetics Alterations in Radiation-Induced Genomic Instability

Umut Aypar, Doctor of Philosophy, 2011

Dissertation Directed by: William F. Morgan, Ph.D., D.Sc., Director of Radiation Biology and Biophysics, Biological Sciences Division, Pacific Northwest National Laboratory

Radiation can lead to carcinogenesis through targeted and non-targeted effects. One non-targeted effect, radiation-induced genomic instability (RIGI), results in an increased frequency of genetic alterations in the progeny of irradiated cells. RIGI is thought to be an early event in radiation-induced carcinogenesis, but it is unknown how this process is initiated. Epigenetic changes, including aberrant DNA methylation and altered microRNA (miRNA) expression, can be induced by radiation exposure and have been associated with some cancers. We are testing the hypothesis that irradiation results in epigenetic alterations that are involved in the initiation and perpetuation of RIGI. The human-Chinese hamster ovary hybrid cell line GM10115 was irradiated using x-rays or iron (Fe) ions and clones were obtained. Irradiation induced DNA damage in GM10115 cells and RIGI in clones (114, 118, CS9, LS12, 115, Fe5.0-8) was determined using micronucleus formation and fluorescence *in situ* hybridization analysis of chromosomal rearrangements. To study epigenetic changes, the post-irradiation status of specific locus, repeat element, genome-wide methylation, and miRNA profiles were evaluated. Results suggest that aberrant DNA methylation and changes in miRNA expression are induced by irradiation. In the unstable clones, results suggest that changes in DNA methylation and aberrant expression of miRNA can be associated with RIGI. Thus, epigenetic changes in

chromosomally unstable clones could suggest that epigenetic aberrations may be perpetuating RIGI.

Epigenetic Alterations in Radiation-Induced Genomic Instability

by

Umut Aypar

Dissertation submitted to the faculty of the Graduate School
of the University of Maryland Baltimore in partial fulfillment
of the requirements for the degree of
Doctor of Philosophy
2011

ProQuest LLC.
789 East Eisenhower Parkway
P.O. Box 1346
Ann Arbor, MI 48106 - 1346

Acknowledgements

Thanks to my mentors William F. Morgan and Janet E. Baulch for being extremely patient and guiding me in the right direction. Thanks also to my thesis committee members Feyruz Rassool, Thomas MacVittie and James Herman for their helpful advice. I want to thank my lab mates and classmates for all of their help and support. Special thanks to my friends, siblings and parents for their love.

Table of Contents

List of Tables

List of Figures

List of Abbreviations

ADP	adenosine diphosphate
Ago	argonaute protein
APC	adenomatous polyposis coli
ATCC	American Type Culture Collection
ATM	ataxia telangiectasia mutated
ATPase	adenosine triphosphatase
BORIS	Brother of the Regulator of Imprinted Sites
BRCA1	breast cancer 1
BRG1	brahma-related gene 1
BRM	brahma
CDH1	cadherin 1
CHO	Chinese hamster ovary
COBRA	combined bisulfite restriction analysis
CpA	cytosine-phosphate-adenine
CpC	cytosine-phosphate-cytosine
CpG	cytosine-phosphate-guanine
CpT	cytosine-phosphate-thymine
Cu/Zn	copper/zinc
DAC	5-aza-2'deoxycytidine
DAVID	Database for Annotation, Visualization and Integrated Discovery
DIE	death inducing effect
DMEM	Dulbecco's Modified Eagle Medium

DNA	deoxyribonucleic acid
DNMT	DNA methyltransferases
E2A/Rad6	ubiquitin-conjugating enzyme E2A, Rad6
FBS	fetal bovine serum
Fe	iron
FISH	fluorescence *in situ* hybridization
FITC	fluorescein isothiocyanate
H3K9me	histone H3 methylated on lysine 9
HAT	histone acetyltransferases
HDAC	histone deacetylases
HP1	heterochromatin protein 1
hprt	hypoxanthine-guanine phosphoribosyltransferase
IL-8	interleukin-8
KAP-1	Kruppel-associated box-associated protein
KRAB	Kruppel-associated box
LET	linear energy transfer
LINE-1	long interspersed nuclear element 1
LOWESS	Locally-Weighted Regression
m	methylated
MBD2	methyl CpG binding domain protein 2
MDR1	multiple drug resistance 1
MeCP2	methyl CpG binding protein 2
MGMT	O-6-methylguanine-DNA methyltransferase

miR-34a	microRNA-34a
miRNA	microRNA
MLH1	mutL homolog 1
MN	micronuclei
mRNA	messenger RNA
MSAP-PCR	methylation-sensitive arbitrarily primed PCR
MSP	methylation-specific PCR
Myc	myelocytomatosis
NFκB	nuclear factor-kappaB
NSRL	NASA Space Radiation Laboratory
oncomiR	oncogenic miRNA
p16	cyclin-dependent kinase inhibitor 2A
PARP	poly-ADP-ribose polymerases
PCR	polymerase chain reaction
PGC-1α	proliferator-activated receptor γ coactivator-1 α
PI	propidium iodide
PPARγ	proliferator-activated receptor γ
pre-miRNA	precursor-miRNA
pri-miRNA	primary-miRNA
PTPR-F	protein tyrosine phosphatase receptor type f
RB1	retinoblastoma
RBE	relative biological effectiveness
RIGI	radiation-induced genomic instability

RISC	RNA-induced silencing complex
RNA	ribonucleic acid
ROS	reactive oxygen species
RT-PCR	reverse transcriptase-PCR
SAT2	spermidine N1-acetyltransferase 2
SCE	sister chromatid exchanges
SNF5	sucrose nonfermenting 5
SOD1	superoxide dismutase 1
SWI2/SNF2	switching 2/sucrose nonfermenting 2
TCA	tricarboxylic acid
TS-miR	tumor-suppressor miRNA
TSLC1	tumor suppressor in lung cancer 1
u	unmethylated
VHL	von Hippel-Lindau
WNT	wingless-integration

Statement on Published Material

This thesis contains material that is or will be published in scientific journals.

Chapter 1 contains the full text of the manuscript *Radiation-Induced Genomic Instability: Are Epigenetic Mechanisms the Missing Link?* International Journal of Radiation Biology 2010. I contributed to this manuscript by writing and making all of the figures. Editing and direction came from William F. Morgan and Janet E. Baulch.

Chapter 2 contains the full text of the manuscript *Radiation-Induced Epigenetic Alterations After Low and High LET Irradiations* Mutation Research 2010. I contributed to this paper by writing the manuscript and performing all experiments except microRNA microarray and qRT-PCR, which were performed by LC Sciences. I have performed the array analysis with the help of Katrina M. Waters. Editing and direction came from William F. Morgan and Janet E. Baulch.

Chapter 3 contains the full text of the manuscript *Epigenetic Alterations in Radiation-Induced Genomically Unstable Clones*, intended for submission to Cancer Research. I contributed to this paper by writing the manuscript and performing all experiments except microRNA microarray, gene expression microarray and qRT-PCR, which were performed by LC Sciences. I have performed the arrays analyses with the help of Katrina M. Waters. Editing and direction came from William F. Morgan and Janet E. Baulch.

Chapter 1: INTRODUCTION: RADIATION-INDUCED GENOMIC INSTABILITY: ARE EPIGENETIC MECHANISMS THE MISSING LINK?

Abstract

Purpose: This review examines the evidence for the hypothesis that epigenetics are involved in the initiation and perpetuation of radiation-induced genomic instability (RIGI).

Conclusion: In addition to the extensively studied targeted effects of radiation, it is now apparent that non-targeted delayed effects such as RIGI are also important post-irradiation outcomes. In RIGI, unirradiated progeny cells display phenotypic changes at delayed times after radiation of the parental cell. RIGI is thought to be important in the process of carcinogenesis, however, the mechanism by which this occurs remains to be elucidated. In the genomically unstable clones developed by Morgan and colleagues, radiation-induced mutations, double-strand breaks, or changes in messenger RNA (mRNA) levels alone could not account for the initiation or perpetuation of RIGI. Since changes in the DNA sequence could not fully explain the mechanism of RIGI, inherited epigenetic changes may be involved. Epigenetics are known to play an important role in

many cellular processes and epigenetic aberrations can lead to carcinogenesis. Recent studies in the field of radiation biology suggest that the changes in methylation patterns may be involved in RIGI. Together these clues have led us to hypothesize that epigenetics may be the missing link in understanding the mechanism behind RIGI.

Introduction

Radiation-induced genomic instability (RIGI) is a delayed, persistent effect of ionizing radiation exposure that can manifest in the unirradiated progeny of irradiated cells. The mechanism by which RIGI is initiated or perpetuated is yet to be understood [1-4]. RIGI may be one of the pathways by which radiation exposure can lead to cancer, therefore, understanding the mechanisms underlying genomic instability may help elucidate the processes involved in the development of radiation-induced carcinogenesis. The mechanisms of RIGI have been extensively studied in the genomically unstable clones developed in the Morgan laboratory [5]. Alterations that involve the DNA sequence, such as radiation-induced mutations or double-strand breaks alone could not account for the initiation or perpetuation of RIGI in these clones, nor could changes in messenger RNA (mRNA) levels [6-8]. Therefore, inherited epigenetic changes that control cellular phenotype without directly altering DNA sequence may be involved.

Epigenetics can play an important role in many cellular processes from gene expression to cellular proliferation and an aberrant epigenetic state of a cell can lead to carcinogenesis [9]. Changes in genomic DNA methylation post-irradiation and its potential correlation with initiation of genomic instability have been suggested [10-12]. Together, these clues have led us to hypothesize that epigenetics may be the missing

mechanistic link between irradiation and genomic instability. In this review, we present evidence that epigenetics, including DNA methylation changes, chromatin remodeling and alterations in microRNA (miRNA) expression, play a role in the initiation and perpetuation of RIGI. We will discuss studies that evaluated radiation-induced epigenetic alterations and how those alterations are involved in RIGI.

Ionizing Radiation

The carcinogenic effects of ionizing radiation exposure were recognized soon after Roentgen discovered x-rays [2, 13]. For many years it was thought that the deposition of energy by irradiation could initiate the processes in radiation-induced carcinogenesis. Targeted direct effects of radiation exposure cause genetic damage through direct deposition of energy in nuclear DNA [14]. This damage includes base damage, cross-links, and single and double strand breaks. If the cell survives then any mis- or un-repaired damage can be replicated and perpetuated in the daughter cells, resulting in mutagenesis and increased risk for carcinogenesis [15]. In addition, targeted indirect effects of radiation exposure can occur via the radiolysis of water. This occurs within nanoseconds by the generation of reactive oxygen species (ROS) that persist only for milliseconds [16]. Targeted indirect effects can cause oxidative damage to DNA, proteins, and lipids through radiation-induced free radicals such as hydroxyl radical ($OH\bullet$), superoxide ($O\bullet_2^-$), and organic radicals ($R\bullet$) [17].

In addition to the targeted effects of irradiation, non-targeted effects also contribute to induced mutagenesis and carcinogenesis. Non-targeted effects result in responses typically associated with targeted effects including sister chromatid exchanges

(SCE), chromosomal rearrangements, micronucleus formation, gene mutations and apoptosis, but they occur in cells not directly exposed to radiation [16]. These non-targeted effects are grouped under the terms radiation-induced bystander effects and RIGI [3, 18]. The bystander effect occurs when a signal produced by a directly irradiated cell elicits a subsequent response in neighboring non-irradiated cells [3]. The bystander effect is mediated via gap junction communication and/or secreted soluble factors [19]. Genomic instability is defined as the increase in acquisition of multiple changes in the genome [20]. RIGI can be observed in cells that survive irradiation at delayed times after exposure and sometimes manifest in their progeny over many generations. Genomic instability can manifest as delayed mutation, decreased plating efficiency, micronucleus formation, increased SCE, chromosomal instability, change in ploidy, gene amplification and microsatellite instability. Of these effects, the best described is chromosomal instability, which involves gross chromosomal rearrangements, mainly chromosomal duplications and/or partial trisomies (reviewed in [3, 21]).

The two non-targeted effects, radiation-induced bystander effects and RIGI, have been studied as separate entities, however, a link between the two was first demonstrated by Kadhim et al. [22] in their initial description of RIGI. This was followed by complementary publications by Watson et al. [23], Lorimore et al. [24], and Lorimore and Wright [25] clearly indicating that RIGI could be induced in cells that had never experienced any radiation traversal. In this review, we will focus primarily on data generated in our laboratory which we appreciate may well provide a biased review of the current understanding of RIGI. Nevertheless we believe our conclusions will have

implications for others studying RIGI and its implications for radiation risk and radiation carcinogenesis.

Genomically Unstable Clones

RIGI has been explored by many investigators (see the special issue of Mutation Research, volume 687, issues 1-2, May 2010). The pioneering studies of RIGI in the progeny of murine stem cells exposed to α–particles by Kadhim et al. [22] first implicated delayed radiation effects as well as potential non-targeted effects, i.e., effects occurring in cells not subject to radiation-induced energy deposition events. RIGI was then described in the progeny of normal human and murine bone marrow cells by the same group [26] and in cultured human lymphocytes by Holmberg et al. [27, 28]. It was shown that chromosomal instability induced by irradiation could be manifested as a wide range of cytogenetic aberrations including telomere structure alterations, micro- and minisatellite instability, hypoxanthine-guanine phosphoribosyltransferase (hprt) mutations, and large scale chromosomal aberrations [29-31]. These studies suggested that the frequency of instability observed is in excess and occurs more spontaneously than the frequency of gene mutations at similar doses, suggesting that the conventional radiation-induced mutations and cytogenetic lesions alone are not responsible for RIGI. A recent review devoted to understanding the mechanism of RIGI *in vivo* has pointed out the importance of the role of inflammatory processes in the radiation response and the need for further research in this area [4]. However, the mechanism(s) by which RIGI is initiated or perpetuated are still poorly understood.

Morgan and colleagues specifically developed unstable clones for use in a series of studies to examine genomic instability mechanisms (Figure 1.1). Clones exhibiting chromosomal instability were derived from the human-hamster hybrid cell line, GM10115, which contains a single copy of human chromosome 4 in a background of 20-24 hamster chromosomes [5]. GM10115 cells were irradiated, and the surviving cells were isolated and clonally expanded [5, 32]. Clones were characterized using cytogenetic analysis of metaphase chromosomes using fluorescence *in situ* hybridization (FISH) for human chromosome 4. An unstable clone was defined as one containing three or more metaphase subpopulations with different rearrangements of the human chromosome [5].

The clones were analyzed for SCE, delayed reproductive cell death, delayed mutation, mismatch repair, and delayed gene amplification [6]. Significant correlation to chromosomal instability was only observed with delayed gene amplification and delayed reproductive cell death. While radiomimetic antibiotics bleomycin and neocarzinostatin, which generate complex double strand breaks that model radiation-induced DNA damage, were effective in the induction of persistent chromosomal instability, the two other double-strand breaking agents, restriction enzymes and hydrogen peroxide, were ineffective at inducing delayed chromosomal instability [33]. These results suggest the quality of DNA damage may be important in the initiation of RIGI, however, DNA lesions including double-strand breaks *per se* does not necessarily lead to chromosomal instability [7, 33]. Ponnaiya et al. [34] demonstrated the dynamic nature of chromosomal instability in the unstable clones as observed by increased frequencies of both chromatid-type and chromosome-type aberrations using FISH and Giemsa staining. Direct evidence

of the involvement of oxidative stress in cells with RIGI was first described by Clutton et al. [35]. In the unstable clones, increased levels of apoptosis were demonstrated to contribute to not only persistent reproductive cell death, but also the existence of oxidative stress and elevated levels of free radical damage [36, 37]. This observation supports the work of Clutton et al. by demonstrating oxidative stress in cells exhibiting RIGI. Additional studies of the clones suggested that the potential source of this chronic oxidative stress may be dysfunctional mitochondria as demonstrated by increased levels of reactive oxygen species (ROS) and impaired mitochondrial function in the unstable clones [37].

This hypothesis for mitochondrial involvement in RIGI was confirmed by Kim et al. [38, 39], as they demonstrated through additional analysis that the mitochondria from unstable cells have impaired respiration. The enzyme activity of manganese superoxide dismutase, a mitochondrial antioxidant enzyme, was decreased in unstable clones suggesting a mitochondrial source of increased cellular ROS. The association of RIGI with elevated ROS and mitochondrial dysfunction was also observed using mass spectrometry [40]. Unstable clone mitochondrial protein profiles included altered levels of acetyl-coenzyme A-acetyltransferase and proteins involved in the tricarboxylic acid cycle (TCA cycle) and oxidative phosphorylation. Additional studies also demonstrated a causative relationship between chronic oxidative stress mediated by hydrogen peroxide and the mutator phenotype that persists for many generations post-irradiation in the unstable clones [41]. It was suggested that the increased levels of hydrogen peroxide resulted from mitochondrial dysfunction originating from complex II of the respiratory chain [42].

In order to test the hypothesis that the delayed instability observed in unstable clones was maintained by factors secreted into the culture medium Nagar et al. [43, 44] performed medium transfer experiments. When the filtered medium from unstable clones were transferred to unirradiated GM10115 cells, the majority of the recipient cells died and some of the survivors manifested delayed genomic instability. This novel epigenetic effect was described as the death inducing effect (DIE) in which a factor or factors secreted by unstable clones mediated instability, possibly by modulating persistent oxidative stress. This study supports the work by Watson et al. [23] as it suggests a link between radiation-induced bystander effects and RIGI [18, 45]. In an effort to identify the DIE factor, experiments performed by Laiakis et al. [46] determined that interleukin-8 (IL-8) was secreted in significant amounts by the unstable clones. The addition of exogenous IL-8 to the stable parental cell line was shown to cause DNA damage initially, but alone was not sufficient to initiate genomic instability. The potential involvement of inflammatory cytokine IL-8 in RIGI is also in agreement with the recent review of the importance of inflammatory processes in the radiation response and RIGI by Wright [4].

To search for mechanisms of initiation and perpetuation of RIGI, levels of gene expression in the unstable clones were studied using cDNA microarray analysis [8, 15, 47, 48]. This microarray analysis revealed lower levels of copper/zinc (Cu/Zn) superoxide dismutase 1 (SOD1) and nuclear-factor-kappaB (NF-kB) p105 in the unstable clones (-3.98-fold, and -3-fold, respectively) [8, 48]. SOD1 catalyzes the removal of harmful superoxide radicals and NF-kB is involved in the regulation of diverse set of cellular functions, including responses to oxidative stress. As a result, both were likely candidates to perpetuate genomic instability in the unstable clones. However, Northern

and Western blot follow up of these microarray data could not confirm the observations [47, 48]. From the same microarray analysis, the ubiquitin-conjugating enzyme E2A, Rad6 (E2A/Rad6) homolog and 26S proteasome subunit adenosine triphosphatase (ATPase) 2 were also found to be under-expressed suggesting a possible defect in the proteasome/ubiquitin pathway in the unstable clones (-3.78-fold, and -2.19-fold, respectively) [15]. Although differences in these two genes involved in the proteasome/ubiquitin pathway were validated in some of the clones, no single gene or molecular pathway was found to be differentially regulated in all of the unstable clones [8]. While not conclusive, these data suggested that there might be multiple molecular pathways and/or events that maintain the unstable phenotype.

Despite these numerous studies of the unstable clones, the mechanism of initiation and perpetuation of RIGI in them is still not understood (Figure 1.1). Non-targeted effects, including RIGI, occur at higher frequencies than would be expected from Poisson statistics of particle hits to surviving cell nuclei or from conventional gene mutation frequencies, invoking epigenetic mechanisms. The fact that these delayed responses affect changes in cellular phenotype without direct radiation exposure of nuclear DNA, and seemingly without altering DNA sequence, also suggests that epigenetics might play a mechanistic role.

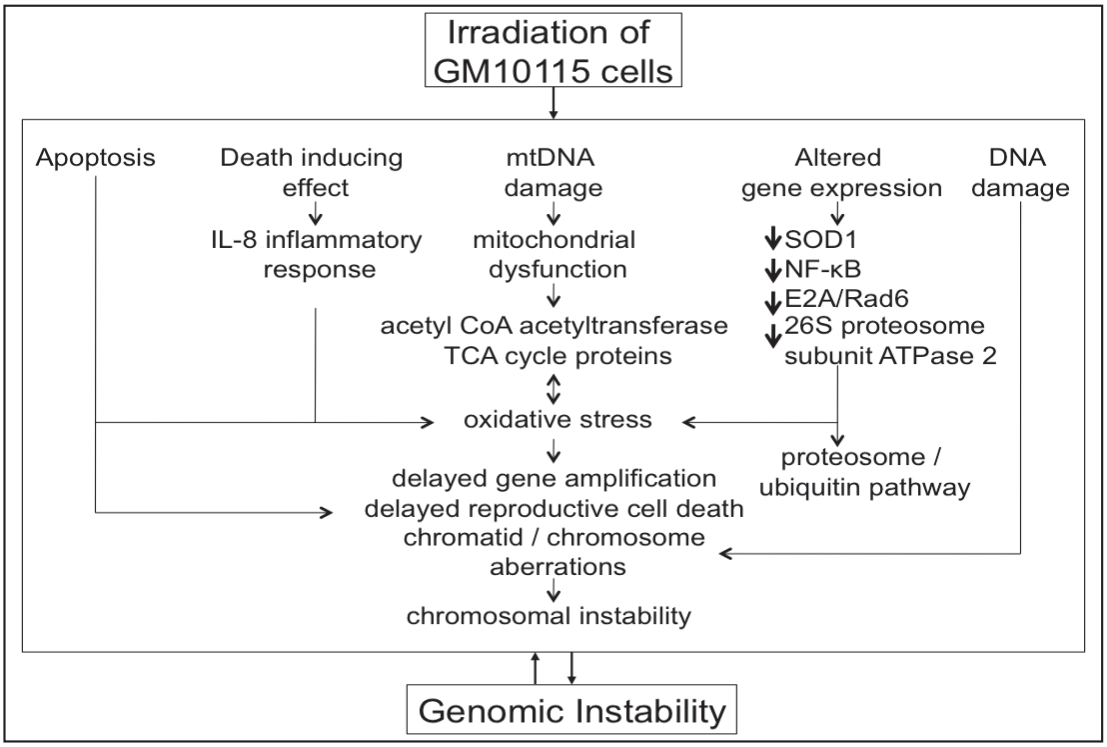

Figure 1.1. Phenotype of genomically unstable clones. Clones exhibiting RIGI were characterized in a series of studies. While the exact mechanisms initiating and perpetuating genomic instability were not identified, numerous inter-related characteristics thought to contribute to the unstable phenotype were identified.

Epigenetics

DNA Methylation

Epigenetics refers to heritable changes in gene expression that take place without alterations in the DNA sequence. Epigenetic changes include molecular modifications such as DNA methylation, chromatin remodeling and miRNA regulated gene expression [49]. The most extensively studied epigenetic modification is DNA methylation. The methylation of mammalian DNA takes place predominantly at cytosine bases in cytosine-

phosphate-guanine (CpG)-dinucleotides through the enzymatic activity of DNA methyltransferases (DNMT) [50]. However, some studies analyzing genome-wide methylation levels have shown that non-CpG methylation is present in significant quantities [51-54]. More recently, the non-CpG methylation has not only been indicated in embryonic stem cells [55] but also in somatic cells [56]. In mammals, there are four types of DNMT: DNMT1, DNMT2, DNMT3a and DNMT3b. DNMT1 functions as the maintenance methyltransferase by copying the methylation pattern of the old DNA strand onto the newly synthesized strand during DNA replication [57]. In cancer and in embryonic stem cells unmethylated CpG sites are targeted for *de novo* methylation by DNMT3a and DNMT3b [58]. DNMT2 has been shown to be capable of tRNA methylation, rather than as a DNA methyltransferase [59].

In normal cells, DNA methylation plays a critical role in the control of gene expression, especially in terms of tissue-specificity and germ-line gene expression. Promoter regions of tumor-suppressor genes are methylated to allow their expression and maintain the normal state of the cell [60]. Genomic imprinting directs hypermethylation to ensure suppression of one of the two parental alleles of a gene for monoallelic expression [61]. Similarly in X-chromosome inactivation, gene-dosage for females is accomplished by hypermethylation of one X-chromosome [62]. Repression of certain repeat elements through hypermethylation can prevent chromosomal instability, translocations, and gene disruption caused by the reactivation of transposable DNA sequences [63]. Cells that have mutations in DNMT3b lack the stabilizing effect of DNA methylation and have prominent nuclear abnormalities [64].

Chromatin Remodeling

Chromatin remodeling is involved in many biological processes including gene expression, DNA replication and repair, chromosome condensation, segregation and apoptosis [65]. Gene transcription is controlled by histone modifications of the histone octamer. Open chromatin is associated with transcriptional activity and is generally characterized by unmethylated DNA cytosines, acetylated histone tails by histone acetyltransferases (HAT) and trimethylation of lysine 4 on histone H3 [50]. Closed chromatin occurs when DNA cytosines become methylated, methyl-binding domains bind to methylated cytosines and acetyl groups are removed from the histone tails by histone deacetylases (HDAC) [50]. DNA becomes coiled into a closed chromatin structure carrying the transcriptional silencing mark histone H3 lysine 9 trimethylation and H3 lysine 27 trimethylation. In addition to methylation and acetylation, histone modifications including ubiquitination and phosphorylation are important in the regulation of gene expression [66]. Phosphorylation of histone H2AX at serine 139 (γH2AX) is one of the most extensively studied of all histone modifications [67]. Gamma H2AX is used as an early marker for induction and repair of DNA double-strand breaks [68, 69]. It also appears to play a functional role in the DNA repair process, maintenance of genome stability, and the early stages of cancer [70, 71].

MiRNA Expression

In addition to DNA methylation and chromatin remodeling, epigenetic changes found in mammalian organisms also include the regulation of gene expression by miRNA. MiRNA are small (~22nt), highly conserved non-coding RNA involved in post-

transcriptional regulation of gene expression either via mRNA degradation or translational inhibition. The synthesis of miRNA requires several processing steps. The primary-miRNA (pri-miRNA) is transcribed by RNA polymerase II and post-transcriptionally modified by addition of a 5'-cap and a 3'-poly (A) tail [72, 73]. In the nucleus, pri-miRNA is processed by the RNaseIII enzyme, Drosha and its cofactor Pasha into precursor-miRNA (pre-miRNA) [74, 75]. The pre-miRNA, a stem-loop structure of ~70nt, is transported to the cytoplasm [76] and further processed by another RNaseIII enzyme, Dicer [77]. The final miRNA strand is loaded into the RNA-induced silencing complex (RISC) in tight association with the argonaute protein (Ago) [78, 79] and directed to the 3'-untranslated region of its target mRNA [80]. MiRNA regulate a number of cellular pathways, such as cellular proliferation, differentiation, and apoptosis [81]. Therefore, deregulation of miRNA synthesis or expression levels may lead to carcinogenesis [82].

Epigenetics and Cancer

DNA Methylation and Cancer

Recent advances in cancer research have shown the importance of epigenetic aberrations in the carcinogenic process [9, 60, 83]. DNA methylation can be involved in the process of carcinogenesis in several ways: modifications in the coding regions of genes as a result of methylated cytosine induced point mutations, initiation of genomic instability through overall depletion of methylcytosines in the genome, and inactivation of gene transcription due to hypermethylation of gene promoters [50]. The induction of point mutations can occur due to spontaneous deamination of methylated cytosine to

thymine, formation of adducts on the adjacent guanine, and formation of pyrimidine dimers. Formation of adducts has been observed following exposure to the carcinogen benzo(a)pyrene diol epoxide present in cigarette smoke and implicated in lung tumorigenesis. Formation of pyrimidine dimers upon exposure of skin to ultraviolet light was shown to cause melanoma. DNA hypomethylation allows upregulation of oncogenes, oncogenic miRNA and transcription of parasitic sequences incorporated in DNA such as repeat elements and transposons, resulting in genomic instability. For example, in acute myeloid leukemia patients hypomethylation of the multiple drug resistance 1 (*MDR1*) promoter region has been shown to lead to overexpression of the *MDR1* gene and establish multidrug resistance [84]. Lastly, promoter hypermethylation silences tumor-suppressor genes and tumor-suppressor miRNA [50]. Many classical tumor-suppressor genes, including retinoblastoma (*RB1*), cylin-dependent kinase inhibitor 2A (*p16*), von Hippel-Lindau (*VHL*), mutL homolog 1 (*MLH1*), breast cancer 1 (*BRCA1*), and adenomatous polyposis coli (*APC*), that cause specific cancer syndromes when mutated are inactivated by methylation in sporadic tumors [50].

Chromatin Remodeling and Cancer

Epigenetic silencing of transcription also occurs through posttranslational histone modification, chromatin remodeling and changes in the nuclear positioning of genes [60]. Deregulation of these and other chromatin processes have been linked to the development and progression of cancer [65, 85, 86]. Some chromatin remodeling modifications observed in cancer cells are alterations in the histone acetyation/deacetylation balance, increased or decreased poly-adenosine diphosphate (ADP)-ribosylation and failures in

ATP-dependent chromatin-remodeling mechanisms [87]. Deregulation of histone acetylation could lead to carcinogenesis in three ways. Histone hypoacetylation at certain promoter regions, induced by reduced HAT activity or increased HDAC activity, could silence tumor-suppressor genes. Conversely, histone hyperacetylation at other promoter regions, induced by elevated HAT activity or decreased HDAC activity, could lead to the activation of oncogenes. Thirdly, carcinogenesis could be triggered by aberrant recruitment of HAT or HDAC.

The second type of chromatin remodeling modification observed in cancer cells is poly-ADP-ribosylation, which is important in the maintenance of genome stability, DNA repair and apoptosis [87]. One of the enzymes involved in this process is poly-ADP-ribose polymerases (PARP) and deficiency of PARP-1 enzyme has been shown to contribute to the development of some cancers [87]. The third type, ATP-dependent chromatin-remodeling, has complexes that all belong to the switching 2/sucrose nonfermenting 2 (SWI2/SNF2) family [87]. These complexes are involved in many processes including DNA repair and genomic stability, therefore, they are important epigenetic mechanisms involved in carcinogenesis. Sucrose nonfermenting 5 (SNF5), brahma-related gene 1 (BRG1) and brahma (BRM) are among the subunits of SNF2 complexes and inactivation or loss of these subunits has been observed in some cancers [87]. Loss of SNF5 leads to chromosomal instability and the gene that codes for it, human *SNF5*, is considered a tumor-suppressor gene, whose mutation or deletion stimulates cell-cycle progression. The subunits of SWI2 complexes are generally associated with highly proliferative cells and are significantly increased in some cancers.

MiRNA Expression and Cancer

Alterations affecting miRNA processing along with alterations of miRNA expression levels, and mutations in miRNA:mRNA interacting sequences have been shown to be associated with cancer [81]. MiRNA expression levels could be altered in many ways including gross genomic alterations, epigenetic changes of the miRNA gene, and point mutations. Alterations affecting miRNA processing could be due to the disruption of the miRNA-processing apparatus and/or alteration in the primary sequence of the pri-miRNA. The interaction between an miRNA and mRNA could be weakened by mutations in the miRNA:mRNA interacting sequences that may arise in early stages of the miRNA synthesis. Two classes of miRNA that are altered in cancer are tumor-suppressor miRNA (TS-miR) and oncogenic miRNA (oncomiR). Altered TS-miR can no longer inhibit the translation of protooncogenes and up-regulated oncomiR suppress the expression of tumor-suppressor genes.

During carcinogenesis, the three epigenetic mechanisms are not completely independent, but rather work in a linked and complex manner [88]. MiRNA gene expression can be controlled by hyper- and/or hypomethylation, and the synthesis of chromatin remodelers and DNMT can be regulated by miRNA. Tumor promotion mediated by c-myelocytomatosis (Myc) is an example of linked epigenetic mechanisms. C-Myc is normally epigenetically silenced by histone acetylation and methylation. Aberrations in this chromatin structure allow for *c-Myc* gene expression, which in turn activates carcinogenic pathways, including wingless-integration (WNT)/β-catenin, crucial for solid tumor development [89-94]. C-Myc also regulates miRNA expression, including miR-421, involved in ATM silencing and down-regulation of the DNA damage

response [95]. The processes by which radiation exposure leads to RIGI are also likely to involve complex epigenetics mechanisms.

Epigenetic Changes After Radiation

DNA Methylation and Radiation

There are multiple reports of altered DNA methylation patterns following exposure to ionizing radiation in plants, rodents, and rodent and human cell lines [11, 12, 96-99]. Plants exposed to 20 and 40Gy of ionizing radiation as the result of the Chernobyl accident showed dose dependent hypermethylation [99]. It was suggested that the radiation-induced hypermethylation might prevent genomic instability and reshuffling of the hereditary material via chromosomal instability or reactivation of transposable elements, allowing the plants to survive in the radiation environment.

In mice and rats, radiation exposure led to dose dependent and sex- and tissue specific global DNA hypomethylation [12, 96, 98, 100-102]. C57/BI male and female mice were whole-body irradiated with 0.5, 1, 2.5, 5Gy of x-rays and methylation analyses were performed in liver, spleen, and lung tissues [12]. Dose dependent DNA hypomethylation was observed in the female liver, as well as in the male and female spleen. In some experimental groups this hypomethylation was associated with increased levels of DNA strand breaks. In spleen and liver of irradiated mice, the radiation-induced DNA hypomethylation correlated with decreased expression of DNA methyltransferases DNMT1 and DNMT3a/b [96]. Thymus tissue of mice exposed to fractionated whole-body x-ray irradiation (0.5Gy) also resulted in DNA hypomethylation that was associated with reduced expression of DNMT1, DNMT3a/b, methyl CpG binding protein 2

(MeCP2) and another methyl-binding protein, methyl CpG binding domain protein 2 (MBD2) [102]. In many of these studies, the global DNA hypomethylation observed post-irradiation along with the decreased expression of proteins involved in maintaining the correct genomic methylation patterns suggested that these changes might play a role in genomic instability [12, 96, 101]. X-ray irradiation of mice was also shown to affect methylation of the promoter of the *p16* tumor-suppressor in a sex- and tissue-specific manner, but not the methylation status of O-6-methylguanine-DNA methyltransferase (*MGMT*) [103]. Together with the evidence for altered promoter methylation in particular cancers [50], this animal data provides a link among radiation exposure, epigenetics and carcinogenesis.

Exposures to low linear energy transfer (LET) gamma-rays were also shown to result in global hypomethylation in the C-1300 N1E-115 (mouse), CHO K-1 (hamster), V79A03 (hamster), and Hela S-3 (human) cell lines [97]. However, another study using one of the same cell lines, CHO K-1, showed no change in methylation after x-ray exposure [11]. The different outcomes in these two studies might suggest differences in changes in epigenetic profiles after different types of radiations. The latter study did also show global hypomethylation in mouse liver tissue after x-rays exposure but demonstrated no change in mouse brain or spleen tissue [11]. Even though each of these studies was performed post-low LET irradiation, different responses were observed. The variability in these findings might suggest the difference in epigenetic responses post-irradiation *in vitro* versus *in vivo* and also among different types of cells and different types of tissues in the animal.

One study has directly correlated RIGI in HPV-G cells with epigenetic changes following exposure to ^{60}Co gamma-radiation [104]. Genomic instability manifested as reproductive cell death, reduced cloning efficiency at successive passages, increased apoptosis, and an increased proportion of chromosomally aberrant cells at 20 passages post-irradiation. While this RIGI was shown to be predominantly associated with DNA hypermethlyation of certain CpG dinucleotides and pericentromeric spermidine N1-acetyltransferase 2 (SAT2) satellite sequences, non-specific DNA hypomethylation was also observed. The majority of the hypermethylated sequences detected were repeat elements. Aberrant methylation status of repeat elements [50] and also SAT2 satellite sequences is known to affect genomic instability [105]. Based on these observations, the authors suggested that DNA methylation alterations following radiation exposure could be involved in initiation and/or perpetuation of RIGI.

The role of ROS in RIGI is well established [35-37] and some studies suggest the involvement of ROS in affecting changes in DNA methylation in relation to cancer and other diseases [106-108]. While ROS alone are not sufficient to induce RIGI, it is known that free radical scavengers can reduce the incidence of instability after irradiation [109, 110]. We hypothesize that ROS production post-irradiation also contributes to radiation-induced DNA methylation changes that can lead to RIGI.

Together these studies suggested radiation-induced global DNA hypomethylation and promoter hypermethylation play a role in genomic instability, most clearly demonstrated by certain CpG dinucleotide hypermethylation (predominantly repeat element and SAT2 satellite sequences) and non-specific DNA hypomethylation [104]. Thus, studies so far found both hypo- and hypermethylation changes post-irradiation. It

remains to be understood which methylation changes have more impact on the cell and contribute to genomic instability. However, hypomethylation of repeat elements and promoter regions of oncogenes and hypermethylation of promoter regions of tumor-suppressor genes post-irradiation play an important role in RIGI and radiation-induced carcinogenesis.

Chromatin Remodeling and Radiation

Gamma H2AX has been used extensively as a measure of double-strand breaks post-irradiation [111]. However, there are fewer studies that try to understand radiation-induced histone modifications as an epigenetic mechanism. In mice, radiation exposure led to decreased trimethylation of histone H4 lysine 20 which the authors suggest might result in relaxed heterochromatin organization that would impair genome stability [102]. It has been shown in human cells that euchromatic regions were more susceptible to radiation-induced DNA damage and gamma H2AX accumulation [112-114]. Cells exposed to gamma-rays have showed chromatin decondensation at sites of double-strand breaks [115]. These changes manifested 15 minutes after irradiation as observed by a decrease in intensity of chromatin labeling, increased histone H4 lysine 5 acetylation, and decreased histone H3 lysine 9 dimethylation. Forty minutes post-irradiation, these changes induced by radiation exposure were replaced by histone modifications typical for condensed chromatin (decreased acetylation of histone H4 lysine 5 and increased methylation of histone H3 lysine 9). The data suggested the need to convert from less to more condensed chromatin after DNA repair. Another study observed rapid binding of SWI/SNF complexes to chromatin in regions of double-strand breaks via interaction with

gamma H2AX suggesting that the repair mechanisms were facilitated by SWI/SNF complex promotion of H2AX phosphorylation [116]. The role of ataxia telangiectasia mutated (ATM) in some of the chromatin changes in response to radiation and as a result its potential role in RIGI has been implicated. In response to double-strand break induction, Kruppel-associated box (KRAB)-associated protein (KAP-1) is phosphorylated in an ATM-dependent manner [117]. Phosphorylated KAP-1 leads to euchromatinization, therefore, these results suggest that chromatin relaxation is a fundamental process in the DNA damage response and that ATM and KAP-1 are primary mediators. It was also suggested that ATM-dependent heterochromatin relaxation is specifically required for the repair of double-strand breaks located within heterochromatin [118]. Another study identified another signaling cascade that helps initiate the DNA damage response by altering chromatin [119]. DNA breaks mobilize heterochromatin protein 1 (HP1)-β, a chromatin factor bound to histone H3 methylated on lysine 9 (H3K9me), which then promotes chromatin changes that initiate the DNA damage response. These studies indicated that radiation exposure affected chromatin remodeling in association with DNA damage and DNA repair. This suggests that radiation-induced aberrations in chromatin remodeling could lead to DNA damage and impaired DNA repair. We hypothesize that this compromised DNA repair and relaxed heterochromatin contributes to the initiation of genomic instability.

MiRNA Expression and Radiation

While changes in expression profiles of miRNA have been observed following irradiation in mouse and human cells [120, 121], the first evidence for functional importance of a miRNA in radiation responses was shown in Drosophila [122]. Following irradiation of fly larvae, the *bantam* miRNA was shown to be up-regulated. This miRNA in turn was shown to bind to the 3'-UTR of the pro-apoptotic gene *hid* and affect its post-transcriptional down-regulation. This miRNA-mediated gene repression resulted in decreased radiation-induced apoptosis and increased larvae survival.

In mouse embryonic stem cells, a group of miRNA and their putative gene targets potentially involved in response to DNA damage were identified post-irradiation [120]. In whole-body irradiated mice, the spleen and thymus tissues showed sex-specific deregulation of miRNA expression [123]. Among these were miRNA-34a (miR-34a) and miR-7, which were thought to be involved in counteracting radiation-induced hypomethylation. MiRNA expression was also significantly affected in the testes of whole-body irradiated mice and a significant difference was observed in miR-709 levels between the control and exposed groups [124]. It was shown that miR-709 targeted the Brother of the Regulator of Imprinted Sites (BORIS), which is an important regulator of DNA methylation and imprinting. This study showed that the radiation-induced DNA damage resulted in increased miR-709 expression in exposed testes that decreased levels of BORIS to prevent massive aberrant erasure of DNA methylation.

Exposure of human fibroblasts to low LET x-rays, at early (0.5 h) time points, resulted in down-regulation of miRNA levels [121]. However, two hours after exposures to 2Gy of radiation, a transient up-regulation of miRNA was observed. MiRNA miR-

579, 608, 548-3p, and 585 were noted for targeting genes involved in radioresponsive mechanisms, such as cell cycle checkpoints and apoptosis. This study suggested that miRNA were down-regulated immediately after irradiation to stimulate DNA repair mechanisms and later up-regulated in order to suppress apoptosis for cell survival. Following gamma-irradiation of A549 human lung carcinoma and IM9 human B lymphoblastic cells a number of miRNA showed more than 2 fold change in 1, 10, 20 and 40 Gy exposed cells [125, 126]. The target genes were involved in apoptosis, regulation of cell cycle, and DNA damage and repair. These studies showed that the miRNA expression in A549 and IM9 human cells was affected by radiation exposure and suggested that the changes might be involved in the regulation of cellular responses to irradiation. A study involving gamma-irradiation of human B lymphoblast cell lines showed dose dependent changes in miRNA expression [127]. Low dose irradiated cells (0.05Gy) demonstrated a decrease in miR-20 and miR-21. MiR-20 and miR-21 have also been shown to increase in tumorigenesis and miR-21 is considered an onco-miRNA. In high dose irradiated cells (10Gy), miR-197 was up-regulated. Carcinogenic characteristics were observed in normal cells following injection of miR-197 suggesting that stimulation of expression of miR197 by high dose radiation could lead to the progression of tumorigenesis. Together, these results suggested that low dose exposure to radiation could suppress progression of cancer by controlling miRNA expression while high dose exposure could promote miRNA-mediated cancer progression. Alteration of miRNA expression due to radiation exposure in relation to p53 wild-type vs. null human colon carcinoma cells has also been shown [128]. In addition, ionizing radiation-induced oxidative stress has been shown to play a role in altering miRNA expression [129].

The role of miRNA in the immune system and in inflammation have been reviewed in the literature [130, 131]. The mechanism of RIGI *in vivo* is thought to be linked to inflammatory processes in the radiation response [4]. Therefore, those miRNA could play an important role in the initiation and/or perpetuation of RIGI.

These studies suggested that radiation exposure alters miRNA profiles in a way that can affect oxidative stress, DNA damage, DNA repair, regulation of cell cycle, apoptosis, tumorigenesis and changes in DNA methylation. While none of these studies directly correlated RIGI with changes in miRNA, the pathways affected by radiation-induced changes in miRNA expression suggest that miRNA play a role in initiation and/or perpetuation of genomic instability.

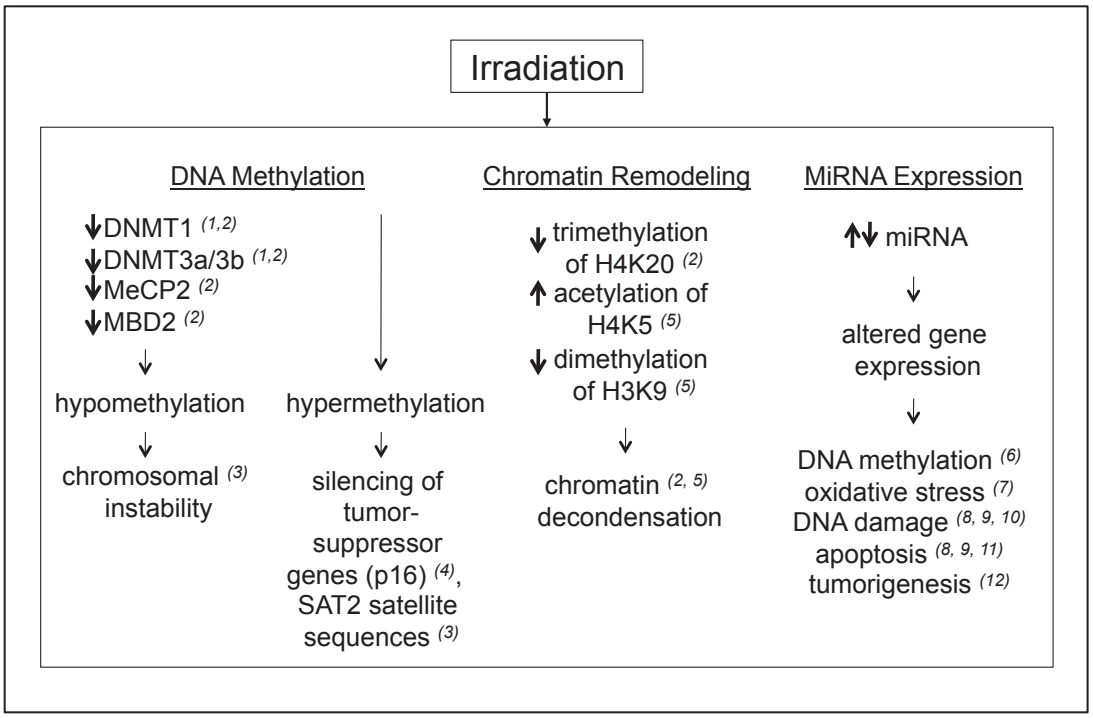

Figure 1.2. Radiation-induced epigenetic alterations. Current work in the field has identified epigenetic changes post-irradiation including altered DNA methylation, chromatin remodeling, and miRNA expression. Some of these changes are presented above. (1: Raiche et al. 2004 [96], 2: Pogribny et al. 2005 [102], 3: Kaup et al. 2006 [104], 4: Kovalchuk et al. 2004 [103], 5: Falk et al. 2007 [115], 6: Ilnytskyy et al. 2009 [123], 7: Simone et al. 2009 [129], 8: Cha et al. 2009 [126], 9: Shin et al. 2009 [125], 10: Ishii and Saiton 2006 [120], 11: Maes et al. 2008 [121], 12: Cha et al. 2009 [127])

Conclusion

Based on the evidence presented here, radiation exposure can induce epigenetic changes including alterations in DNA methylation, chromatin remodeling and miRNA expression (Figure 1.2). RIGI was linked to alterations in global, repeat element and tumor-suppressor promoter methylation. Chromatin remodeling was also affected by irradiation in a manner that could contribute to genomic instability. Radiation exposure led to relaxed heterochromatin organization that could lead to DNA damage, impaired DNA repair and eventually genomic instability. Altered miRNA expression levels were also shown post-irradiation. At low radiation doses, miRNA changes could be involved in suppressing radiation-induced apoptosis, stimulating DNA repair, counteracting radiation-induced hypomethylation, and suppressing the progression of cancer, but higher doses of radiation could lead to tumorigenic progression.

The mechanisms underlying the RIGI observed in unstable clones developed by Morgan and colleagues remain unclear. However, the evidence presented in this review supports the hypothesis that epigenetic mechanisms may be involved (Figure 1.3). Induction of epigenetic changes could be an initiating factor in this instability. These changes may be heritable and persist at delayed times post-irradiation in the progeny of the irradiated cells. Additionally or alternatively, epigenetic alterations may be a late arising delayed effect of irradiation driving the perpetuation of the instability.

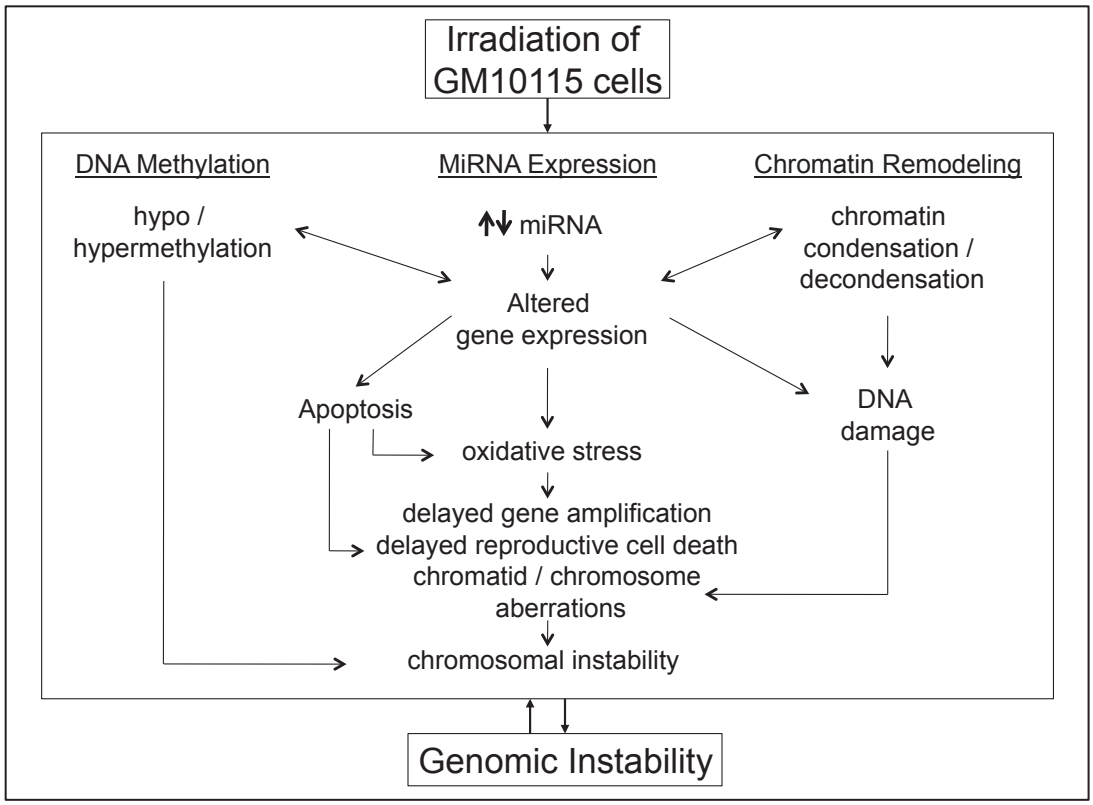

Figure 1.3. Hypothesized model for the contribution of epigenetic alterations to radiation-induced genomic instability in the unstable clones.

Chapter 2: RADIATION-INDUCED EPIGENETIC ALTERATIONS AFTER LOW AND HIGH LET IRRADIATIONS

Abstract

Epigenetics, including DNA methylation and microRNA (miRNA) expression, could be the missing link in understanding the delayed, non-targeted effects of radiation including radiation-induced genomic instability (RIGI). This study tests the hypothesis that irradiation induces epigenetic aberrations, which could eventually lead to RIGI, and that the epigenetic aberrations induced by low linear energy transfer (LET) irradiation are different than those induced by high LET irradiations. GM10115 cells were irradiated with low LET x-rays and high LET iron (Fe) ions and evaluated for DNA damage, cell survival and chromosomal instability. The cells were also evaluated for specific locus methylation of *nuclear factor-kappa B* (*NFκB*), *tumor suppressor in lung cancer 1* (*TSLC1*) and *cadherin 1* (*CDH1*) gene promoter regions, long interspersed nuclear element 1 (LINE-1) and Alu repeat element methylation, CpG and non-CpG global methylation and miRNA expression levels. Irradiated cells showed increased micronucleus induction and cell killing immediately following exposure, but were

chromosomally stable at delayed times post-irradiation. At this same delayed time, alterations in repeat element and global DNA methylation and miRNA expression were observed. Analyses of DNA methylation predominantly showed hypomethylation, however, hypermethylation was also observed. We demonstrate that miRNA expression levels can be altered after x-ray irradiation and that these miRNA are involved in chromatin remodeling and DNA methylation. A higher incidence of epigenetic changes was observed after exposure to x-rays than Fe ions even though Fe ions elicited more chromosomal damage and cell killing. This distinction is apparent at miRNA analyses at which no validated miRNA were altered after high LET irradiations while two miRNA were altered after low LET irradiations. This study also shows that the irradiated cells acquire epigenetic changes suggesting that epigenetic aberrations may arise in the cell without initiating chromosomal instability.

Introduction

Radiation-induced carcinogenesis is a well-recognized process, but the underlying mechanisms are not well understood [2]. Radiation-induced genomic instability (RIGI) is thought to be an early event in radiation carcinogenesis, however, the mechanisms underlying this process remain to be elucidated [1]. In order to understand the initiation and perpetuation of RIGI, studies have evaluated numerous endpoints including double-strand breaks, mutations, gene expression, disruption of mitochondrial processes, cell cycle arrest, and apoptotic cell death [132]. Despite these efforts, the mechanisms by which RIGI is initiated and perpetuated are still unknown. Recent studies have shown radiation-induced epigenetic changes including DNA methylation and microRNA

(miRNA) expression [132]. In addition to playing a role in the radiation response, aberrant genomic DNA methylation and miRNA profiles have also been shown to be associated with cancer [9]. Therefore, we are testing the hypothesis that the immediate effects of low and high linear energy transfer (LET) radiation exposure result in different epigenetic alterations in cells that could eventually lead to RIGI.

Mammalian DNA is thought to be predominantly methylated at cytosine bases in cytosine-phosphate-guanine (CpG)-dinucleotides through the enzymatic activity of DNA methyltransferases (DNMT) [50]. In normal cells, DNA methylation is involved in controlling gene expression, especially in terms of tissue-specificity and germ-line gene expression. Hypomethylation of the promoter regions of tumor-suppressor genes allow their expression and maintains the normal state of the cell [133]. Certain repeat elements, including long interspersed nuclear elements 1 (LINE-1) and Alu elements, are repressed through hypermethylation to prevent chromosomal instability, translocations, and gene disruption caused by the reactivation of transposable DNA sequences [63]. In cancer cells, global hypomethylation can lead to the initiation of genomic instability [50]. In addition, hypermethylation of tumor-suppressor genes can lead to their transcription inactivation.

In addition to CpG methylation, non-CpG methylation has also been demonstrated [51-54]. Non-CpG methylation is prevalent in embryonic stem cells and appears to be mediated by DNMT3a [55]. In somatic cells, non-CpG methylation of the *proliferator-activated receptor γ (PPARγ) coactivator-1 α* (*PGC-1α*) promoter occurs by DNMT3b [56]. Similar to CpG methylation, hypermethylation of non-CpG methylation of the *PGC-1α* promoter resulted in repression of its expression. However, only limited

studies have described non-CpG methylation and it is controversial as to whether or not it exists in mammalian somatic cells [134]. For example, Rein et al. [135] have described conflicting results to those reported by Woodcock et al., that suggested non-CpG methylation to be more dominant methylation site than CpG sites [54].

MiRNA expression is also an epigenetic mechanism involved in the regulation of gene expression. MiRNA are small (~22 nucleotides), highly conserved non-coding RNA involved in post-transcriptional regulation of gene expression either via mRNA degradation or translational inhibition. In normal cells, miRNA expression plays an important role in the regulation of cellular pathways including cellular proliferation, differentiation, and apoptosis [81]. In cancer cells, deregulation of miRNA synthesis or expression levels are observed [82].

These epigenetic changes could be the missing link between radiation exposure, RIGI, and radiation-induced carcinogenesis. Therefore, it is important to understand the changes in epigenetic profiles following irradiation. This study will shed light on the effects of radiation dose and LET on epigenetics. Low LET x-rays are commonly used in the clinic for diagnostic and treatment measures. High LET iron (Fe) ions are prominent in outer space and understanding their effect is important for the health of astronauts. To date, studies have predominantly evaluated low LET radiation effects on epigenetic changes, while little is known regarding high LET radiation effects.

In this study, GM10115 cells were irradiated using either low LET x-rays or high LET Fe ions. The initiation of radiation-induced DNA damage and cell killing were determined through micronucleus and clonogenic cell survival assays, respectively. The post-irradiation status of specific locus, repeat element, and genome-wide DNA

methylation, and miRNA profiles were evaluated to determine the effect of dose and radiation quality on epigenetic changes. The results of these experiments show differences in DNA methylation changes and miRNA expression alterations based on dose and LET of the radiation used.

Materials & Methods

Cell culture:

The human-hamster hybrid cell line, GM10115, contains a single copy of human chromosome 4 in a background of 20-24 hamster chromosomes (Human Genetic Mutant Cell Repository, Camden, NJ). AA8 is a Chinese hamster ovary (CHO) cell line (American Type Culture Collection (ATCC)). These cell lines were maintained in high glucose Dulbecco's Modified Eagle Medium (DMEM) containing 10% fetal bovine serum (FBS, Hyclone, Logan, UT), 2 mM L-glutamine (Invitrogen, Carlsbad, CA), 0.2 mM L-proline (Sigma, St. Louis, MO) at 34°C (AA8 at 37°C) with 5% CO_2. RKO is a human colorectal carcinoma cell line (ATCC), which was maintained in low glucose Dulbecco's Modified Eagle Medium (DMEM) containing 10% FBS (Hyclone, Logan, UT), 2 mM L-glutamine (Invitrogen, Carlsbad, CA) at 37°C with 5% CO_2. Cell cultures were routinely screened for the presence of mycoplasma (Bionique Testing Laboratories, Inc., Saranac Lake, NY).

Cells treated with the DNA methylation inhibitor 5-aza-2'deoxycytidine (DAC, Sigma) were plated at a low density ($1x10^6$ cells in T-175 flasks) 24 hours before treatment. Every 24 hours fresh medium containing 5 μM DAC was added to cultures for 5 days prior to harvesting.

Irradiations:

GM10115 cells were irradiated with low LET (2 keV/μm) x-rays using Pantak HF320 x-ray machine (250-kV peak, 13mA; half-value layer, 1.65-mm copper) at a dose rate of 2.4 Gy/min with doses of 0.5, 1 and 2Gy (Radiation Oncology Research Laboratory, University of Maryland, Baltimore). For high LET radiations, cells were irradiated with Fe ions ($^{56}Fe^{+26}$, 1GeV/amu, 150 keV/μm) at dose rates of 0.2Gy/min with doses of 0.1 and 1Gy. All high LET radiations were performed at the NASA Space Radiation Laboratory (NSRL, Brookhaven National Laboratory, Upton, NY) in experimental cycle NSRL-08B (2008). Beam dosimetry was provided by the NSRL and a detailed characterization of this beam has been published previously [136]. Following irradiation cell cultures were returned to 34°C for 1 h (to allow for media deactivation), harvested by trypsinization, and then used in subsequent experiments or frozen in aliquots at -80°C.

Clonogenic cell survival:

As an initial response, the effect of irradiation on cell survival was measured by clonogenic cell survival. Within two hours after irradiation, GM10115 cells were plated in 100-mm-diameter culture dishes at densities calculated to yield 50 - 100 cell colonies per dish. Following 14 days incubation, cells were fixed, stained with crystal violet in 20% ethanol, and colonies >50 cells counted. The number of colonies divided by the number of plated cells was used to calculate the plating efficiency and survival fraction for each treatment. A total of three biological replicates were performed. The doses used for Fe ions (0.1Gy and 1Gy) correspond to similar relative biological effectiveness (RBE) at 0.5Gy and 2Gy of x-rays respectively (Figure 2.2A).

Micronucleus analysis:

As an indicator of the initial radiation response, chromosomal integrity was measured by the frequency of micronucleus formation at first cell cleavage post-irradiation using the cytokinesis block technique [137]. Within two hours after irradiation, $1x10^6$ irradiated or control GM10115 cells were plated in T-25 culture flasks in the presence of 2.0 μg/ml cytochalasin B and incubated for 36 h at 34°C. We had previously determined 36 h to be the time at which irradiated GM10115 cells are predominantly binucleated. At the end of the incubation, cells were fixed with ice-cold methanol:acetic acid (3:1), and stored at 4°C. The fixed cells were stained with acridine orange (0.01% in phosphate buffered saline), and examined using fluorescence microscopy (Nikon Eclipse TE2000-E, Melville, NY). At least 500 binucleated cells with well-defined cytoplasm were scored for micronucleus formation (Figure 2.1). The frequency of micronuclei was calculated as a percent of micronucleated cells to total number of binucleated cells scored. A total of three biological replicates were performed.

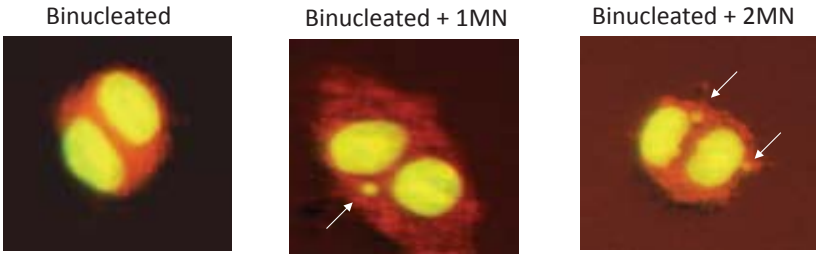

Figure 2.1. Micronuclei (MN) pictures of binucleated cells. The cells are stained with acridine orange which makes cytoplasm appear red and nucleus appear green.

Clonal expansion:

Delayed radiation responses were evaluated in clonally expanded single GM10115 cells at 16 - 20 population doublings post-irradiation. Clones with 50 - 100 cells were picked at random using sterile Dacron swabs dipped in trypsin and were expanded to mass culture in 25-cm^2 flasks. At 16 - 20 population doublings each culture was harvested for cytogenetic and DNA methylation analyses. For miRNA analyses, populations of irradiated cells grown for 16 - 20 population doublings after irradiation were used.

Analysis of chromosomal instability:

The clones were characterized by cytogenetic analysis of metaphase chromosomes using fluorescence *in situ* hybridization (FISH) for human chromosome 4. The biotin labeling of the pBluescript vector-based library of human chromosome 4-specific DNA sequences (pBS4) and the details of the FISH procedure have been described previously [5]. Metaphase spreads were scored using a Zeiss Axioskop microscope equipped with a dual-band pass fluorescein isothiocyanate (FITC)/Texas Red filter set. A stable clone was defined as one that contained a homogenous metaphase population with a unique rearrangement (translocation) or no rearrangement of the human chromosome with hamster chromosomes. An unstable clone was defined as one that contained three or more metaphase subpopulations with different rearrangements of the human chromosome. Each of these rearranged subpopulations constituted ≥ 5% of the 200 metaphases scored.

DNA isolation and bisulfite treatment:

DNA was extracted from cells using the DNeasy kit using standard methods (Qiagen, Valencia, CA) and stored in TE buffer at -20°C. Bisulfite modification of genomic DNA was performed using the EpiTect bisulfite kit using standard methods (Qiagen). Bisulfite treated DNA was used in specific locus, bisulfite sequencing and repeat element methylation analyses. Bisulfite treatment selectively deaminates cytosine but not 5-methylcytosine to uracil [138] and during PCR uracil is replaced by thymine. This leads to a primary sequence change in the DNA that allows cytosine to be distinguished from 5-methylcytosine.

Specific locus methylation:

Promoter methylation of *nuclear factor-kappa B* (*NFκB*), *tumor suppressor in lung cancer 1* (*TSLC1*) and *cadherin 1* (*CDH1*) were studied using the methylation-specific PCR (MSP) assay [139]. The genomic sequences for the promoter regions of human *NFκB* p105, hamster *TSLC1*, and hamster *CDH1* [140-142] were used to design methylation specific primers in the *MSPprimer* program, www.mspprimer.org. A 20 μl PCR was carried out in RNase-free water using 20 ng bisulfite treated genomic DNA, 10 μl HotStarTaq Plus Master Mix (1 unit of HotStarTaq DNA Polymerase, 200 μM of each dNTP, 1.5 mM $MgCl_2$; Qiagen), 5 (*TSLC1*, *CDH1*) or 10 (*NFκB*) picomoles of each PCR primer. Primer sequences are as follows: *NFκB* unmethylated (u*NFκB*), forward 5'-AAG TAG TTT AGA TGT TAG TGA ATG-3' and reverse 5'-AAA CCC CCA AAA AAC ACC TAC CAA ACC CAA TAA TCA AAA AAC A-3'; *NFκB* methylated (m*NFκB*), forward 5'-AAG TAG TTT AGA TGT TAG TGA ATG-3' and reverse 5'-

CCA AAA AAC GCC TAC CGA ACC CAA TAA TCG AAA AAC G-3'; *TSLC1* unmethylated (u*TSLC1*), forward 5'-TTT ATA GGG TTT TGT TTT TAG GTG G-3' and reverse 5'-AAA AAC TAC CTC CCA AAC CCA AAC A-3'; *TSLC1* methylated (m*TSLC1*), forward; 5'-TTT ATA GGG TTT TGT TTT TAG GTG G-3' and reverse 5'-CTC CCG AAC TCC CGA ACC CGA ACG-3'); *CDH1* unmethylated (u*CDH1*) forward 5'-GAT TTG AAT GAA TGT GAA TTA GGA AGT TTT TTT AGG TTG GTT TTG-3' and reverse 5'-TAA CCA AAC AAA CAC CAA ACA AAC ACA AAA CTC AAA TAC AAT CA-3'); *CDH1* methylated (m*CDH1*), forward 5'-ATT CGA ACG AAT GTG AAT TAG GAA GTT TTT TTA GGT CGG TTT C-3' and reverse 5'-CCG AAC AAA CAC GAA ACT CGA ATA CGA TCG-3'. PCR cycling conditions were 95°C for 15 s, annealing temperature (u*NFκB*; 48.9°C, m*NFκB*; 47.3°C, u*TSLC1*; 55.0°C, m*TSLC1*; 55.0°C, u*CDH1*; 52.0°C, m*CDH1*; 48.6°C) for 15 s and 72°C for 15 s for 40 cycles. Control bisulfite treated DNA was included for all PCR. MDA-MB-231 (human breast cancer), u*NFκB* reaction; HL60 (human promyelocytic leukemia), m*NFκB* reaction; AA8 (Chinese hamster ovary), u*TSLC1* and m*CDH1* reactions; NIH3T3 (mouse embryonic fibroblast), m*TSLC1* reaction; 410.4 (mouse mammary cancer) u*CDH1* reaction. DNA of these cell lines used as controls were obtained from colleagues. Controls without DNA were performed for all PCR. PCR products were resolved on 3% agarose gels (Sigma). Gels were stained using ethidium bromide. Images were captured using a MultiImage Light Cabinet camera with ChemiImager 4400 software (Alpha Innotech Corporation, San Leandro, CA). Two technical replicates were performed for each sample.

Bisulfite sequencing:

Promoter methylation of *NFκB* was further studied by bisulfite sequencing. Primers were generated from the genomic sequence for the promoter region of human *NFκB* p105 [140]. Each PCR reaction was performed in a total volume of 20 μl under the following conditions: RNase-free water using 160 ng of bisulfite treated DNA, 10 μl HotStarTaq Plus Master Mix, 10 pmol of the *NFκB* primers (forward; 5'-AAG TAG TTT AGA TGT TAG TGA ATG-3', reverse; 5'-AAA CTC TAA CTT CCT AAC AAA AC-3'). PCR cycling conditions were 95°C for 15 s, annealing temperatures 55°C for 15 s and 72°C for 15 s for 40 cycles. PCR products were resolved on 3% agarose gels to confirm reaction quality. Gels were stained using ethidium bromide and images were digitally captured. For sequencing, the PCR products were treated with ExoSAP-IT (USB, Cleveland, OH) and bisulfite sequencing was performed at the Institute for Genome Sciences, University of Maryland Biopark. Three technical replicates were performed.

Repeat element methylation:

DNA methylation of LINE-1 and Alu repeat elements was evaluated by combined bisulfite restriction analysis (COBRA) [143]. For analysis of LINE-1 a 50 μl PCR was carried out in RNase-free water, 25 μl HotStarTaq Plus Master Mix, 100 picomoles of each PCR primer (forward; 5'-TTG AGT TGT GGT GGG TTT TAT TTA G-3', reverse; 5'-TCA TCT CAC TAA AAA ATA CCA AAC A-3') and 100 ng of bisulfite-treated genomic DNA. PCR cycling conditions were 95°C for 30 s, 50°C for 30 s and 72°C for 60 s for 35 cycles. The final PCR product was digested with 10 U of HinfI restriction enzyme (Fermentas, Glen Burnie, MD). The digested PCR products were separated by

electrophoresis on 2.0% Metaphor high-resolution agarose gels (Lonza, Rockland, ME). For analysis of Alu elements a 50 μl PCR was carried out in RNase-free water, 25 μl HotStarTaq Plus Master Mix, 50 pmol of forward primer (5'-GAT CTT TTT ATT AAA AAT ATA AAA ATT AGT-3'), 50 pmol of reverse primer (5'-GAT CCC AAA CTA AAA TAC AAT AA-3'), and 100 ng of bisulfite-treated genomic DNA. PCR cycling conditions were 96°C for 90 s, 43°C for 60 s and 72°C for 120 s for 35 cycles. The PCR product was then digested with 10 U of MboI (Fermentas). The digested PCR product was then separated by high-resolution agarose gel electrophoresis (2.5% Metaphor agarose, Lonza). Gels were stained using ethidium bromide, images were digitally captured and the intensity of bands on the gel was quantified using Quantity One software (BioRad, Hercules, CA). The optical densities were used to calculate the percent of the total repetitive element DNA that is methylated and the percent repetitive element DNA that is unmethylated. A total of four technical replicates were performed.

The restriction enzymes used, MboI and HinfI, both have cytosine in their cut site, therefore only methylated cytosines will be cut at these intact restriction sites. After gel electrophoresis, the top uncut band represents unmethylated or mutated sequences and the lower, cut bands represent methylated repeat elements. For in-depth description of this assay please refer to the method paper [143].

Global DNA methylation:

Global DNA methylation was evaluated by methylation-sensitive arbitrarily primed PCR (MSAP-PCR) [144]. Restriction enzyme digestion of 2 μg of genomic DNA was performed by using either 20 units of RsaI, 20 units each of RsaI and methylation-

sensitive restriction enzyme HpaII, or 20 units each of RsaI and methylation-sensitive restriction enzyme MspI at 37°C for 16 h. Restriction digested DNA was amplified using arbitrarily primed PCR with a single primer (MLG2: 5'-AAC CCT CAC CCT AAC CCC GG-3'). PCR reactions were performed in a total volume of 50 μl under the following conditions: RNase-free water, 25 μl HotStarTaq Plus Master Mix, 50 pmol of the MLG2 primer and 200 ng of genomic DNA. Five cycles at low-stringency conditions of 94°C for 30 s, 40°C for 60 s, 72°C for 90 s were done before increasing the stringency of the PCR to 94°C for 15 s, 55°C for 15 s, 72°C for 60 s for another 30 cycles. PCR products were resolved on high-resolution 1.8% Metaphor agarose gels (Lonza). Gels were stained using ethidium bromide. Images were digitally captured and the intensity of bands on the gel was quantified using Quantity One. Four technical replicates were performed.

The RsaI restriction enzyme was used to generate smaller fragments of DNA and reduce the number potential artifacts that might be amplified in the arbitrarily primed PCR. HpaII does not cut DNA if the internal cytosine of its restriction site (C*C*GG) is methylated and therefore the bands generated in the PCR of DNA digested by RsaI+HpaII lane are methylated at the internal cytosine. MspI is unable to cut DNA when the external cytosine (*C*CGG) is methylated and so the bands generated in the PCR of DNA digested by RsaI+MspI are methylated at the external cytosine. All the restriction enzymes were titrated and the concentrations were chosen in excess to ensure complete digestion for all reactions. Each new lot of enzyme was tested for consistent activity and result as compared to the previous lot. The MLG2 primer was designed with a 3' end complementary to the recognition sequence of the HpaII and MspI cut site,

CCGG. Thus, whenever the restriction enzymes are unable to digest the DNA, it is amplified and a band is observed on the gel. An increase in band intensity indicates an increase in methylation. Band intensity was measured to numerically determine the change in DNA methylation. For the HpaII and the MspI lane, eleven and nine bands were analyzed for each sample, respectively. The mean percent methylation for all bands from each dose group was normalized to the corresponding mean percent methylation for all bands from sham-irradiated controls.

The bands observed on the MSAP-PCR gels were cut out and the DNA fragments purified from the agarose using the MinElute Gel Extraction Kit (Qiagen). These PCR products were sequenced at the Biopolymer-Genomics Core (University of Maryland School of Medicine) using the MLG2 primer. The sequences were identified using National Center for Biotechnology Information (NCBI) blasts**.**

RNA isolation and miRNA analysis:

Total RNA was extracted from sham irradiated control, Fe ion, and x-ray irradiated GM10115 cells at 16 - 20 population doublings post exposure using the miRNeasy Mini Kit (Qiagen) following kit procedures. The extracted RNA was quantified using a NanoDrop ND-1000 spectrophotometer (NanoDrop Technologies, Wilmington, DE), and immediately stored at -80°C until analysis.

MiRNA microarray analysis of total RNA (5 μg) was performed by LC Sciences LLC (Houston, TX). Quality control for the integrity of total RNA, enrichment of miRNA from total RNA, labeling, hybridization to μParaflo® microfluidics chip and scanning were performed using miRHuman/Mouse/Chinese Hamster miRNA array chips,

based on Sanger miR-Base Release 12.0. Preliminary statistical analyses were performed on raw data normalized by the Locally-Weighted Regression (LOWESS) method on the background-subtracted data. Student's t-tests were then performed to identify differences in miRNA expression. Two technical replicates were performed.

Prediction of miRNA targets:

Candidate miRNA, that changed ≥ 1.5-fold with a microarray intensity signal ≥ 100 and p-value ≤ 0.05, were picked for target prediction. Four different computational programs, TargetScan [145], PicTar [146], MicroRNA.org [147], MicroCosm (miRBase) [148-150] were used to predict miRNA targets. Targets were merged across the four databases using the bioinformatics resource manager program version 2.1 and overlapping targets in all databases were subject to the Database for Annotation, Visualization and Integrated Discovery (DAVID) [151, 152] pathway analysis. DAVID analysis was performed based on gene ontology GOTERM BP 3, 4, and 5. Pathways were identified using the Functional Annotation Clustering feature (high classification stringency) and those with p-value ≤ 0.05.

qRT-PCR analysis of miRNA:

The miRNA expression profiles obtained from the microarray data were validated using qRT-PCR. Total RNA used for the microarray analysis was reverse transcribed to cDNA template and TaqMan miRNA assay was performed in triplicate by LC Sciences. The hsa-let-7a miRNA, which was expressed equally in all the samples on the microarray, was used as an internal control. Among the candidate miRNA identified by the array,

those with an intensity signal ≥ 500 were validated with qRT-PCR.

Statistical analyses:

Means and standard errors were calculated for all data points from two - four technical replicates. The means were compared between samples by Student's t-test analysis using the StatPlus Mac software package (AnalystSoft, Vancouver, BC). P-values ≤ 0.05 were considered statistically significant.

Results

Clonogenic cell survival

The initial direct effect of irradiation on cell survival was measured by clonogenic cell survival. A statistically significant dose-dependent decrease in surviving fraction was observed with increasing doses of radiation (Figure 2.2A). Immediate effects of radiation exposure on cell killing were higher with high LET Fe ions versus low LET x-ray radiation exposure. At the same 1Gy dose, high LET irradiation induced almost two times more cell killing than low LET irradiation ($p = 0.01$). RBE for cell killing was determined using these data. Similar amounts of cell killing were observed after 0.5Gy and 2Gy of x-rays and 0.1Gy and 1Gy of Fe ions, respectively. The delayed effects experiments, including cytogenetics, DNA methylation and miRNA expression, were performed using doses of similar RBE for cell killing for the two types of radiation.

Micronucleus Analysis

The initial direct effects of low and high LET irradiation on chromosomal integrity were measured by the frequency of micronucleus formation [137]. A statistically significant dose-dependent increase in percent micronuclei was observed after either x-ray or Fe ion irradiations (Figure 2.2B). Immediate effects of radiation exposure on chromosomal integrity were higher with high LET as compared to low LET radiation exposure. At the same doses, 1Gy of high LET irradiation induced three times more micronuclei than 1Gy of low LET irradiation ($p = 0.03$). Comparing micronucleus induction based on the RBE established for cell killing, there was no significant difference in micronucleus induction between 0.5Gy of x-rays and 0.1Gy of Fe ions. However, 1Gy of Fe ions induced a significant increase in percent micronuclei relative to 2Gy of x-rays ($p = 0.03$).

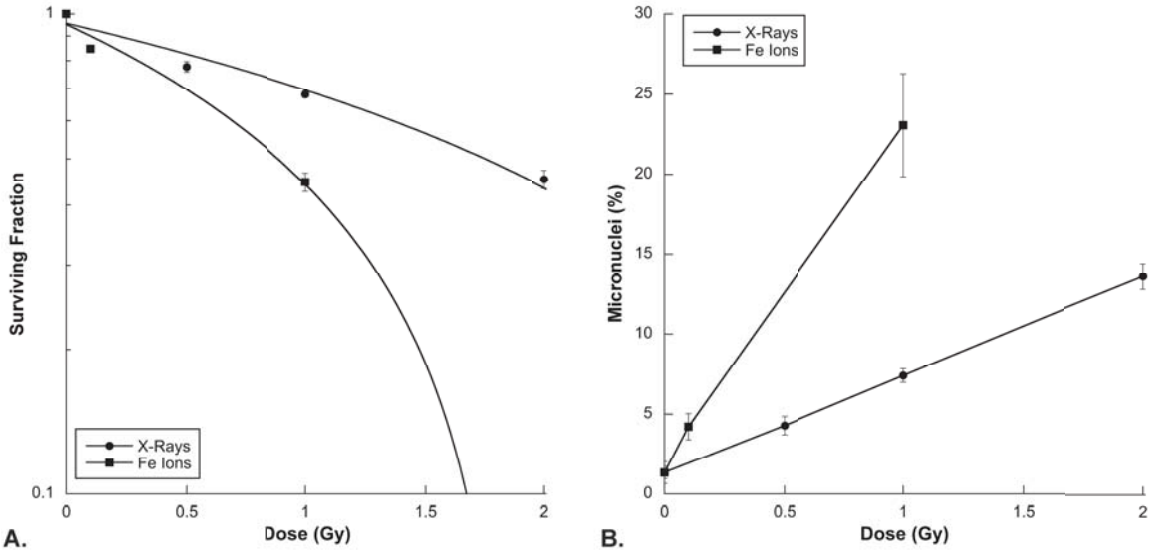

Figure 2.2. Immediate effects of low (x-rays) and high LET (Fe ions) radiation on chromosomal integrity and cell survival. (A) Surviving fraction of GM10115 cells versus doses of radiation. RBE of the doses used is determined based on clonogenic cell survival. (B) Percent micronucleus induction in binucleated GM10115 cells versus doses of radiation.

Fluorescence in situ hybridization

At 16 - 20 population doublings post-irradiation clonally expanded cells obtained from unirradiated control and irradiated cells were tested for chromosomal instability using FISH for human chromosome 4. Following x-irradiation, two, four, and six clones were evaluated for the 0Gy, 0.5Gy and 2Gy groups, respectively. Following Fe ion irradiation, two, four, and six clones were evaluated for the 0Gy, 0.1Gy and 1Gy groups, respectively. No chromosomally unstable clones were identified for any experimental group (data not shown).

Specific Locus Methylation

Promoter methylation of the *NFκB*, *TSLC1* and *CDH1* genes was studied using MSP assay [139]. The *NFκB* locus was chosen since changes in its expression have been linked to cancer and it is also involved in cellular responses to irradiation [153, 154]. It has also been identified as an important gene candidate that could be involved in RIGI [48]. Promoter regions of tumor-suppressor genes including *TSLC1*, *CDH1* are hypermethylated in cancer [155, 156]. Since radiation exposure can lead to cancer, our goal was to see if low and high LET irradiations at these doses lead to changes in promoter methylation. At 16 - 20 population doublings after low or high LET irradiations, no changes in DNA methylation at the CpG sites analyzed for the promoter regions of *NFκB* (four CpG), *TSLC1* (three CpG) and *CDH1* (nine CpG) were observed (Figure 2.3).

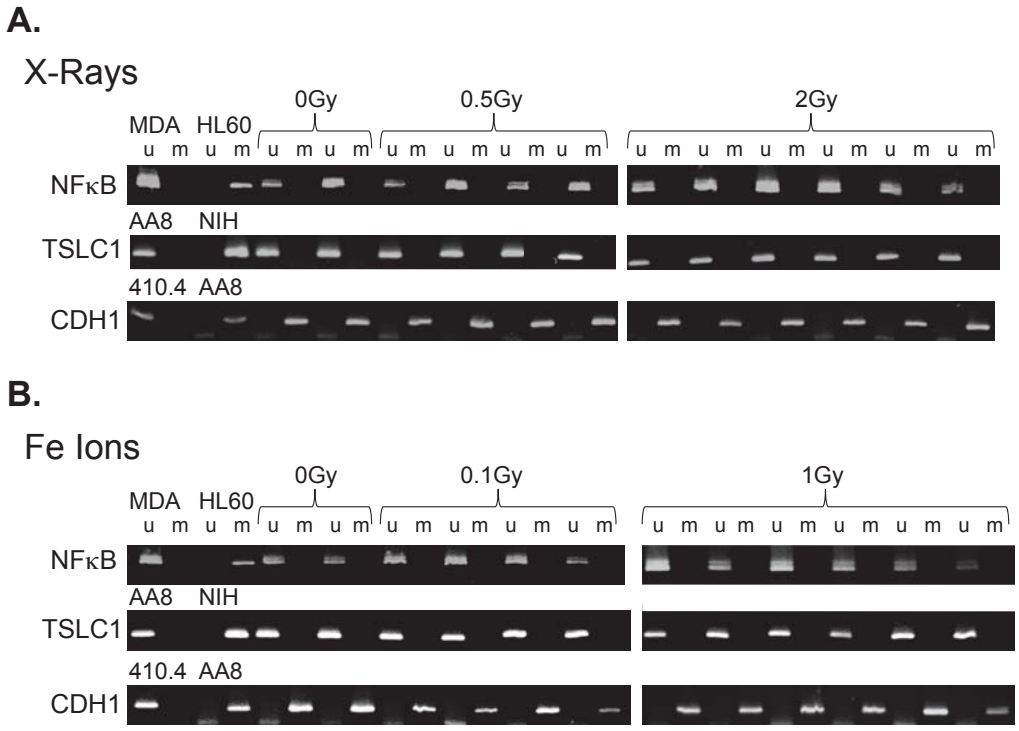

Figure 2.3. Methylation specific PCR assay for the methylation status of the promoter regions of *TSLC1*, *CDH1* and *NFκB*. (A) Methylation status of the clones observed after irradiation of x-rays and (B) Fe ions. For each radiation experiment, two clones were obtained from sham-irradiated cells, four clones from low dose and six clones from high dose irradiated cells. The lanes marked with 'u' signify PCR products using primers specific to unmethylated promoter sequence and those marked 'm' signify PCR products using primers specific to methylated promoter sequence. MDA (MDA-MB-231), positive control for u*NFκB*. HL60, positive control for m*NFκB*. AA8, positive control for u*TSLC1* and m*CDH1*. NIH (NIH3T3), positive control for m*TSLC1*. 410.4, positive control for u*CDH1*.

Bisulfite sequencing

Aberrant expression of *NFκB* has been shown to be potentially involved in RIGI [48], therefore its promoter methylation was studied more deeply using bisulfite sequencing (Figure 2.4). Within the *NFκB* promoter region twenty CpG sites were sequenced for each clone; control, low LET or high LET irradiated. The first two CpG sites were generally methylated for all clones irrespective of experimental group. The last two CpG sites did not sequence accurately due to their proximity to the primer binding site. The remaining sixteen CpG were unmethylated and no differences were observed among clones. These bisulfite sequencing results also serve as confirmation of the results obtained in the *NFκB* MSP assay.

A.

5'-
taaaatatatatttcggctcaagctttcttatgtggggaggtaatccacccgaagtatccccagcctgtacctaatacagtgcccagcacta
aagcagctcagatgccagtgaatggtggccactgggaggcctgtcagtgggtgccagtagcggtctcttcagagaaaaagaaaac
tcccctctgccagatcagtattttatgagctgtgaaccaaaaccattgctaccaccatcactataattctatcacagtaattatcataaggcct
aacaatgccttgtagatgaacattctgagtaactgctctataaccaggagatttaagaccgcaccaaaaaccagtagagggttatacttta
ctgggcacaagtcgtttatgataacgaaattgtagtttaatctgtgaagagatgtgaatgtaactgagacacgcttaaatggaatatacag
atgagctttatttttatatctggcatgcttggatccatgccgaccctccagctgctcgggcctgccttagggctatggaccgcatgactctatc
agcggcactgccaccgccgccgcctccgtgctgcctgcgttcccgaccattgggccggcaggcgcttcctgggggcttccctaccgg
ctccagcccttgggattcgggagc**gccctgctaggaagccagagccc**cgcaggggccgc-3'

B.

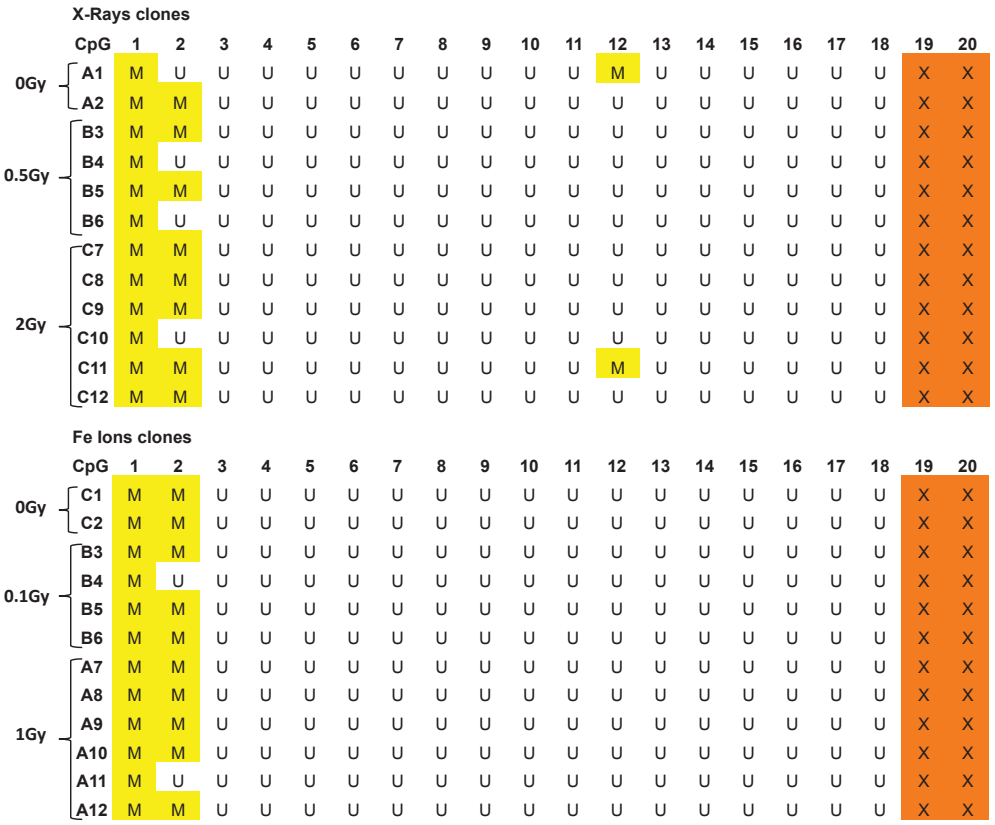

Figure 2.4. *NFκB* bisulfite sequencing of x-rays and Fe ions clones. (A) Genomic sequence of *NFκB* promoter region. The binding regions of bisulfite sequencing forward and reverse primers are bold and underlined. The twenty CpG sites detected in the sequencing are highlighted in yellow. (B) The methylation status of the twenty CpG sites is shown. The first two CpG sites were generally methylated for all clones irrespective of experimental group. The last two CpG sites did not sequence accurately due to their proximity to the primer binding site. The remaining sixteen CpG were mainly unmethylated and no differences were observed among clones. Methylated CpG sites are highlighted in yellow. Orange highlighted CpG sites did not sequence accurately.

LINE-1 and Alu Methylation

DNA methylation of LINE-1 and Alu repeat elements was evaluated by COBRA [143]. The assay was validated using DNA from DAC-treated cells. The validation for LINE-1 elements was performed using both human (RKO) and hamster (AA8) cells in addition to GM10115 cells, since the GM10115 cells are human/hamster hybrids. DAC treatment of RKO and GM10115 cells resulted in 21.8% and 2.5% decreases in LINE-1 methylation, respectively (RKO: $p = 0.007$, GM10115: $p = 0.004$). Five digestion fragments were quantified for methylation analysis. Four were of human origin and the extra band observed in GM10115 cells was confirmed to be of hamster origin with the use of the AA8 (hamster) cell line. Validation of Alu elements showed 4.2% and 2.2% decreases in methylation after DAC treatment of RKO and GM10115 cells, respectively (RKO: $p = 0.003$, GM10115: $p = 0.007$). No Alu band was observed for the AA8 hamster cell line since Alu elements are specifically of human origin.

The COBRA assay was performed on low and high LET clones. For the LINE-1 elements, hypomethylation was observed at high doses of both low and high LET radiation relative to controls (2Gy: $p = 0.05$, 1Gy: $p = 0.004$; Figure 2.5A). While hypermethylation ($p = 0.05$) was observed after 0.5Gy of low LET radiation, there was no change in LINE-1 methylation at 0.1Gy of high LET radiation relative to controls. In both low and high LET irradiations, when comparing the two doses for each, the changes in DNA methylation were significantly different suggesting a variation in response based on dose (0.5Gy vs 2Gy $p = 0.02$, 0.1Gy vs 1Gy $p = 0.005$, respectively).

Hypomethylation of Alu elements was observed for the high doses of both low and high LET clones relative to controls (2Gy: $p = 0.02$, 1Gy: $p = 0.03$; Figure 2.5B).

While a trend for hypomethylation was observed after 0.5Gy of low LET radiation, there was no change in Alu methylation observed after 0.1Gy of high LET radiation when compared to unirradiated clones. When comparing the two doses for each radiation type, the observed changes in methylation were statistically different for only the high LET irradiation (0.1Gy vs 1Gy $p = 0.01$). However, when comparing doses at which RBE for cell killing is similar (0.5Gy x-rays vs 0.1Gy Fe ions, 2Gy x-rays vs 1Gy Fe ions), there was no statistically significant difference between the methylation changes.

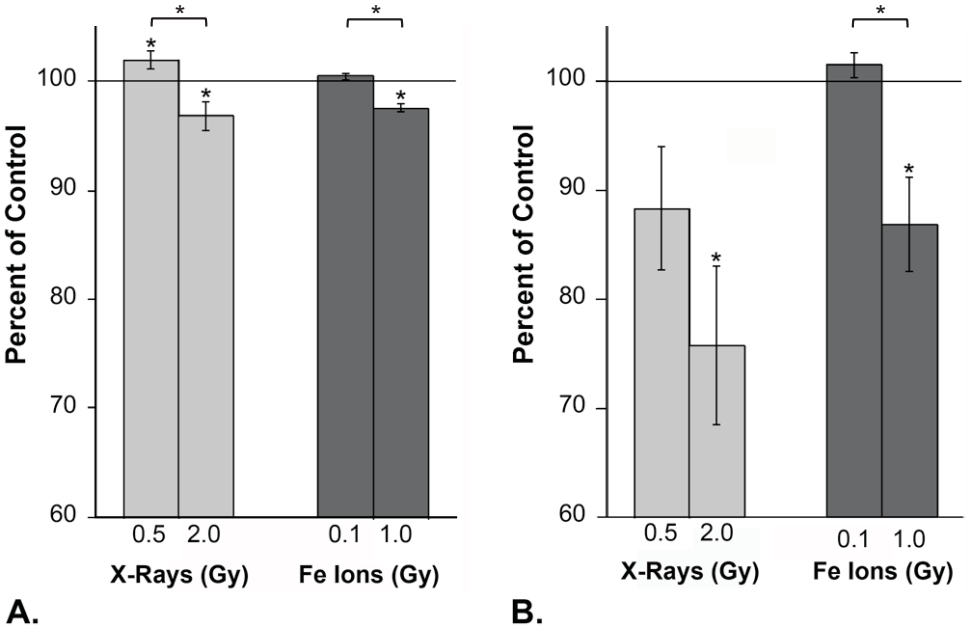

Figure 2.5. Changes in repeat element DNA methylation post-irradiation. (A) LINE-1 percent methylation and (B) Alu percent methylation of x-ray and Fe ion irradiated clones. For each dose the percent DNA methylation is normalized to control (mean value of two clones). The data at low doses (0.5Gy x-rays or 0.1Gy Fe ions) represent the mean value of four clones and at high doses (2Gy x-rays or 1Gy Fe ions) the mean value of six clones. Error bars indicate mean +/- SEM. * $p \leq 0.05$ versus sham-irradiated control or otherwise indicated comparisons, Student's t-test. Changes in percent methylation compared to control are LINE-1: 1.95, -3.22, 0.40, -2.45 and Alu: -11.70, -24.15, 1.42, -13.16 for LINE-1: 0.5Gy, 2Gy, 0.1Gy, 1Gy and Alu: 0.5Gy, 2Gy, 0.1Gy, 1Gy, respectively. The raw mean numbers are LINE-1 x-rays: 0Gy = 68.6, 0.5Gy = 69.9, 2Gy = 66.4; LINE-1 Fe ions: 0Gy = 69.2, 0.1Gy = 69.5, 1Gy = 67.5; Alu x-rays: 0Gy = 17.8, 0.5Gy = 15.8, 2Gy = 13.5; and Alu Fe ions: 0Gy = 22.1, 0.1Gy = 22.4, 1Gy = 19.2.

Global DNA Methylation

Global DNA methylation was evaluated by MSAP-PCR [144]. For all clones, methylation at the internal cytosine (HpaII; CpG) was evaluated for eleven bands or cytosine residues and methylation at the external cytosine (MspI; cytosine-phosphate-cytosine (CpC)) was evaluated for nine bands or cytosine residues (Figure 2.6).

At the CpG sites, statistically significant hypermethylation of bands #1, 2, 5, 6, 9 and 11 was observed after 0.5Gy of low LET irradiation ($p = 0.03$, 0.004, 0.03, 0.03, 0.003, 0.03, respectively; Figure 2.7A). There was no statistically significant change in methylation of bands after 2Gy of low LET irradiation. The mean methylation of all these bands together suggested global hypermethylation at the CpG sites relative to controls after low LET irradiation. This hypermethylation was only statistically significant after 0.5Gy low LET irradiation ($p = 0.01$; Figure 2.8A). High LET irradiation resulted in statistically significant hypermethylation of bands #2 and 4 at the CpG sites after 0.1Gy ($p = 0.01$, 0.009, respectively), however, statistically significant hypomethylation of bands #4 and 11 after 1Gy ($p = 0.04$, 0.002, respectively; Figure 2.7B). Although not statistically significant, the mean methylation of all these bands together suggested high LET irradiation caused hypermethylation after 0.1Gy and hypomethylation after 1Gy irradiation at the CpG sites when compared to unirradiated controls (Figure 2.8A). In both low and high LET irradiations, when comparing the two doses for each, the changes in DNA methylation were significantly different suggesting a variation in response based on dose (0.5Gy vs 2Gy $p = 0.01$, 0.1Gy vs 1Gy $p = 0.001$, respectively).

At the CpC sites, statistically significant hypermethylation of band #8 was observed after 0.5Gy of low LET irradiation ($p = 0.03$), however, statistically significant hypomethylation of bands #5 and 8 after 1Gy ($p = 0.02$, 0.001, respectively; Figure 2.7C). The mean methylation of all these bands together suggested hypermethylation after low LET irradiation though not statistically significant (Figure 2.8B). High LET irradiation resulted in statistically significant hypomethylation of bands #7, 8 and 9 at the CpC sites after 0.1Gy ($p =0.02$, 0.01, 0.02, respectively), and statistically significant hypomethylation of bands #5, 6, 7, 8 and 9 after 1Gy ($p = 0.03$, 0.03, 0.02, 0.002, 0.03, respectively; Figure 2.7D). The mean methylation of all these bands together suggested high LET irradiation caused hypomethylation after 0.1Gy and 1Gy irradiations at the CpC sites when compared to unirradiated controls (Figure 2.8B). However, statistically significant results were observed only after 1Gy of high LET irradiation ($p = 0.03$). There was no statistically significant difference between the two doses for either low or high LET irradiations. When comparing doses at which RBE for cell killing is similar, there was no statistically significant difference between the methylation changes of both CpG and CpC sites (0.5Gy x-rays vs 0.1Gy Fe ions, 2Gy x-rays vs 1Gy Fe ions).

The quantitated eleven amplified DNA bands from the HpaII PCR and the nine amplified DNA bands from the MspI PCR were also isolated and sequenced (Figure 2.6). Two of the HpaII sequences (bands #4 and 10) were identified as CpG islands and one of the MspI sequences (band #9) was identified as a *protein tyrosine phosphatase receptor type f (PTPR-F)* promoter sequence (Figures 2.9, 2.10 and 2.11). The remaining seventeen sequences were unknown.

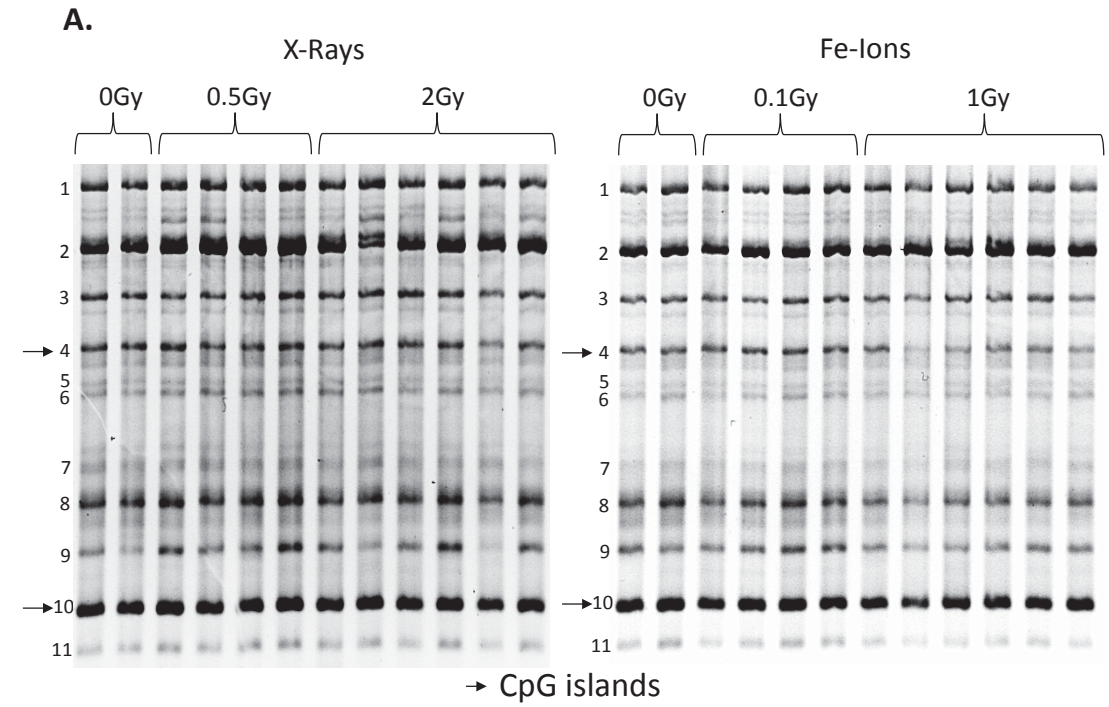
A.
X-Rays
Fe-Ions
0Gy
0.5Gy
2Gy
0Gy
0.1Gy
1Gy
1
2
3
4
5
6
7
8
9
10
11
CpG islands

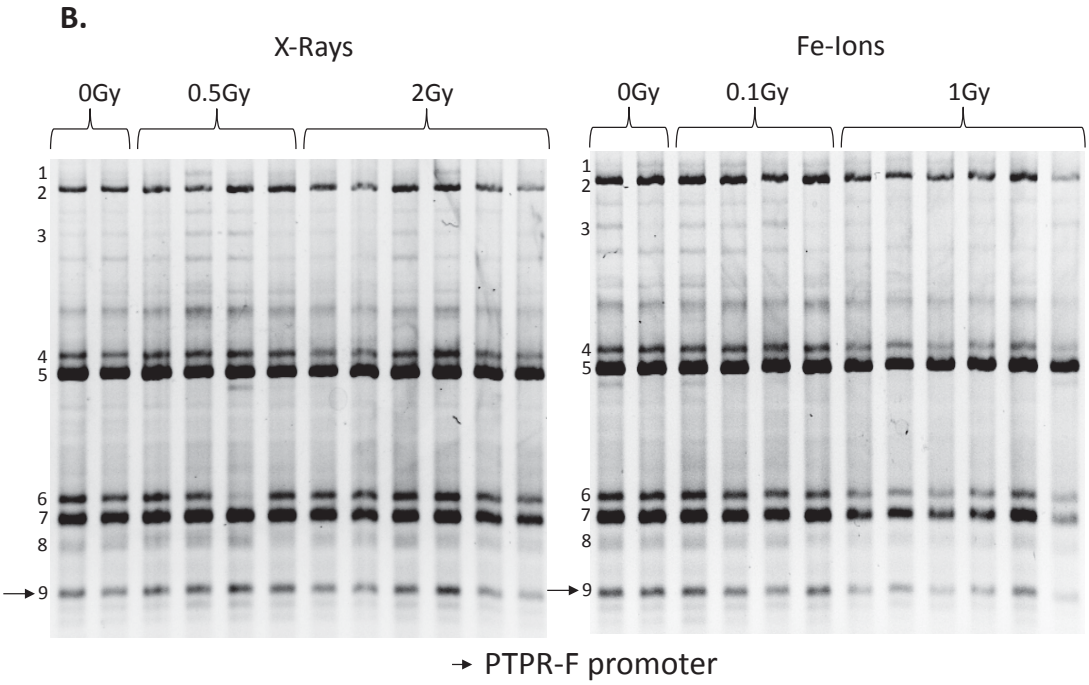
B.
X-Rays
Fe-Ions
0Gy
0.5Gy
2Gy
0Gy
0.1Gy
1Gy
1
2
3
4
5
6
7
8
9
PTPR-F promoter

Figure 2.6. Agarose gel pictures of the MSAP assay in the x-ray and Fe ion irradiated clones. (A) Internal cytosine (CpG) methylation and (B) External cytosine (CpC) methylation of clones. For the internal and the external cytosine, eleven and nine bands were analyzed for each sample, respectively. An increase in band intensity indicates an increase in methylation. These bands were also sequenced. At CpG, two were identified to be CpG islands (band #4: ~490bp, band #10: ~175bp) and at CpC, one was identified to be *protein tyrosine phosphatase receptor type f* (PTPR-F) promoter (band #9: ~130bp).

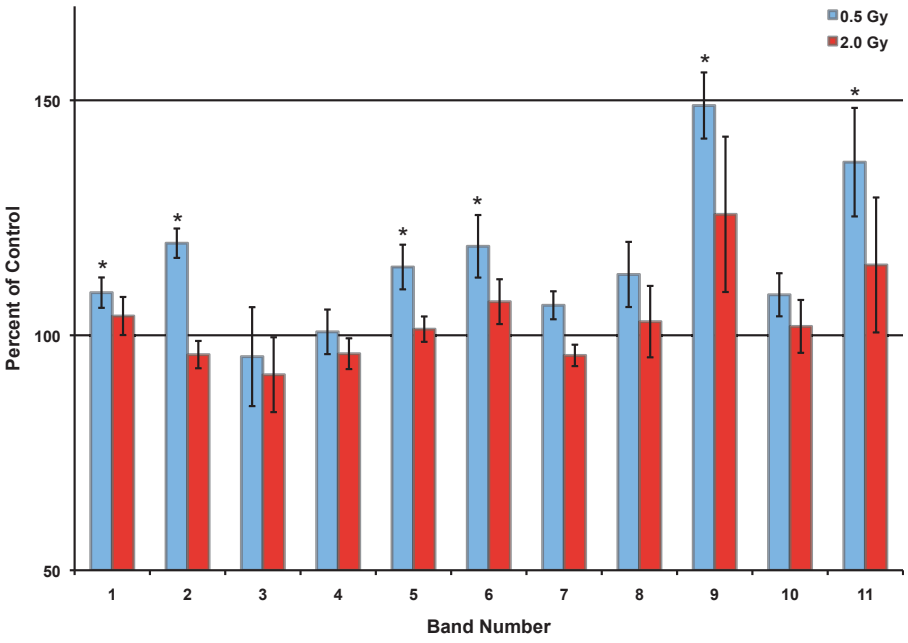
0.5 Gy
2.0 Gy
150
100
50
Percent of Control
1
2
3
4
5
6
7
8
9
10
11
Band Number

A.

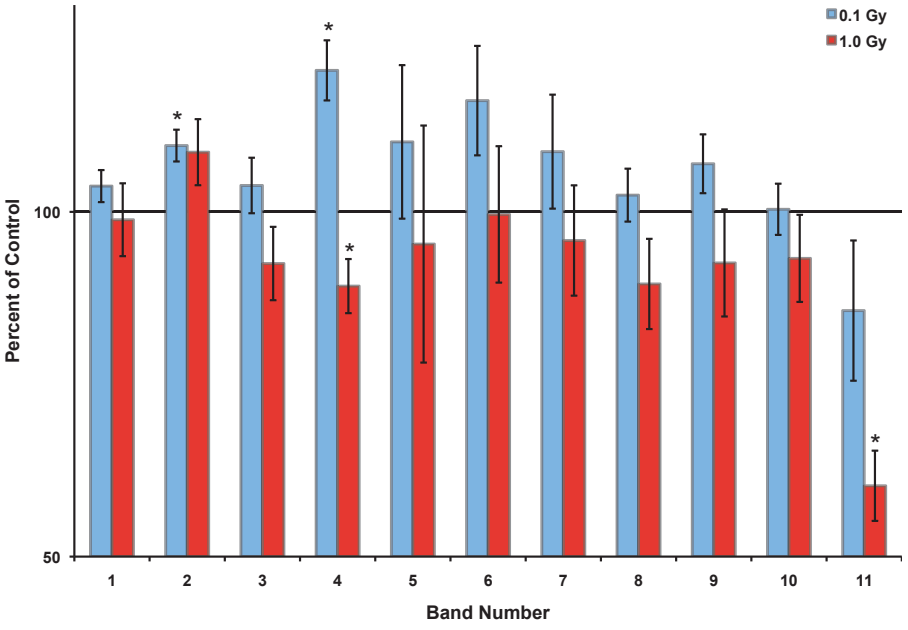
0.1 Gy
1.0 Gy
100
50
Percent of Control
1
2
3
4
5
6
7
8
9
10
11
Band Number

B.

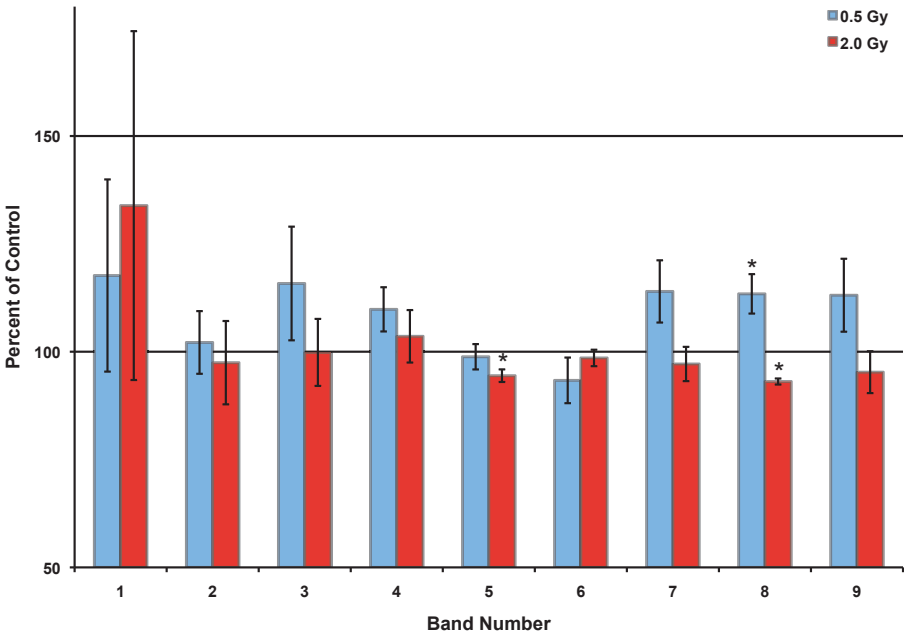
0.5 Gy
2.0 Gy
150
100
50
Percent of Control
1
2
3
4
5
6
7
8
9
Band Number

C.

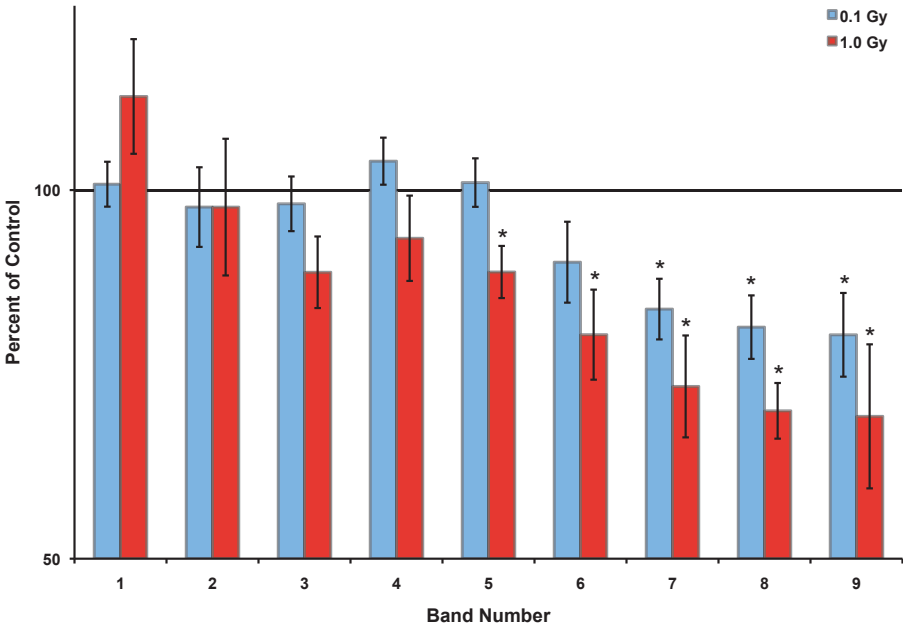
0.1 Gy
1.0 Gy
100
50
Percent of Control
1
2
3
4
5
6
7
8
9
Band Number

D.

Figure 2.7. Effects of irradiation on DNA methylation of each MSAP band observed. (A) Internal cytosine (CpG) percent methylation of x-ray clones. (B) CpG percent methylation of Fe ion clones. (C) External cytosine (CpC) percent methylation of x-ray clones. (D) CpC percent methylation of Fe ion clones. For the internal and the external cytosine, eleven and nine bands were analyzed for each sample, respectively. The mean percent methylation for each band from each dose group was normalized to the mean percent methylation of control. The control was determined as the mean value of two unirradiated clones. The data at low doses (0.5Gy x-rays or 0.1Gy Fe ions) represent the mean value of four clones and at high doses (2Gy x-rays or 1Gy Fe ions) the mean value of six clones. Error bars indicate mean +/- SEM. * $p \leq 0.05$ versus sham-irradiated control, Student's t-test. Changes in percent methylation compared to control and the raw mean numbers are shown on Table 2.1.

A.

Band	0 Gy	0.5 Gy	2.0 Gy	% Δ 0.5 Gy	% Δ 2.0 Gy
1	2088.4	2281.7	2188.1	9.07	4.10
2	4293.7	5140.6	4126.2	19.59	-4.11
3	1852.7	1758.8	1689.2	-4.54	-8.39
4	1866.8	1879.7	1799.8	0.73	-3.92
5	767.2	875.2	779.1	14.53	1.30
6	1061.2	1243.0	1121.0	18.93	7.15
7	1295.7	1378.2	1243.4	6.38	-4.28
8	2536.2	2816.4	2560.9	12.94	2.91
9	1245.2	1815.7	1478.3	48.89	25.74
10	4071.6	4375.1	4106.0	8.62	1.89
11	607.3	784.3	648.4	36.84	14.97

B.

Band	0 Gy	0.1 Gy	1.0 Gy	% Δ 0.1 Gy	% Δ 1.0 Gy
1	1790.3	1860.8	1770.2	3.74	1.14
2	3305.7	3626.7	3601.7	9.61	8.66
3	1467.1	1522.2	1352.6	3.83	-7.49
4	1497.1	1798.3	1334.9	20.52	-10.77
5	757.3	810.3	680.8	10.15	-4.67
6	1003.1	1158.4	991.5	16.14	-0.37
7	1064.0	1156.6	1025.7	8.73	-4.15
8	2424.2	2480.2	2150.8	2.43	-10.46
9	1401.5	1506.2	1290.2	6.98	-7.41
10	3464.9	3466.2	3185.0	0.37	-6.74
11	547.1	477.2	334.3	-14.32	-39.73

C.

Band	0 Gy	0.5 Gy	2.0 Gy	% Δ 0.5 Gy	% Δ 2.0 Gy
1	1029.3	977.5	967.0	17.66	33.87
2	2763.3	2727.9	2565.9	2.15	-2.54
3	1485.9	1593.7	1414.4	15.82	-0.16
4	2314.2	2517.3	2350.1	9.82	3.57
5	4958.2	4905.5	4673.3	-1.17	-5.56
6	2220.4	2108.4	2173.2	-6.64	-1.45
7	3333.7	3771.1	3198.5	13.98	-2.85
8	998.1	1131.8	929.7	13.41	-6.91
9	1295.0	1436.4	1207.1	13.09	-4.74

D.

Band	0 Gy	0.1 Gy	1.0 Gy	% Δ 0.1 Gy	% Δ 1.0 Gy
1	1046.5	1063.9	1104.9	0.80	12.70
2	2972.7	2878.1	2730.4	-2.31	-2.31
3	1636.1	1628.7	1444.2	-1.86	-11.15
4	2402.9	2483.2	2158.7	3.92	-6.54
5	4530.9	4549.9	3927.7	1.02	-11.11
6	2428.6	2205.6	1880.4	-9.78	-19.61
7	4000.4	3413.6	2819.8	-16.14	-26.63
8	1187.1	1006.5	821.2	-18.59	-29.94
9	1548.5	1295.7	1029.5	-19.63	-30.69

Table 2.1. Raw mean numbers and changes in percent methylation compared to control. (A) Internal cytosine (CpG) methylation of x-ray clones. (B) CpG methylation of Fe ion clones. (C) External cytosine (CpC) methylation of x-ray clones. (D) CpC methylation of Fe ion clones.

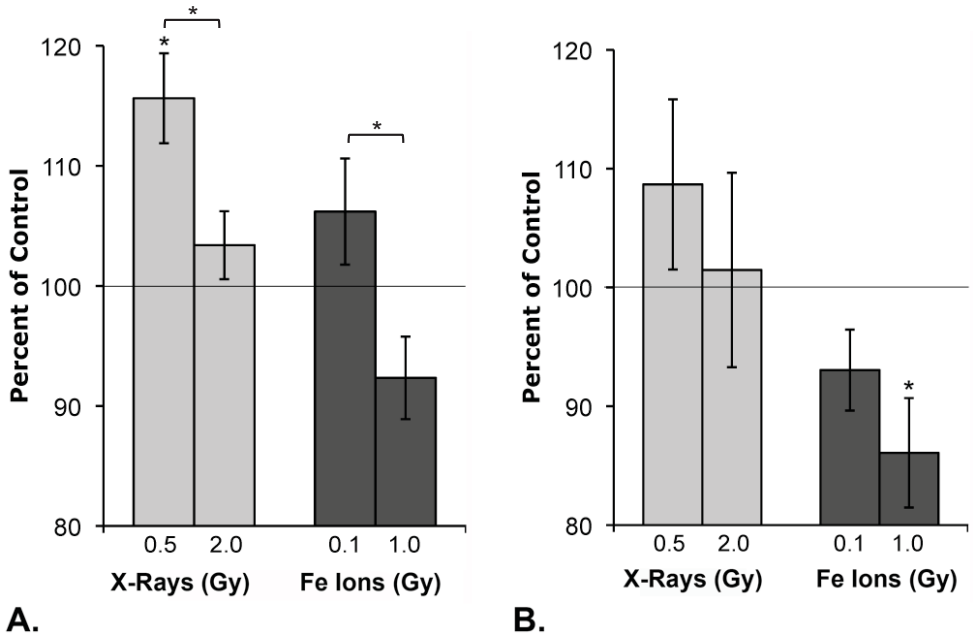

Figure 2.8. Effects of irradiation on global DNA methylation. (A) Internal cytosine (CpG) percent methylation and (B) External cytosine (CpC) percent methylation of x-ray and Fe ion clones. For the internal and the external cytosine, eleven and nine bands were analyzed for each sample, respectively. The mean percent methylation for all bands from each dose group was normalized to the mean percent methylation of control. The control was determined as the mean value of two unirradiated clones. The data at low doses (0.5Gy x-rays or 0.1Gy Fe ions) represent the mean value of four clones and at high doses (2Gy x-rays or 1Gy Fe ions) the mean value of six clones. Error bars indicate mean +/- SEM. * $p \leq 0.05$ versus sham-irradiated control or otherwise indicated comparisons, Student's t-test. Changes in percent methylation compared to control are CpG: 15.64, 3.40, 6.20, -7.66 and CpC: 8.68, 1.47, -6.95, -13.92 for CpG: 0.5Gy, 2Gy, 0.1Gy, 1Gy and CpC: 0.5Gy, 2Gy, 0.1Gy, 1Gy, respectively. The raw mean numbers are CpG x-rays: 0Gy = 1971.5, 0.5Gy = 2213.5, 2Gy = 1976.4; CpG Fe ions: 0Gy = 1702.0,

0.1Gy = 1805.7, 1Gy = 1610.7; CpC x-rays: 0Gy = 2266.5, 0.5Gy = 2352.2, 2Gy = 2164.4; and CpC Fe ions: 0Gy = 2417.1, 0.1Gy = 2280.6, 1Gy = 1990.8.

```
>emb|AL669824.13| Mouse DNA sequence from clone RP23-396G1 on chromosome 2 Contains
the 5' end of the gene for a novel protein containing HEAT
repeat domains, the gene for the orthologue of H. sapiens
chromosome 20 open reading frame 77 (C20orf77), the Tgm2 gene
for transglutaminase 2 C polypeptide and a CpG island, complete
sequence
Length=139077

 Score =  407 bits (450),  Expect = 3e-110
 Identities = 309/363 (86%), Gaps = 30/363 (8%)
 Strand=Plus/Plus

Query  1       TTTCTGTCCTTACTGTACCGTGTCTCAGGGCTTTGTTCCTTTTCACTGCCAAGCAATACT  60
               ||||||||||||||||| ||||| |||||||||| |||||||||||||||||| ||||||
Sbjct  102170  TTTCTGTCCTTACTGTAGCGTGTATCAGGGCTTCGTTCCTTTTCACTGCCAAGTAATACT  102229

Query  61      CCATGGTCCATACACCATAGTTTATTTGTCTC----TTAAGTTAATGGACAGGTGGGTTG  116
               ||||||||||||| |||||||||| |||||    |||||||| ||| ||||||||||||
Sbjct  102230  CCATGGTCCATACAGCATAGTTTATTGGTCTCTTAATTAAGTTAGTGGGCAGGTGGGTTG  102289

Query  117     CTTCCACTTTTTATCCAATGCGGATGACGGCACCGACAACATCATTGAACATCTTTCTGT  176
               ||| |||||||| ||    ||||||||||||||||||||||||| ||||||||||||||
Sbjct  102290  CTTTCACTTTTTCTCTCCTGCGGATGACGGCACCGACAACATCACTGAACATCTTTCTGT  102349

Query  177     GTGCACGCGTGCTTCCATTTCTCATGGATAAATATCTG---CAGGTGGAATAAGTGGGAA  233
               || |||| |||||     |||||||||||    | ||||   ||   |  |||||||  |||
Sbjct  102350  GTCCACGGGTGCT----TTTCTCATGGAT---TTTCTGGTTCA--TACAATAAGTACGAA  102400

Query  234     ATAGGGTAACTCCTTACTTATCACTCTGGTCTTCTGAGCCTTACTTTCTCAGCCCCCGGG  293
               |      |||||||||||||||| |||||||||||||| |||||||||         |
Sbjct  102401  A------AACTCCTTACTTATCACTTTGGTCTTCTGAGCCTGACTTTCTCA--------G  102446

Query  294     GCTACTAATGGGGAAACAATGTGTGGATAAACCCAAGGCTTCCAATGTCCAGGGTCCTGG  353
               |||||||||||||||||| ||||||||||||||||||||||||||||||||||||||||
Sbjct  102447  GCTACTAATGGGGAAACAGTGTGTGGATAAACCCAAGGCTTCCAATGTCCAGGGTCCTGG  102506

Query  354     AAA  356
               |||
Sbjct  102507  AAA  102509
```

```
101521 gagccgagat gacaggcatg tactaactaa gatgcttcat atttcttgct ataggacagc
101581 agctgaggac actgtctaga ggcagctcgt tagccatcgt gaagggtgta gatcaagtgt
101641 gacctgcagc tggctggaat ggacatggta ctgaacgatt aagggtttac gaaggcccca
101701 gggaccctct gactttaccc agtgggcagg agtacccgta atcacggaca actgtctaca
101761 gaatgcaccg taccctcaaa cggacggcac cacctcctct ctgctccctc atttcacaaa
101821 acaaagaagc cggaagggaa tgggatgttt actgagcatg cccaagcaaa tcccccagac
101881 agaacccagg ctgcggctct cagctcagcc ttctcccttc ccctgctcat actaatcatt
101941 tagatggctt tattgagata gaactcacat gccgtacaag ttagttcaat ggcctccagt
102001 ccagacaact gcacccatga agacagtcta cagaattccc ataatcccct agttccaact
102061 ccccatccct ccgcatctca aggcccaggc agccacctgt ctccttcctc tctataggtg
102121 catcacacat tctgacagct ttggtttctg ttttcttcca cttagcctat ttctgtcctt
102181 actgtagcgt gtatcagggc ttcgttcctt ttcactgcca agtaatactc catggtccat
102241 acagcatagt ttattggtct cttaattaag ttagtgggca ggtgggttgc tttcactttt
102301 tctctcctgc ggatgacggc accgacaaca tcactgaaca tctttctgtg tccacgggtg
102361 cttttctcat ggattttctg gttcatacaa taagtacgaa aaactcctta cttatcactt
102421 tggtcttctg agcctgactt tctcaggcta ctaatgggga aacagtgtgt ggataaaccc
102481 aaggcttcca atgtccaggg tcctggaaac aagcctgccc ctttcctgtc ctccccacat
102541 cctctcccct cctctcttta ggccattctt cagagagcgg tgggacaact cctctctaac
102601 tgctgggtct tgggtaagtc tgtgacctga gattccacgg ctctgacagt agctgtggat
102661 tcatgggaac agagttacag agcagctttt tgtgtctgta aattttctca acactcactg
102721 agagtctggt cctgttcaag gctggacacg acttccgtgg gcacagcttc tcattttgat
102781 ggcttatttc ttttcccact tgacacagaa cccacgggct tcatggtgtt catggtccct
```

Figure 2.9. The sequence of the HpaII band #4 - CpG island. The NCBI blast results are shown on the top. On the bottom, the sequence attained from sequencing is highlighted in pink. The rest of the sequence was obtained from the NCBI. The potential enzyme cut site, CCGG, is highlighted in yellow.

```
>emb|AL627074.11|  Mouse DNA sequence from clone RP23-465A17 on chromosome 3 Cont
a glycine cleavage system protein H (aminomethyl carrier)
(Gcsh) pseudogene, a lysosomal associated protein transmembrane
pseudogene, the 3' end of the Spata5 gene for spermatogenesis
associated 5, a px19-lie protein (PX19) pseudogene
and a CpG island, complete sequence
Length=177133

 Score =  183 bits (202),  Expect = 1e-43
 Identities = 103/104 (99%), Gaps = 0/104 (0%)
 Strand=Plus/Minus

Query  1       AGCTTTTCCAGAGAGGCATTTCCTTCCTTGAGGTCCTCACAGAAAAGTCTGCTTTATTTT  60
               ||||||||||||||||||||||||||||||||||||||||||||||||||||||||||||
Sbjct  162798  AGCTTTTCCAGAGAGGCATTTCCTTCCTTGAGGTCCTCACAGAAAAGTCTGCTTTATTTT  162739

Query  61      TAGTAATATCCTGGCTCCTGGTATTGTGTTTGTGCACATAATCC  104
               |||||||||||||||||||||||| ||||||||||||||||
Sbjct  162738  TAGTAATATCCTGGCTCCTGGTATTGTATTTGTGCACATAATCC  162695
```

```
162361 actgcacatt gtgcatcctg cgttccagca gcccagcctt cttggcttga cagtgtgctg
162421 caccctcctc ttctgattca ttttactctg atttcttcct ttcctgtgga cttaatcagc
162481 cagcccggca ctgaggacga attccattcg gaaacacact ggggaagaag gcaaaagaat
162541 tttggcaaaa tcacaaaatg ggaataataa tacagagatc ggaatggaac acccacccat
162601 ctcaccggg tgctgggaga attaattaac gtctgtaaag gcctttgagt tccttggggg
162661 gacgtgccac cagacagcta gcgttattgt ggaggatta tgtgcacaaa tacaatacca
162721 ggagccagga tattactaaa aataaagcag acttttctgt gaggacctca aggaaggaaa
162781 tgcctctctg gaaaagctta actctccttt aattccatcg cttgggctgc cggggacaga
162841 acagcaaagc cgagattcca ctgtgagaag aggattatgt tttctgagca ttgtcaaggt
162901 gctggggaac aaaacaaaat cgctggtttg ccaaaagaag gttatagtct ttggacaaga
162961 gattaagaga ctgtttggct agtgcacttc gtagcctgtc cgcaggggga aaaggcaaca
163021 ggaaagcaaa tgtttgtttg catttgaggg aaaagagttt tttacaaaac gggaagaaag
163081 ggaactgcct cagatgaaag ccgccatcag cagcggcgcc ctcagtaaat ctcccagaat
163141 tccccatgta ttttttcca tctgcgtgtc tctcaagcag acacttccaa atcctagatg
163201 gttaaaacaa ggaagaaccc tgcttgtgtt tacagaggaa gaccacgtta actttatacg
```

Figure 2.10. The sequence of the HpaII band #10 - CpG island. The NCBI blast results are shown on the top. On the bottom, the sequence attained from sequencing is highlighted in pink. The rest of the sequence was obtained from the NCBI. The potential enzyme cut site, CCGG, is highlighted in yellow.

```
>emb|AL807774.10| Mouse DNA sequence from clone RP23-198L2 on chromosome 4 Contains
the 5' end of the Ptprf gene for protein tyrosine phosphatase
receptor type F and a CpG island, complete sequence
Length=67374

 Score =  194 bits (214),  Expect = 1e-46
 Identities = 124/134 (93%), Gaps = 1/134 (0%)
 Strand=Plus/Minus

Query  1      GGAGACATCGCTTGGCCTTCACATATGAGCACAAGGACAATGCCTCCCCTCCAGGCCTAG  60
              ||||||||| ||||||||||||||||||||||||||||| ||||||||||||||||||| |
Sbjct  47636  GGAGACATCACTTGGCCTTCACATATGAGCACAAGGACA-TGCCTCCCCTCCAGGCCTCG  47578

Query  61     GAGCAGGGCAGCAGGGGCAGGTCCGCAAGGACCTTGTGCTCAGAGTTTGACAATGTGGCC  120
              ||||||||||||||||||||||| ||| |||||| ||||||||||||||||||| ||| |
Sbjct  47577  GAGCAGGGCAGCAGGGGCAGGTCTGCATGGACCCTGTGCTCAGAGTTTGACAATCTGGTC  47518

Query  121    TGAGCCCTGGCTTT  134
              |||| | |||||||
Sbjct  47517  TGAGACTTGGCTTT  47504
```

```
46741 agcggttaag agcactgact gctctttcag gggtcctgag ttcaattccc agcaaccaca
46801 tggtggctca caaccaacta taatggaatc cgatgccctc ttctggtgtg tctgaagata
46861 gctacaaggt actcatatac atttaattaa ttaatttaaa aaaacagtga agatattttt
46921 cccttctgtt cacaaggagc caccagatgt gaatgaccag gtcaagaaag tttccctcac
46981 cagggcttag gcagtcaccc tgcaatcttc ggtggtcttg gcatttatga atagagaagc
47041 ccacctgtct tttctgctca ccaccctgaa tgtcagtaat gtgaggttta tttggtggtc
47101 ctgtacctct gcccagttta gtggctgtga tactcacagg taggagggct gaagccccgc
47161 cccacccccg ccccctggct gaaggcggca gacccactca ctgctaaact agctaggctt
47221 ctgctttggg tcactcagac ctacattctg gggccaccac agccatctca ggctctcaaa
47281 ctattggtct ctgtcccatc tctcacctac tttttggccc ctatttggta tagtacatat
47341 gaaggctggg cagaagaaca ctgggacccc tatggtctaa tttcagaatg tatagcacct
47401 ggctgcccac aaactcaggg gaatgaaaca gaggctcagg ccctgaggcc acaggatgag
47461 agaacagtct tgggggggggg gactagatgg catatgaaga aataaagcca agtctcagac
47521 cagattgtca aactctgagc acagggtcca tgcagacctg cccctgctgc cctgctccga
47581 ggcctggagg ggaggcatgt ccttgtgctc atatgtgaag gccaagtgat gtctcctggc
47641 agcagtgctg tgtctgctgt gtcccagccc cagggtgcag ggtgagggaa gcgccagatg
47701 tcagttccca ctctctattc acccctttgtc cagatcctgg gcccactgga tgcccctcaa
47761 gttcatgacg tcagtacatc tcttagctgg ttgaaatcga attacatttc agcctgagtc
47821 cccaccccac caggtcagca gcagttctgt tatccctcac agctgccttt accctccct
47881 tgctgaaagt gcaagaattc tggggctttg cacagcccca aagttggtcc gtctgtgctc
47941 ctgagccttt cagggagagc tttaaacaga tactcgaaca gtggccatca ctgtaatggg
48001 gtatcccact atgcactgtc cacttctcca aggcctcact ttcccatcct cattcccct
48061 tcatcccagg ctctttctag gcagctccac ccttcacaaa gcttcagcct ttagtccttg
48121 gcgtggttcc ccctgcccac ccccccagcc accgacagct gctttccaag gtggtggggt
48181 agacagtgct gtttacctgc cctcccgcat gcctctgacg gacgtacgtc aagaagagct
48241 cagaagacac aatcaccagt tcgccttcct cccggtacag atgggagaga aaggctgagt
48301 cccttgaaca caaaagcctg gctaatgtct ctgcttcctt gccagtgagt cactgtggtg
48361 gagcatgata caggagctga tttctcaatg gaacaagcta atgatgactt cacctagca
48421 ggactcccta atgtccttat cgccaagtga agccacccac acctgctcct tcctgcccat
48481 ccccgtggtt tctaagggac tggaggttgc tgtccagcag atgctctgac ttcttcaagg
```

Figure 2.11. The sequence of the MspI band #9 - PTPR-F promoter. The NCBI blast results are shown on the top. On the bottom, the sequence attained from sequencing is highlighted in pink. The rest of the sequence was obtained from the NCBI. The potential enzyme cut sites CCTG and CAGG are highlighted in gray and green, respectively.

MiRNA

Microarrays were used to identify the miRNA differentially expressed between the irradiated groups and the unirradiated controls based on defined criteria ($p \leq 0.05$, signal ≥ 100, and fold change ≥ 1.5; Table 2.2). After low LET irradiations, six miRNA were differentially expressed compared to control (hsa-miR-1305, hsa-miR-1826, hsa-miR-720, mmu-miR-34c*, mmu-miR-680, mmu-miR-720). Only three miRNA, however, were changed after high LET irradiations compared to control (hsa-miR-107, hsa-miR-181d, mmu-miR-674). Among the candidate miRNA identified by the microarray, those with a signal equal to or above 500 were validated with qRT-PCR (Table 2.2). Mmu-miR-680 could not be validated at 0.5Gy (fold change = 1.19). MiRNA differentially expressed after high LET irradiations were not validated with qRT-PCR due to low intensity signal (<500). Final validation of these miRNA requires knockdown or overexpression analysis and eventually a biological readout.

	Fold Change Microarray		Fold Change qRT-PCR	
	0.5 Gy	2.0 Gy	0.5 Gy	2.0 Gy
miRNA				
hsa-miR-1826	-1.54	-2.38	-1.44	-2.42
mmu-miR-680	3.07	3.33	1.19	2.00

Table 2.2. MiRNA altered after x-ray irradiation, identified by microarray analysis and validated by qRT-PCR.

The gene targets for these miRNA were identified using four different databases and the merged list of gene targets was used for pathway analysis using the DAVID database. Two major pathways, including chromatin remodeling, and DNA methylation were identified with those miRNA differentially expressed after low LET irradiations relative to control ($p \leq 0.05$). Mmu-miR-680 had no known statistically significant pathways thought to contribute to RIGI but hsa-miR-1826 is involved in both chromatin remodeling and DNA methylation including DNMT1 (Table 2.3). The gene targets were not validated.

	Chromatin remodeling	DNA methylation
miRNA		
hsa-miR-1826	TBL1XR1, AEBP2, ING4, SATB2, BRCC3, HP1BP3, CREBBP, PHF17, WHSC1L1, SETD7, DNMT1, JMJD1C, HDAC9, SMC1A, BAZ2A	ATRX, ATF7IP, WHSC1L1, DNMT1, BAZ2A

Table 2.3. Target genes of altered miRNA and the functional pathways in which they are involved.

Discussion

Immediate effects of radiation exposure on chromosomal integrity and cell survival showed more damage with high LET versus low LET radiation exposure. At the same doses (1Gy), high LET irradiation induced three times more micronuclei and almost two times more cell killing than low LET irradiation. Based on cell killing, similar number of cells survived after 1Gy of high LET and 2Gy of low LET radiation, therefore high LET irradiation was able to elicit the same effects at much lower doses. To account for this difference, doses at similar RBE based on cell killing between low and high LET

radiation were used to study the changes in epigenetics. When the methylation changes for both repeat element and genome-wide DNA methylation were compared at doses that RBE for cell killing is similar, there was no statistically significant difference. Cell killing post-irradiation demonstrates a dose-dependent response analogous to the targeted effects of irradiation including DNA damage as observed by the micronucleus assay. However, non-targeted effects, such as epigenetics and RIGI, may not be dose, LET or RBE dependent.

In addition to radiation quality and radiation dose, dose rate also determines the RBE. Generally as the dose rate is lowered and the exposure time extended, the biological effect of a given dose is reduced. The effects of low LET irradiations are more dependent on dose rate than densely ionizing high LET irradiations. Dose rate effect has been shown for the induction of delayed micronuclei [157, 158]. Limoli et al. demonstrated the lack of dose rate effect in the induction of chromosomal aberrations [32, 159]. The difficulty in making a conclusion regarding radiation quality and dose rate effects on the generation of RIGI has been reviewed [160]. It has also been stated that the induction of RIGI after low LET irradiation is mostly dose dependent rather than dose rate [161]. Considering the non-targeted nature of changes in epigenetics, they may also not be dose rate dependent.

NFκB has been shown to be involved in cellular responses to radiation and cancer [153, 154]. In addition, previous studies in our lab have identified it as an important gene candidate potentially involved in RIGI [48]. *TSLC1* and *CDH1* genes also play a role in cancer progression and it has been shown that their promoter regions are hypermethylated in cancer cells [155, 156]. Since radiation exposure can lead to cancer, we measured the

promoter methylation of *NFκB, TSLC1 and CDH1* to determine if low and high LET irradiation cause alterations in DNA methylation of these promoter regions. At the doses examined and after 16 - 20 population doublings post-irradiation, neither low LET x-rays nor high LET Fe ions were capable of causing changes in DNA methylation at these promoter regions. These results were in agreement with unpublished data from the Baulch lab as they observed no change in *cyclin-dependent kinase inhibitor 2A* (*p16*) or *O^6-methylguanine-DNA methyltransferase* (*MGMT*) promoter methylation after both low LET x-ray and high LET Fe ion irradiations. Results were also in agreement with the observations of Kovalchuk et al. demonstrating a lack of change in *MGMT* promoter methylation following *in vivo* low LET x-ray irradiation of mice [103]. This same study by Kovalchuk et al., however, showed changes in *p16* promoter methylation in liver tissue *in vivo*. It is possible that our current study may be limited in observing such changes since an *in vitro* cell culture model was used. Endpoints observed in complex tissue systems or whole organisms could be different than those observed in cells *in vitro*. Also, methylation changes might occur at different promoter regions of different genes or such changes may be acquired at later post-irradiation times.

LINE-1 and Alu repeat elements comprise about 30 percent of the human genome and they are normally hypermethylated [162, 163]. Hypomethylation of these repeat elements can lead to genomic instability and cancer [164-166]. Both low and high LET radiation exposures resulted in hypomethylation of repeat elements LINE-1 and Alu, except for the hypermethylation of LINE-1 at 0.5Gy of low LET radiation relative to controls. These results are in agreement with the low LET radiation studies in the literature [167]. Unpublished data from the Baulch lab showed significant

hypomethylation of LINE-1 elements in the RKO cancer cell line following exposure to 1Gy of low LET x-rays. In the same study, hypomethylation of LINE-1 and Alu elements was observed in both RKO and AG01522D cell lines after 0.1 and 1Gy of high LET Fe ion irradiation while in our study we observed hypomethylation only at the higher doses. Radiation-induced hypermethylation of repeat elements is not commonly observed in the literature, however, unpublished data from the Baulch lab demonstrated hypermethylation in the AG01522D human diploid skin fibroblast cell line post 1Gy of low LET x-rays. Since any aberration in DNA methylation may be detrimental to the cell, the radiation-induced change itself may be more important than the direction of the change. While the differences in the cell lines could account for the different observations, the non-targeted nature of epigenetic changes could also account for the variability in observed responses. Epigenomic instability is a delayed, non-targeted effect of irradiation similar to genomic instability. Non-targeted effects occur at higher frequencies than expected from Poisson statistics of particle hits to surviving cell nuclei or from conventional gene mutation frequencies. Even for low LET radiation studies in the literature, there are many differences in terms of changes in methylation that may be due to radiation doses, dose rates, cell lines, *in vivo* vs *in vitro* or post-irradiation time points [132]. The changes in repeat element methylation observed in this assay are not large percent changes. However, the LINE-1 assay evaluates just two CpG sites and the Alu assay evaluates one CpG site. As a result, the changes in this assay may represent a large global change in methylation. Hypomethylation observed in the repeat elements could potentially lead to instability. However, FISH analysis suggested chromosomal stability in these clones, therefore, the methylation analyses suggest that the

hypomethylation observed might arise in the cell without initiating RIGI. It should be noted that in this study RIGI was based on the stability of chromosome 4 in the human/hamster cell line and even though it was found to be stable, other end points for genomic instability may be present and may reveal a long-term effect [6]. Since hypomethylation leads to genomic instability in cancer, even though RIGI is not observed in these clones, it could be that radiation-induced hypomethylation may possibly lead to RIGI at later times or in clones that were not investigated in this study.

In cancer cells, the general trend of genome-wide methylation is hypomethylation [168]. This is in reference to CpG methylation, as DNA is thought to be predominantly methylated at these sites. Numerous studies in the past and also more recently have identified methylation at non-CpG sites [51-53, 55, 56]. However, it is controversial as to whether or not it exists in mammalian somatic cells [134]. For example, Rein et al. [135] have stated that non-CpG methylation does not occur and those reported by Woodcock et al. may be an experimental artifact [54]. In our global DNA methylation assay, we measure both the CpG methylation (internal cytosine methylation) and non-CpG methylation (external cytosine methylation). Non-CpG methylation can occur at cytosine-phosphate-adenine (CpA), cytosine-phosphate-thymine (CpT), and CpC sites but with this assay we are only measuring CpC methylation. At the CpG site, 0.5Gy of low LET irradiation resulted in global hypermethylation and 1Gy of high LET irradiation resulted in a trend in global hypomethylation. At the CpC site, global hypomethylation after high LET irradiations were observed. However, the methylation status of the individual bands needs to be validated for direct evidence of CpC methylation. In terms of low LET radiation-induced global CpG methylation, both hyper and hypomethylation

have been shown [132]. After low LET ^{60}Co gamma-radiation, Kalinich et al. only observed hypomethylation, whereas, Kaup et al. observed both global hypomethylation and hypermethylation [97, 104]. Unpublished data from the Baulch lab observed hypomethylation after low LET x-rays and hypermethylation after high LET Fe ions irradiations. Even though the direction of methylation change between the studies are not always in agreement, the difference in the induction of methylation changes between low LET x-rays and high LET Fe ions are demonstrated in both of these studies. In terms of global non-CpG methylation, the literature provides no comparisons since non-CpG methylation post-irradiation has not been evaluated previously. The genomic regions that were measured to determine global DNA methylation were sequenced. Many sequences were unknown possibly due to the lack of a known complete hamster genome sequence. The sequences could also be repeat elements. A study using the same technique in human cell lines also could not identify sequences and those identified were mostly repeat elements [104]. This assay also suggests that methylation changes might arise in the cell without initiating RIGI. However, the methylation status of the sequences was not validated with bisulfite sequencing or any other method, therefore, strong conclusions are not possible at this point.

The different outcomes in epigenetic changes between low and high LET radiations have also been observed with miRNA results. MiRNA regulate a number of cellular pathways and deregulation of miRNA expression levels can lead to cancer [81, 82]. In terms of validated miRNA, while two were altered post-low LET irradiation, none was altered after high LET irradiation based on our criteria. A number of studies have shown changes in miRNA using different cell lines and doses of low LET

irradiations [132]. However, the changes in miRNA expression post-high LET irradiations have not been studied previously. Even though different miRNA have been identified, the non-validated functional roles of the miRNA are in agreement with many studies in the literature [132]. Low LET radiation exposed mouse embryonic stem cells showed alteration in the expression of miRNA that target genes involved in response to DNA damage [120]. Maes et al. observed alterations in miRNA expression in post low LET x-ray irradiated human fibroblasts and these miRNA target genes involved in radioresponsive mechanisms, such as cell cycle checkpoints and apoptosis [121]. The changes in these pathways induced by alterations in miRNA expression are those observed in cells with RIGI [132]. Alterations in the expression of miRNA and especially those involved in the pathways mentioned above have also been shown to be present in cancer cells [81]. The clones in this study are stable suggesting that the lack of changes in miRNA expression might be the reason behind the non-initiation of RIGI. The research thus far have not shown direct initiation of RIGI due to radiation-induced changes in miRNA expression, therefore, it could be that miRNA expression changes may not play a role in RIGI. Though further examination will help better determine the relationship between radiation-induced miRNA changes and RIGI.

This study shows that epigenetic changes including subtle alterations in DNA methylation and a few miRNA expression changes do occur both post low or high LET irradiations. Different doses and qualities (LET) of radiation can show different effects on the epigenetics of the cell. Differences in these epigenetic responses might be predicted, since the mechanisms of DNA damage induced by x-rays and Fe ions and DNA repair following irradiations are known to be different [169, 170]. Low LET

radiations, like x-rays, produce sparse ionizations within the irradiated cells while high LET radiations, like Fe ions, produce dense or clustered ionizations along their beam track. DNA damage induced by x-rays is mainly through indirect effects like oxidative stress while Fe ions induce direct DNA damage. DNA repair after high LET irradiations is much slower than after low LET irradiations [171]. In addition, the induction of oxidative stress by Fe ions is shown to be lower than x-rays [172]. Thus, oxidative stress plays a more significant role in inducing damage after x-ray exposure. Studies have shown reactive oxygen species induction of epigenetic changes [106-108]. Therefore, oxidative stress may be contributing to elevated levels of epigenetic changes after x-ray irradiations.

Our study is one of the few that has studied DNA methylation and miRNA expression changes after high LET irradiation. We observed clear LET and dose dependence of irradiation on cell killing and micronucleus induction, direct effects of irradiation. Using RBE equivalent doses for cell killing, we also observed differences in miRNA expression at delayed times post irradiation that were based on LET. A higher number of miRNA were altered after low LET x-ray exposure than after high LET Fe ion exposure and the magnitude of the changes observed following x-ray exposure suggested possible dose dependence. While our DNA methylation data also suggest possible dose dependence, LET dependence of radiation-induced changes in DNA methylation is less clear. The literature demonstrates that delayed non-targeted radiation effects including bystander effects and genomic instability are not always dose, dose rate, LET or RBE dependent [160]. Whether radiation-induced epigenetic changes are also independent of these factors remains to be clarified.

Chapter 3: EPIGENETIC ALTERATIONS IN RADIATION-INDUCED GENOMICALLY UNSTABLE CLONES

Abstract

Radiation-induced genomic instability (RIGI) is thought to be important in the process of carcinogenesis, however, the mechanism by which this occurs remains to be elucidated. Morgan and colleagues developed genomically unstable clones in which they studied the mechanism of RIGI. Radiation-induced mutations, double-strand breaks, or changes in messenger RNA (mRNA) levels alone could not account for the perpetuation of RIGI, therefore, epigenetics, including DNA methylation and microRNA (miRNA) expression, could be the missing link. This study tests the hypothesis that epigenetic aberrations are perpetuated in chromosomally unstable clones with RIGI. Stable and unstable clones were characterized based on chromosomal instability. The clones were evaluated for specific locus methylation of *nuclear factor-kappa B* (*NFκB*), *tumor suppressor in lung cancer 1* (*TSLC1*) and *cadherin 1* (*CDH1*) gene promoter regions, long interspersed nuclear element 1 (LINE-1) and Alu repeat element methylation, CpG and non-CpG global methylation, miRNA and gene expression levels. In stable clones, compared to

controls, only a few changes were observed in DNA methylation and in miRNA expression. In the unstable clones, alterations in repeat element and global DNA methylation and miRNA expression were observed. DNA methylation analyses predominantly showed hypomethylation, however hypermethylation was also observed. MiRNA with altered expression levels in unstable clones are involved in apoptosis and chromatin remodeling. This study shows that epigenetic alterations can be perpetuated in unstable clones with RIGI.

Introduction

Radiation-induced genomic instability (RIGI) is a delayed, long-lasting effect of ionizing radiation that manifests in the unirradiated progeny of irradiated cells as an increased heritable frequency of nuclear genetic alterations. RIGI is a non-targeted phenomenon that is thought to contribute to radiation carcinogenesis, however, the mechanisms underlying this process are poorly understood [1, 2]. What initiates RIGI and causes it to persist over time is still unknown, even after evaluating numerous endpoints including double-strand breaks, mutations, gene expression, disruption of mitochondrial processes, cell cycle arrest, and apoptotic cell death [132]. Potential mechanisms may involve epigenetic alterations, including changes in DNA methylation and microRNA (miRNA) expression. Epigenetic aberrations are observed following irradiation, associated with genomic instability, and found in cancer cells [132]. Therefore, we are testing the hypothesis that epigenetic aberrations are perpetuated in chromosomally unstable clones with RIGI.

In cancer cells, global hypomethylation can lead to the initiation of genomic instability [50]. Especially, hypomethylation of repeat elements, including long interspersed nuclear elements 1 (LINE-1) and Alu elements, can lead to chromosomal instability, translocations, and gene disruption caused by the reactivation of transposable DNA sequences [63]. In addition, hypermethylation of tumor-suppressor genes can lead to their transcription inactivation and oncogene transcription can be activated due to hypermethylation of their gene promoters.

MiRNA expression plays an important role in the regulation of cellular pathways including cellular proliferation, differentiation, and apoptosis [81]. Deregulation of miRNA synthesis or expression levels can result in disruption of these cellular pathways that could lead to carcinogenesis [82]. Certain miRNA, such as miR-34c, have also been shown to be involved in the control of genomic instability [173].

These epigenetic changes could be missing links in the mechanism of RIGI [132]. Therefore, it is important to understand the changes in epigenetic profiles in unstable clones with RIGI. To date, studies have predominantly evaluated radiation-induced epigenetic changes, while little is known regarding epigenetic aberrations in the progeny of the irradiated cells with RIGI.

Only one study has directly correlated RIGI with epigenetic changes [104]. In HPV-G cells, following exposure to ^{60}Co gamma-radiation, RIGI manifested as reproductive cell death, reduced cloning efficiency at successive passages, increased apoptosis, and an increased proportion of chromosomally aberrant cells at 20 passages post-irradiation. In these cells, RIGI was shown to be predominantly associated with DNA hypermethlyation of mostly repeat elements and pericentromeric spermidine N1-

acetyltransferase 2 (SAT2) satellite sequences. However, non-specific DNA hypomethylation was also observed.

In this study, GM10115 cells and stable and unstable clones developed from irradiated GM10115 cells are being used. The status of specific locus, repeat element, and genome-wide DNA methylation, miRNA, and gene expression profiles were evaluated to determine the correlations between epigenetic alterations and RIGI. The results of these experiments show differences in DNA methylation changes and miRNA expression alterations based on instability.

Materials & Methods

Cell culture:

The human-hamster hybrid cell line, GM10115, contains a single copy of human chromosome 4 in a background of 20-24 hamster chromosomes (Human Genetic Mutant Cell Repository, Camden, NJ). AA8 is a Chinese hamster ovary (CHO) cell line (American Type Culture Collection (ATCC)). These cell lines were maintained in high glucose Dulbecco's Modified Eagle Medium (DMEM) containing 10% fetal bovine serum (FBS, Hyclone, Logan, UT), 2 mM L-glutamine (Invitrogen, Carlsbad, CA), 0.2 mM L-proline (Sigma, St. Louis, MO) at 34°C (AA8 at 37°C) with 5% CO_2. RKO is a human colorectal carcinoma cell line (ATCC), which was maintained in low glucose Dulbecco's Modified Eagle Medium (DMEM) containing 10% fetal bovine serum (FBS, Hyclone, Logan, UT), 2 mM L-glutamine (Invitrogen, Carlsbad, CA) at 37°C with 5% CO_2. Cell cultures were routinely screened for the presence of mycoplasma (Bionique Testing Laboratories, Inc., Saranac Lake, NY).

Cells treated with the DNA methylation inhibitor 5-aza-2'deoxycytidine (DAC, Sigma) were plated at a low density ($1x10^6$ cells in T-175 flasks) 24 hours before treatment. Every 24 hours fresh medium containing 5 μM DAC was added to cultures for 5 days prior to harvesting.

Analysis of chromosomal instability:

Stable and unstable colonies were isolated from irradiated parental GM10115 cells by isolating and clonally expanding a surviving irradiated cell [5, 6, 32]. Two stable (114, 118) and four unstable clones (CS9, LS12, 115 and Fe5.0-8), isolated from GM10115 cells irradiated with 10Gy of X-rays or 5Gy of iron ions were used in this study (Table 3.1). The clones were characterized by cytogenetic analysis of metaphase chromosomes using fluorescence *in situ* hybridization (FISH) for human chromosome 4 (Figure 3.1). The biotin labeling of the pBluescript vector-based library of human chromosome 4-specific DNA sequences (pBS4) and the details of the FISH procedure have been described previously [5]. Metaphase spreads were scored using a Zeiss Axioskop microscope equipped with a dual-band pass fluorescein isothiocyanate (FITC)/Texas Red filter set. A stable clone was defined as one that contained a homogenous metaphase population with a unique rearrangement (translocation) or no rearrangement of the human chromosome with hamster chromosomes. An unstable clone was defined as one that contained three or more metaphase subpopulations with different rearrangements of the human chromosome. Each of these rearranged subpopulations constituted ≥ 5% of the 200 metaphases scored.

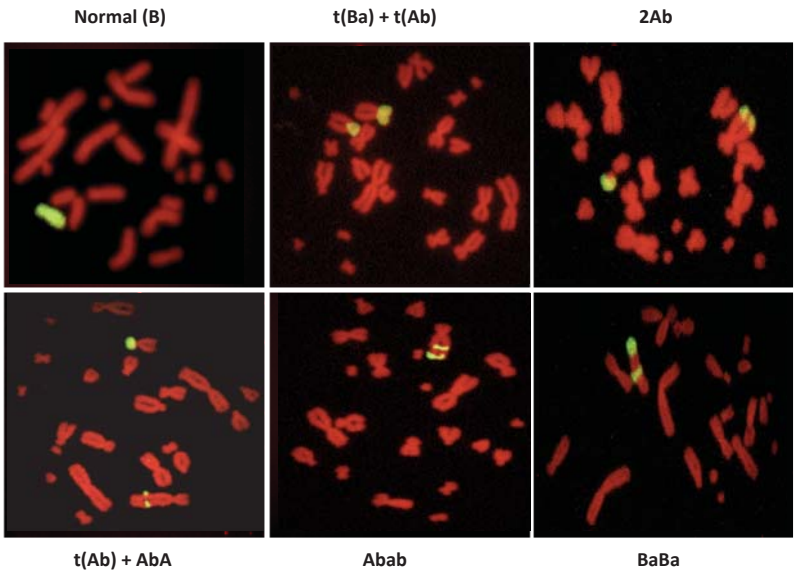

Figure 3.1. Fluorescence *in situ* hybridization (FISH) pictures of normal, stable and unstable clones showing different types of subpopulations. FISH is performed on human chromosome 4, which is labeled by fluorescein isothiocyanate (FITC; green fluorescing). Hamster chromosomes are stained with propidium iodide (PI; red fluorescing).

Clones	Radiation	Classification	Number of Subpopulations[a]	Aberrant Metaphases[b]	Metaphases Counted
GM10115	-	Parental	1	0%	200
114	10Gy X-rays	Stable	1	100%	200
118	10Gy X-rays	Stable	1	0%	200
CS9	10Gy X-rays	Unstable	4	100%	200
LS12	10Gy X-rays	Unstable	5	100%	207
115	10Gy X-rays	Unstable	4	100%	206
Fe5.0-8	5Gy Fe ions	Unstable	3	95%	200

[a] Number of different abnormal metaphase subpopulations showing distinct types of chromosome aberrations
[b] Percentage of metaphases scored showing chromosomal aberrations

Table 3.1. Classification of clones based on the number of chromosomal aberrations acquired at delayed times post-irradiation.

DNA isolation and bisulfite treatment:

DNA was extracted from cells using the DNeasy kit using standard methods (Qiagen, Valencia, CA) and stored in TE buffer at -20°C. Bisulfite modification of genomic DNA was performed using the EpiTect bisulfite kit using standard methods (Qiagen). Bisulfite treated DNA was used in specific locus methylation, bisulfite sequencing and repeat element methylation analyses. Bisulfite treatment selectively deaminates cytosine but not 5-methylcytosine to uracil [138] and during PCR uracil is replaced by thymine. This leads to a primary sequence change in the DNA that allows cytosine to be distinguished from 5-methylcytosine.

Specific locus methylation:

Promoter methylation of *nuclear factor-kappa B* (*NFκB*), *tumor suppressor in lung cancer 1* (*TSLC1*) and *cadherin 1* (*CDH1*) were studied using the methylation-specific PCR (MSP) assay [139]. The genomic sequences for the promoter regions of human *NFκB* p105, hamster *TSLC1*, and hamster *CDH1* [140-142] were used to design methylation specific primers in the *MSPprimer* program, www.mspprimer.org. A 20 μl PCR was carried out in RNase-free water using 20 ng bisulfite treated genomic DNA, 10 μl HotStarTaq Plus Master Mix (1 unit of HotStarTaq DNA Polymerase, 200 μM of each dNTP, 1.5 mM $MgCl_2$; Qiagen), locus specific MSP PCR primers (5 pmol *TSLC1*, *CDH1;* 10 pmol *NFκB*). Primer sequences are as follows: *NFκB* unmethylated (u*NFκB*), forward 5'-AAG TAG TTT AGA TGT TAG TGA ATG-3' and reverse 5'-AAA CCC CCA AAA AAC ACC TAC CAA ACC CAA TAA TCA AAA AAC A-3'; *NFκB* methylated (m*NFκB*), forward 5'-AAG TAG TTT AGA TGT TAG TGA ATG-3' and

reverse 5'-CCA AAA AAC GCC TAC CGA ACC CAA TAA TCG AAA AAC G-3'; *TSLC1* unmethylated (u*TSLC1*), forward 5'-TTT ATA GGG TTT TGT TTT TAG GTG G-3' and reverse 5'-AAA AAC TAC CTC CCA AAC CCA AAC A-3'; *TSLC1* methylated (m*TSLC1*), forward; 5'-TTT ATA GGG TTT TGT TTT TAG GTG G-3' and reverse 5'-CTC CCG AAC TCC CGA ACC CGA ACG-3'); *CDH1* unmethylated (u*CDH1*) forward 5'-GAT TTG AAT GAA TGT GAA TTA GGA AGT TTT TTT AGG TTG GTT TTG-3' and reverse 5'-TAA CCA AAC AAA CAC CAA ACA AAC ACA AAA CTC AAA TAC AAT CA-3'); *CDH1* methylated (m*CDH1*), forward 5'-ATT CGA ACG AAT GTG AAT TAG GAA GTT TTT TTA GGT CGG TTT C-3' and reverse 5'-CCG AAC AAA CAC GAA ACT CGA ATA CGA TCG-3'. PCR cycling conditions were 95°C for 15 s, annealing temperature (u*NFκB*; 48.9°C, m*NFκB*; 47.3°C, u*TSLC1*; 55.0°C, m*TSLC1*; 55.0°C, u*CDH1*; 52.0°C, m*CDH1*; 48.6°C) for 15 s and 72°C for 15 s for 40 cycles. Control bisulfite treated DNA was included for all PCR. MDA-MB-231 (human breast cancer), u*NFκB* reaction; HL60 (human promyelocytic leukemia), m*NFκB* reaction; AA8 (Chinese hamster ovary), u*TSLC1* and m*CDH1* reactions; NIH3T3 (mouse embryonic fibroblast), m*TSLC1* reaction; 410.4 (mouse mammary cancer) u*CDH1* reaction. DNA of these cell lines used as controls were obtained from colleagues. Controls without DNA were performed for all PCR. PCR products were resolved on 3% agarose gels (Sigma). Gels were stained using ethidium bromide. Images were captured using a MultiImage Light Cabinet camera with ChemiImager 4400 software (Alpha Innotech Corporation, San Leandro, CA). Two technical replicates were performed for each sample.

Bisulfite sequencing:

Promoter methylation of *NFκB* was further studied by bisulfite sequencing. Primers were generated from the genomic sequence for the promoter region of human *NFκB* p105 [140]. Each PCR reaction was performed in a total volume of 20 μl under the following conditions: RNase-free water using 160 ng of bisulfite treated DNA, 10 μl HotStarTaq Plus Master Mix, 10 pmol of the *NFκB* primers (forward; 5'-AAG TAG TTT AGA TGT TAG TGA ATG-3', reverse; 5'-AAA CTC TAA CTT CCT AAC AAA AC-3'). PCR cycling conditions were 95°C for 15 s, annealing temperatures 55°C for 15 s and 72°C for 15 s for 40 cycles. PCR products were resolved on 3% agarose gels to confirm reaction quality. Gels were stained using ethidium bromide and images were digitally captured. For sequencing, the PCR products were treated with ExoSAP-IT (USB, Cleveland, OH) and bisulfite sequencing was performed at the Institute for Genome Sciences, University of Maryland Biopark. Three technical replicates were performed.

Repeat element methylation:

LINE-1 and Alu repeat element DNA methylation was evaluated by combined bisulfite restriction analysis (COBRA) [143]. For analysis of LINE-1 a 50 μl PCR was carried out in RNase-free water using 25 μl HotStarTaq Plus Master Mix, 100 picomoles of each PCR primer (forward; 5'-TTG AGT TGT GGT GGG TTT TAT TTA G-3', reverse; 5'-TCA TCT CAC TAA AAA ATA CCA AAC A-3') and 100 ng of bisulfite-treated genomic DNA. PCR cycling conditions were 95°C for 30 s, 50°C for 30 s and 72°C for 60 s for 35 cycles. The final PCR product was digested with 10 U of HinfI restriction enzyme (Fermentas, Glen Burnie, MD). The digested PCR products were separated by

electrophoresis on 2.0% Metaphor high resolution agarose gels (Lonza, Rockland, ME). For analysis of Alu elements a 50 μl PCR was carried out in RNase-free water using 25 μl HotStarTaq Plus Master Mix, 50 pmol of forward primer (5'-GAT CTT TTT ATT AAA AAT ATA AAA ATT AGT-3'), 50 pmol of reverse primer (5'-GAT CCC AAA CTA AAA TAC AAT AA-3'), and 100 ng of bisulfite-treated genomic DNA. PCR cycling conditions were 96°C for 90 s, 43°C for 60 s and 72°C for 120 s for 35 cycles. The PCR product was then digested with 10 U of MboI (Fermentas). The digested PCR product was then separated by high resolution agarose gel electrophoresis (2.5% Metaphor agarose, Lonza). Gels were stained using ethidium bromide, images were digitally captured and the intensity of bands on the gel were quantified using Quantity One software (BioRad, Hercules, CA). The optical densities were used to calculate the percent of the total repetitive element DNA that is methylated and the percent repetitive element DNA that is unmethylated. A total of four technical replicates were performed.

The restriction enzymes used, MboI and HinfI, both have cytosine in their cut site therefore only methylated cytosines will be cut at these intact restriction sites. After gel electrophoresis, the top uncut band represents unmethylated or mutated sequences and the lower, cut bands represent methylated repeat elements.

Global DNA methylation:

Global DNA methylation was evaluated by methylation-sensitive arbitrarily primed PCR (MSAP-PCR) [144]. Restriction enzyme digestion of 2 μg of genomic DNA was performed by using either 20 units of RsaI, 20 units each of RsaI and methylation-sensitive restriction enzyme HpaII, or 20 units of each of RsaI and methylation-sensitive

restriction enzyme MspI at 37°C for 16 h. Restriction digested DNA was amplified using arbitrarily primed PCR with a single primer (MLG2: 5'-AAC CCT CAC CCT AAC CCC GG-3'). PCR reactions were performed in a total volume of 50 μl under the following conditions: RNase-free water, 25 μl HotStarTaq Plus Master Mix, 50 pmol of the MLG2 primer and 200 ng of genomic DNA. Five cycles at low-stringency conditions of 94°C for 30 s, 40°C for 60 s, 72°C for 90 s were done before increasing the stringency of the PCR to 94°C for 15 s, 55°C for 15 s, 72°C for 60 s for another 30 cycles. PCR products were resolved on high resolution 1.8% Metaphor agarose gels (Lonza). Gels were stained using ethidium bromide. Images were digitally captured and the intensity of bands on the gel were quantified using Quantity One. Four technical replicates were performed.

The RsaI restriction enzyme was used to generate smaller fragments of DNA and reduce the number potential artifacts that might be amplified in the arbitrarily primed PCR. HpaII does not cut DNA if the internal cytosine of its restriction site (C*C*GG) is methylated and therefore the bands generated in the PCR of DNA digested by RsaI+HpaII lane are methylated at the internal cytosine. MspI is unable to cut DNA when the external cytosine (*C*CGG) is methylated and therefore the bands generated in the PCR of DNA digested by RsaI+MspI are methylated at the external cytosine. All the restriction enzymes were titrated and the concentrations were chosen in excess to ensure complete digestion for all reactions. Each new lot of enzyme was tested for consistent activity and result as compared to the previous lot. The MLG2 primer was designed with a 3' end complementary to the recognition sequence of the HpaII and MspI cut site, CCGG. Therefore, whenever the restriction enzymes are unable to digest the DNA, it is

amplified and a band is observed on the gel. An increase in band intensity indicates an increase in methylation. Band intensity was measured to determine numerically the change in DNA methylation. For the HpaII and the MspI lane, eleven and nine bands were analyzed for each sample, respectively. The mean percent methylation for all bands from each dose group was normalized to the corresponding mean percent methylation for all bands from sham-irradiated controls.

The bands observed on the MSAP-PCR gels were cut out and the DNA fragments purified from the agarose using the MinElute Gel Extraction Kit (Qiagen). These PCR products were sequenced at the Biopolymer-Genomics Core (University of Maryland School of Medicine) using the MLG2 primer. The sequences were identified using National Center for Biotechnology Information (NCBI) blasts.

The validation of the methylation status of the identified three bands was performed by bisulfite sequencing. Each PCR reaction was performed in a total volume of 20 μl under the following conditions: RNase-free water using 50 ng of bisulfite treated DNA, 10 μl HotStarTaq Plus Master Mix, 10 pmol of the primers CpG1 (forward; 5'-TGA TTT TAT TTA GTG GGT AGG AGT A-3', reverse; 5'-TAA ATT CTA TCT CAA TAA AAC CAT C-3'), CpG2 (forward; 5'-TAT TGG GGA AGA AGG TAA AAG A-3', reverse; 5'-CCT TCC TTA AAA TCC TCA CAA-3'), PTPR-F (forward; 5'-AGG GGA ATG AAA TAG AGG TT-3', reverse; 5'-ACC TTA TAC TCA AAA TTT AAC AAT C-3'). PCR cycling conditions were 95°C for 15 s, annealing temperature 49°C for 15 s and 72°C for 15 s for 40 cycles. PCR products were resolved on 3% agarose gels to confirm reaction quality. Gels were stained using ethidium bromide and images were digitally captured. For sequencing, the PCR products were cloned into competent

bacteria using the TOPO cloning kit (Invitrogen, Carlsbad, CA) and subsequent plasmid mini preparation (Invitrogen, Carslbad, CA). Sequencing was performed at the Biopolymer-Genomics Core (University of Maryland School of Medicine) using the T3 primer (5'-ATT AAC CCT CAC TAA AGG GA-3'. For each sample, ten clones were sequenced.

RNA isolation, miRNA and gene expression analysis:

Total RNA was extracted from GM10115 cells, stable and unstable clones using the miRNeasy Mini Kit (Qiagen) following kit procedures. The extracted RNA was quantified using a NanoDrop ND-1000 spectrophotometer (NanoDrop Technologies, Wilmington, DE), and immediately stored at -80°C until analysis.

MiRNA microarray and gene expression microarray analyses of total RNA were performed by LC Sciences LLC (Houston, TX). For miRNA microarray, quality control for the integrity of total RNA, enrichment of miRNA from total RNA, labeling, hybridization to μParaflo® microfluidics chip and scanning were performed using miRHuman/Mouse/Chinese Hamster miRNA array chips, based on Sanger miR-Base Release 12.0. Preliminary statistical analyses were performed on raw data normalized by the Locally-Weighted Regression (LOWESS) method on the background-subtracted data. Student's t-tests were then performed to identify differences in miRNA expression. Two technical replicates were performed.

For gene expression microarray analysis, quality control for the integrity of total RNA was performed and then the Affymetrix's GeneChip IVT Express kit was used for cDNA synthesis and *in vitro* transcription. To measure mRNA levels the Affymetrix

GeneChip Mouse Genome 430 2.0 Array was used, with data processed by the Affymetrix software Command Console and Expression Console using MAS5.0 Analysis Algorithms. Three technical replicates were performed.

Prediction of miRNA targets:

Candidate miRNA, that changed ≥ 1.5-fold with a microarray intensity signal ≥ 100 and p-value ≤ 0.05, were picked for target prediction. Three different computational programs, TargetScan [145], MicroRNA.org [147], MicroCosm (miRBase) [148-150] were used to predict miRNA targets. Targets from the three databases were combined. The potential miRNA targets were merged with gene targets identified by the gene expression microarray using the Bioinformatics Resource Manager program version 2.1 and overlapping targets in all databases were subject to the Database for Annotation, Visualization and Integrated Discovery (DAVID) [151, 152] pathway analysis. DAVID analysis was performed based on gene ontology GOTERM BP 3, 4, and 5. Pathways were identified using the Functional Annotation Clustering feature (high classification stringency).

qRT-PCR analysis of miRNA:

Candidate miRNA identified by the array with an intensity signal ≥ 500 and involved in pathways of interest were validated using qRT-PCR. Total RNA used for the microarray analysis was reverse transcribed to cDNA template and TaqMan miRNA assay was performed in triplicate by LC Sciences. The hsa-miR-16 miRNA, which was expressed equally in all the samples on the microarray, was used as an internal control.

Statistical analyses:

Means and standard errors were calculated for all data points from two - four technical replicates. The means were compared between samples by Student's t-test analysis using the StatPlus Mac software package (AnalystSoft, Vancouver, BC). P-values ≤ 0.05 were considered statistically significant.

Results

Specific Locus Methylation

NFκB, *TSLC1* and *CDH1* promoter methylation was ascertained using methylation-specific PCR (MSP) assay [139]. Changes in the expression of *NFκB* gene have been linked to cancer [153]. *NFκB* is also involved in cellular responses to irradiation and was identified as an important gene candidate that could be involved in RIGI [48, 154]. *TSLC1* and *CDH1* tumor-suppressor genes are also involved in cancer and their promoter regions are hypermethylated in cancer cells [155, 156]. We investigated these genes to see if clones with RIGI acquired any changes in their promoter methylation since RIGI is thought to be an early event in radiation carcinogenesis. Four, three and nine CpG sites were analyzed for *NFκB*, *TSLC1* and *CDH1* promoter regions, respectively. Neither in stable nor in unstable clones changes in DNA methylation at these CpG sites were observed (Figure 3.2A).

For the unstable clones LS12 and 115, very faint bands were observed in the unmethylated *NFκB* lane. PCR with primers designed to amplify the entire *NFκB* promoter region in order to determine the decrease in band intensity observed in the unmethylated *NFκB* lane was performed. These results showed a faint band in unstable

clone LS12 and no band in unstable clone 115 suggesting potential mono- and bi-allelic deletion of this region, respectively (Figure 3.2B). This might also suggest that LS12 clone is heterogeneous and *NFκB* promoter is deleted in subpopulations of cells. FISH analysis for chromosome 4 also shows a heterogeneous LS12 clone with 5 different subpopulations, therefore, some of these subpopulations may have lost a piece of chromosome 4 that includes *NFκB* promoter.

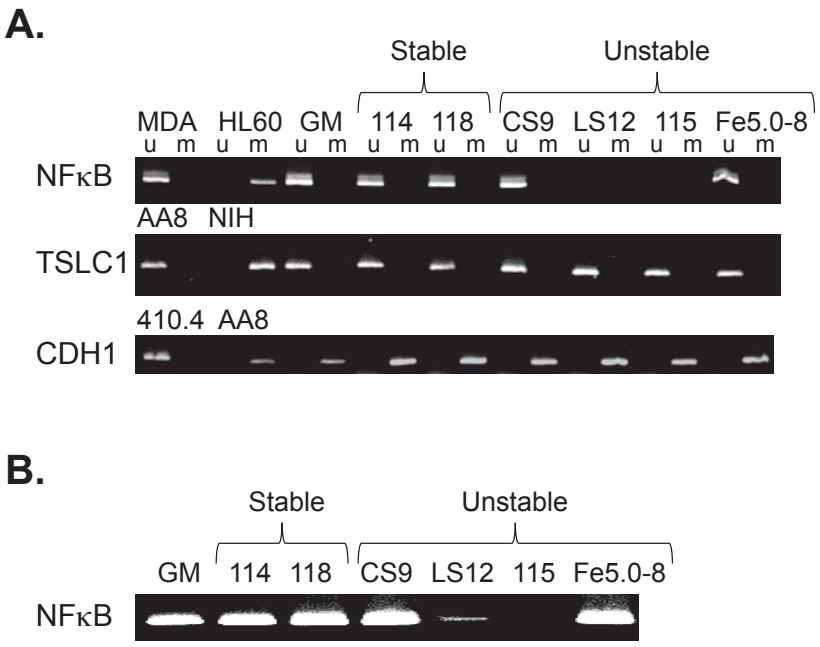

Figure 3.2. Methylation status of the promoter regions of *TSLC1*, *CDH1* and *NFκB* using methylation specific PCR assay. (A) Methylation status of the stable and unstable clones. The lanes marked with 'u' signify PCR products using primers specific to unmethylated promoter sequence and those marked 'm' signify PCR products using primers specific to methylated promoter sequence. MDA (MDA-MB-231), positive control for u*NFκB*. HL60, positive control for m*NFκB*. AA8, positive control for u*TSLC1* and m*CDH1*. NIH (NIH3T3), positive control for m*TSLC1*. 410.4, positive control for u*CDH1*. (B) PCR of complete *NFκB* promoter region.

Bisulfite sequencing

Promoter methylation of *NFκB* was studied in more detail using bisulfite sequencing since it has been shown to be potentially involved in RIGI in unstable clones [48]. For each clone (control, stable or unstable) twenty CpG sites were sequenced within the *NFκB* promoter region (Figure 3.3). The first two CpG were generally methylated for all clones. The last two CpG did not sequence accurately due to their proximity to the primer binding site. The remaining sixteen CpG were unmethylated and no differences were observed among clones (114, 118, CS9, LS12, Fe5.0-8) compared to control GM10115. These bisulfite sequencing results also serve as confirmation of the results obtained in the *NFκB* MSP assay. In addition, these results confirmed the very faint band observed in the unmethylated *NFκB* lane for the unstable clone LS12 since the bisulfite sequencing showed unmethylated CpG sites. The *NFκB* promoter region sequence was not amplified by PCR for the unstable clone 115, therefore no bisulfite sequencing could be performed.

A.

5'-
taaaatatatatttcggctcaagctttcttatgtggggaggtaatccacccgaagtatccccagcctgtacctaatacagtgcccagcacta
aagcagctcagatgccagtgaatggtggccactgggaggcctgtcagtgggtgccagtagcggtctcttcagagaaaaagaaaac
tcccctctgccagatcagtattttatgagctgtgaaccaaaaccattgctaccaccatcactataattctatcacagtaattatcataaggcct
aacaatgccttgtagatgaacattctgagtaactgctctataaccaggagatttaagaccgcaccaaaaaccagtagagggttatacttta
ctgggcacaagtcgtttatgataacgaaattgtagtttaatctgtgaagagatgtgaatgtaactgagacacgcttaaatggaatatacag
atgagctttatttttatatctggcatgcttggatccatgccgaccctccagctgctcgggcctgccttagggctatggaccgcatgactctatc
agcggcactgccaccgccgccgcctccgtgctgcctgcgttcccgaccattgggccggcaggcgcttcctgggggcttccctaccgg
ctccagcccttgggattcgggagcg**gccctgctaggaagccagagccc**cgcaggggccgc-3'

B.

CpG	1	2	3	4	5	6	7	8	9	10	11	12	13	14	15	16	17	18	19	20
GM	M	M	U	U	U	U	U	U	U	U	U	U	U	U	U	U	U	U	X	X
114	M	M	U	U	U	U	U	U	U	U	U	U	U	U	U	U	U	U	X	X
118	M	M	U	U	U	U	U	U	U	U	U	U	U	U	U	U	U	U	X	X
CS9	M	U	U	U	U	U	U	U	U	U	U	U	U	U	U	U	U	U	X	X
LS12	M	M	U	U	U	U	U	U	U	U	U	U	U	U	U	U	U	U	X	X
115	X	X	X	X	X	X	X	X	X	X	X	X	X	X	X	X	X	X	X	X
FE	M	M	U	U	U	U	U	U	U	U	U	U	U	U	U	U	U	U	X	X

Figure 3.3. *NFκB* bisulfite sequencing of stable and unstable clones. (A) Genomic sequence of *NFκB* promoter region. The binding regions of bisulfite sequencing forward and reverse primers are bold and underlined. The twenty CpG sites detected in the sequencing are highlighted in yellow. (B) The methylation status of the twenty CpG sites is shown. The first two CpG sites were generally methylated for all clones irrespective of experimental group. The last two CpG sites did not sequence accurately due to their proximity to the primer binding site. The remaining sixteen CpG were mainly unmethylated and no differences were observed among clones. Methylated CpG sites are highlighted in yellow. Orange highlighted CpG sites did not sequence accurately. Green labeled clone 115 could not be sequenced since the promoter region did not amplify.

LINE-1 and Alu Methylation

LINE-1 and Alu repeat element DNA methylation was evaluated by COBRA [143]. DNA from DAC-treated cells was used to validate the assay. For LINE-1 elements, both human (RKO) and hamster (AA8) cells in addition to GM10115 cells were used for validation since the GM10115 cells are human/hamster hybrids. RKO and GM10115 cells resulted in 21.8% and 2.5% decreases in LINE-1 methylation after DAC treatment, respectively (RKO, $p = 0.007$; GM10115, $p = 0.004$). For methylation analysis, five digestion fragments were quantified. Four were of human origin and the extra band observed in GM10115 cells was confirmed to be of hamster origin with the use of the AA8 (hamster) cell line. Alu elements validation showed 4.2% and 2.2% decreases in methylation after DAC treatment of RKO and GM10115 cells, respectively (RKO: $p = 0.003$, GM10115: $p = 0.007$). For the AA8 hamster cell line, no Alu band was observed since Alu elements are of human origin.

The COBRA assay was performed on stable and unstable clones. For the LINE-1 elements, hypermethylation was observed in the unstable clones CS9 and LS12 relative to controls (CS9, $p = 0.02$; LS12, $p = 0.01$; Figure 3.4A). No change in methylation was observed for any of the stable clones.

Hypomethylation of Alu elements was observed for the unstable clones 115 and Fe5.0-8 relative to controls (115, $p = 0.03$; Fe5.0-8, $p = 0.005$; Figure 3.4B). There was no change in methylation for any of the stable clones.

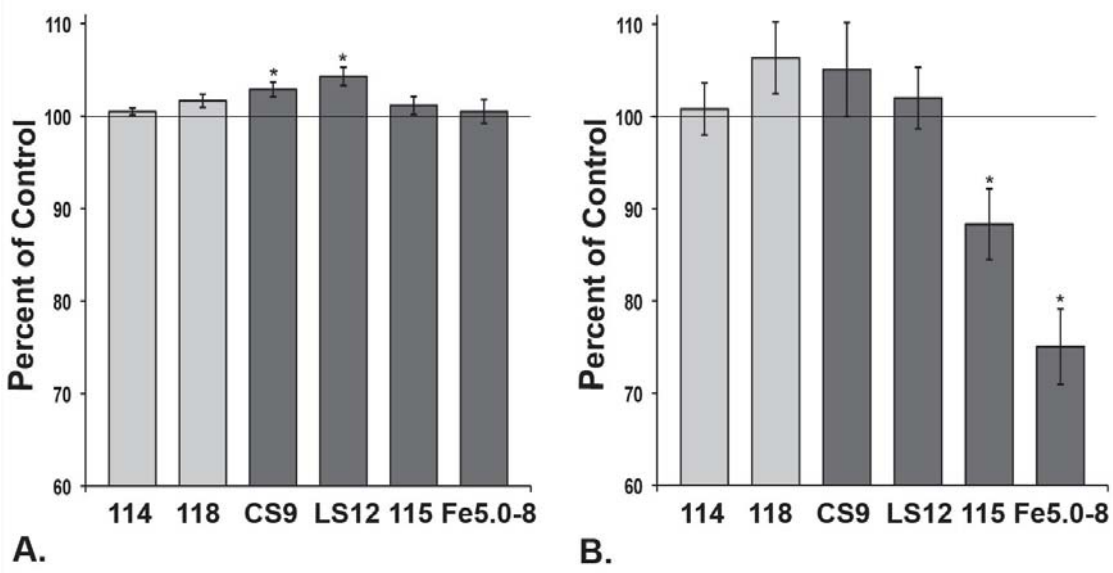

Figure 3.4. Altered repeat element DNA methylation in the clones. (A) LINE-1 percent methylation and (B) Alu percent methylation of stable and unstable clones. For each clone the percent DNA methylation is normalized to control. Error bars indicate mean +/- SEM. * $p \leq 0.05$ versus GM10115 control, Student's t-test. Change in percent methylation compared to control is LINE-1: 0.50, 1.67, 2.89, 4.29, 1.16, 0.51 and Alu: 0.81, 6.37, 5.10, 2.01, -11.67, -24.95 for LINE-1: 114, 118, CS9, LS12, 115, Fe5.0-8 and Alu: 114, 118, CS9, LS12, 115, Fe5.0-8, respectively. The raw mean numbers are LINE-1: GM = 70.83, 114 = 71.17, 118 = 72.00, CS9 = 72.87, LS12 = 73.85, 115 = 71.64, Fe5.0-8 = 71.70, Alu: GM = 19.76, 114 = 19.92, 118 = 21.04, CS9 = 20.75, LS12 = 20.12, 115 = 17.40, Fe5.0-8 = 14.78.

Global DNA Methylation

Global DNA methylation was evaluated by MSAP-PCR [144]. For all clones, methylation at the internal cytosine (HpaII; CpG) was evaluated for eleven bands or cytosine residues and methylation at the external cytosine (MspI; cytosine-phosphate-cytosine (CpC)) was evaluated for nine bands or cytosine residues (Figure 3.5).

At the CpG sites, statistically significant hypermethylation of band #2 was observed in the stable clone 118 ($p = 0.01$), however, there was statistically significant hypomethylation of bands #8 and 9 in the stable clone 118 ($p = 0.04$, 0.04, respectively) and the unstable clones 115 ($p = 0.001$, 0.05, respectively) and Fe5.0-8 ($p = 0.04$, band #9 only; Figure 3.6A). The mean methylation of all the bands together suggested no change in methylation in either the stable or unstable clones relative to control (Figures 3.7A).

At the CpC sites, statistically significant hypomethylation of bands #1, 2, 3, 6, 8 and 9 was observed (Figure 3.7B). In the stable clone 114, only band #8 was hypomethylated ($p = 0.01$). In the unstable clone LS12, bands #1, 2, 6 and 8 were hypomethylated ($p = 0.02$, 0.04, 0.0006, 0.008, respectively). In the unstable clone 115, bands #1, 6 and 9 were hypomethylated ($p = 0.005$, 0.04, 0.04, respectively). In the unstable clone Fe5.0-8, bands #1, 2 and 3 were hypomethylated ($p = 0.005$, 0.04, 0.007, respectively). The mean methylation of all the bands together indicated statistically significant hypomethylation in the unstable clones LS12, 115 and Fe5.0-8 relative to control (LS12, $p = 0.002$; 115, $p = 0.003$; Fe5.0-8, $p = 0.002$; Figures 3.7B). However, no statistically significant change in methylation was observed in any of the stable clones.

The quantitated amplified DNA from the HpaII and the MspI PCR were also isolated and sequenced (Figure 3.5). Seventeen sequences out of the twenty sequenced

were unknown, two of the HpaII sequences (bands #4 and 10) were identified as CpG islands and one of the MspI sequences (band#9) was identified as a *protein tyrosine phosphatase receptor type f (PTPR-F)* promoter sequence (Figures 3.8, 3.9 and 3.10).

The validation of the methylation status of these three bands was performed by bisulfite sequencing. For each band, ten clones were sequenced for one stable (118) and one unstable clone (115). There was no difference in the methylation patterns of these sequences between the stable and unstable clones 118 and 115. For band#4, out of the two possible CpG sites one was unmethylated and the other was methylated, however, CCGG site could not be identified (Figure 3.8). For band #10, all five CpG sites including the CCGG site were methylated (Figure 3.9). For band #9, four potential CpC sites were unmethylated and a CpG site was methylated (Figure 3.10). CCGG site could not be identified and CpC methylation was not present.

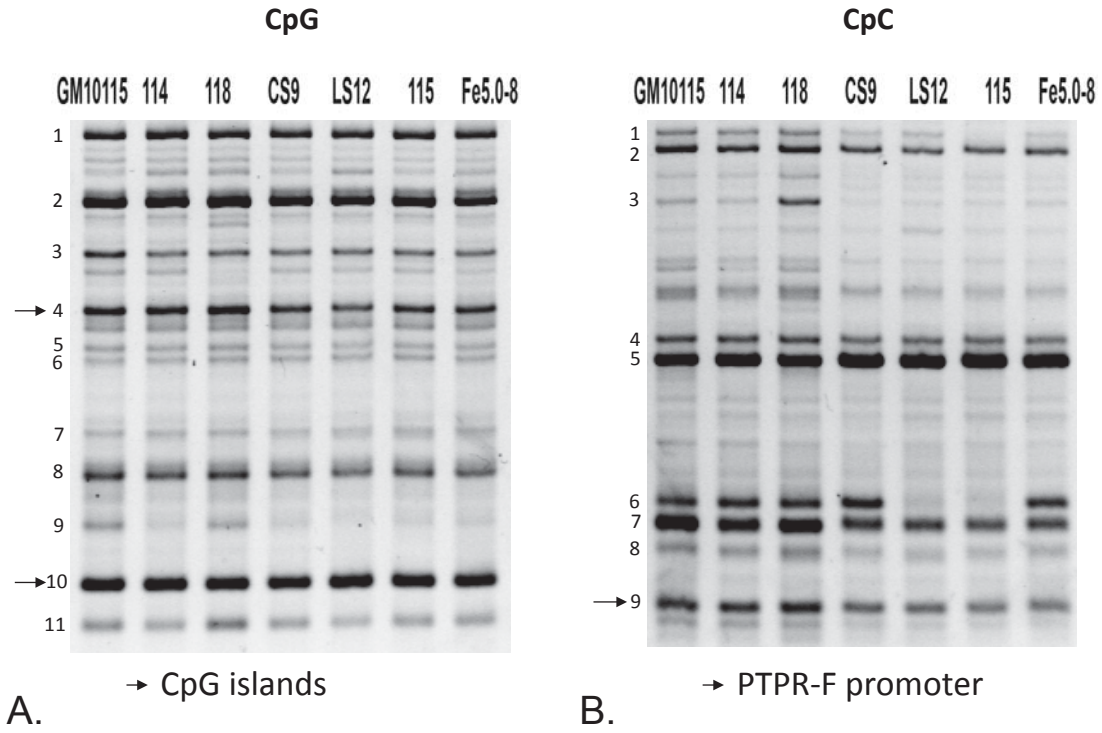

Figure 3.5. Agarose gel pictures of the global DNA methylation assay in the clones. (A) Internal cytosine (CpG) methylation and (B) External cytosine (CpC) methylation of stable and unstable clones. For the internal and the external cytosine, eleven and nine bands were analyzed for each sample, respectively. An increase in band intensity indicates an increase in methylation. These bands were also sequenced. At CpG, two were identified to be CpG islands (band #4: ~490bp, band #10: ~175bp) and at CpC, one was identified to be *protein tyrosine phosphatase receptor type f* (PTPR-F) promoter (band #9: ~130bp).

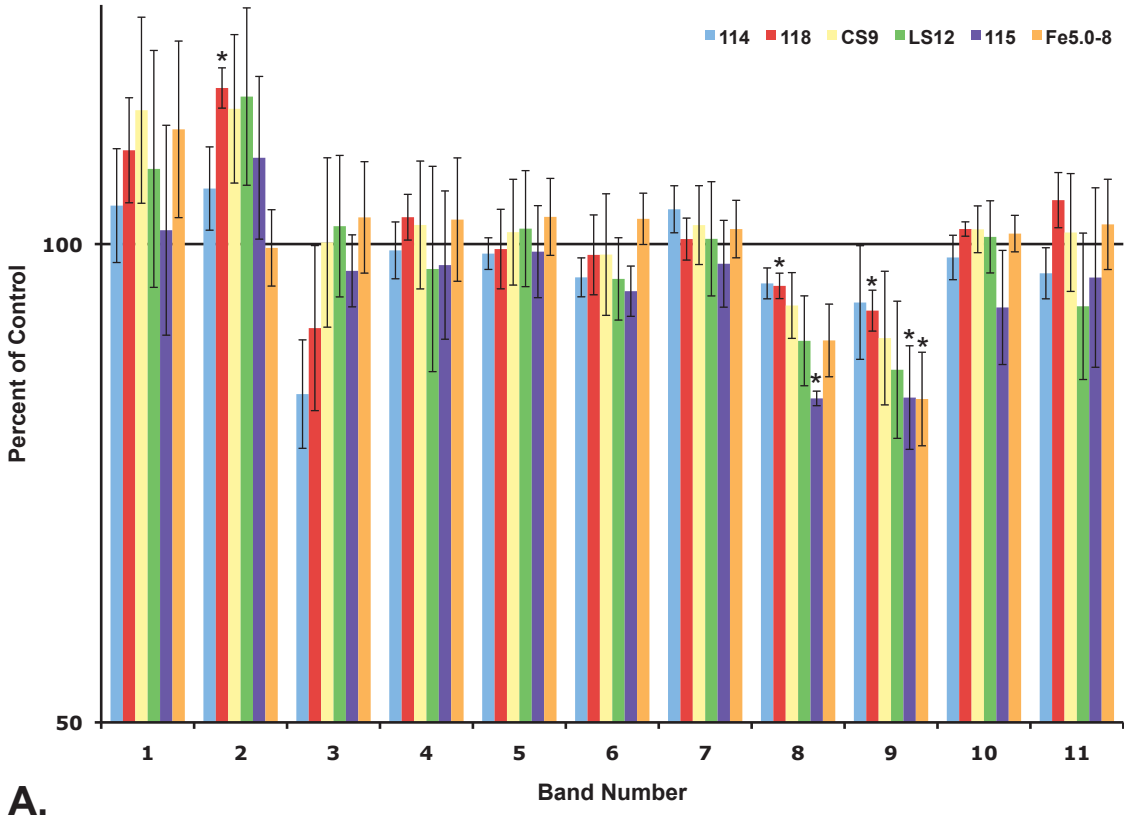
114
118
CS9
LS12
115
Fe5.0-8
Percent of Control
100
50
1
2
3
4
5
6
7
8
9
10
11
Band Number

A.

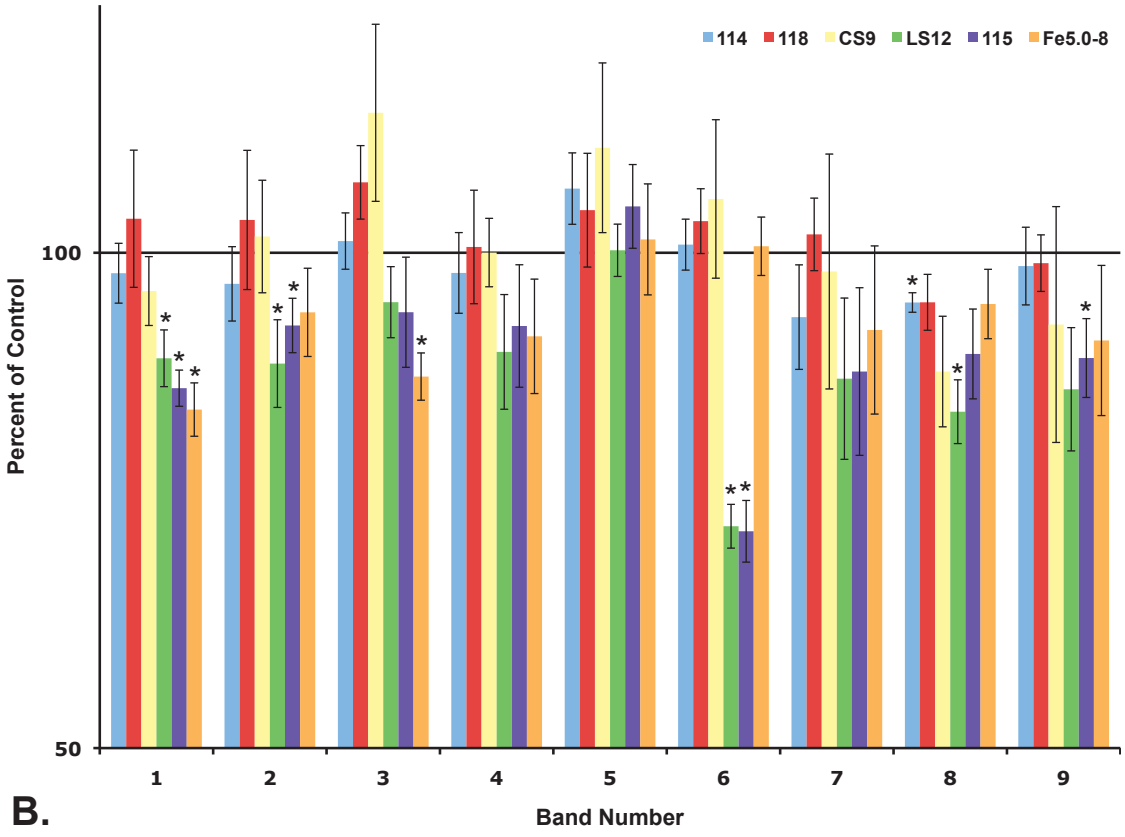
114
118
CS9
LS12
115
Fe5.0-8
Percent of Control
100
50
1
2
3
4
5
6
7
8
9
Band Number

B.

Figure 3.6. Changes in DNA methylation of each MSAP band observed in the clones. (A) Internal cytosine (CpG) percent methylation of stable and unstable clones. (B) External cytosine (CpC) percent methylation of stable and unstable clones. For the internal and the external cytosine, eleven and nine bands were analyzed for each sample, respectively. The mean percent methylation for each band from each clone was normalized to the mean percent methylation of control. Error bars indicate mean +/- SEM. * $p \leq 0.05$ versus GM10115 control, Student's t-test. Changes in percent methylation compared to control and the raw mean numbers are shown on Table 3.2.

A.

Band	GM	114	118	CS9	LS12	115	Fe	% Δ 114	% Δ 118	% Δ CS9	% Δ LS12	% Δ 115	% Δ Fe
1	2782.3	2863.4	3025.6	3124.8	2940.9	2763.4	3073.6	4.02	9.80	13.99	7.86	1.45	11.99
2	2810.0	2952.6	3260.0	3185.5	3204.0	3025.3	2782.2	5.80	16.31	14.14	15.42	9.02	-0.40
3	1976.3	1617.2	1726.1	1937.2	1995.7	1931.8	2010.0	-15.68	-8.78	0.17	1.87	-2.80	2.79
4	1532.4	1511.5	1578.9	1548.8	1458.7	1469.6	1550.6	-0.66	2.81	1.99	-2.60	-2.20	2.56
5	1176.7	1163.8	1169.7	1187.7	1189.4	1161.8	1205.8	-1.00	-0.52	1.24	1.61	-0.79	2.84
6	1747.7	1688.0	1728.8	1723.8	1678.6	1658.9	1791.6	-3.48	-1.13	-1.10	-3.64	-4.92	2.64
7	1742.5	1808.3	1752.7	1778.4	1755.3	1711.2	1768.0	3.64	0.52	1.98	0.55	-2.06	1.57
8	2549.4	2443.9	2438.6	2380.7	2285.1	2138.5	2288.3	-4.11	-4.37	-6.42	-10.12	-16.13	-10.07
9	1356.7	1263.4	1258.3	1212.6	1167.5	1130.3	1127.6	-6.11	-6.96	-9.83	-13.14	-16.05	-16.20
10	3169.9	3112.4	3215.2	3215.7	3198.5	2925.4	3202.9	-1.40	1.57	1.54	0.75	-6.63	1.09
11	1335.3	1286.3	1396.1	1334.4	1224.9	1262.6	1348.8	-3.06	4.59	1.21	-6.50	-3.50	2.06

B.

Band	GM	114	118	CS9	LS12	115	Fe	% Δ 114	% Δ 118	% Δ CS9	% Δ LS12	% Δ 115	% Δ Fe
1	1205.0	1180.5	1251.4	1159.1	1076.9	1041.8	1017.6	-2.06	3.44	-3.86	-10.65	-13.67	-15.83
2	1730.4	1662.2	1759.2	1745.4	1519.9	1592.0	1604.7	-3.14	3.31	1.64	-11.19	-7.34	-6.01
3	1341.2	1357.5	1441.6	1531.0	1278.4	1268.4	1174.6	1.18	7.11	14.13	-4.99	-6.00	-12.50
4	1767.9	1731.7	1776.3	1771.7	1589.3	1637.5	1618.1	-2.03	0.59	0.02	-10.01	-7.39	-8.43
5	3533.7	3749.0	3681.6	3868.1	3529.9	3654.8	3520.0	6.48	4.30	10.60	0.25	4.68	1.35
6	1341.4	1355.6	1379.7	1422.2	969.7	966.9	1348.0	0.82	3.19	5.43	-27.60	-28.11	0.66
7	1828.0	1666.5	1832.4	1702.6	1531.2	1558.9	1609.2	-6.50	1.86	-1.89	-12.71	-11.99	-7.80
8	1188.1	1126.5	1123.4	1047.8	993.7	1066.8	1129.2	-5.02	-5.00	-11.99	-16.05	-10.21	-5.17
9	1135.5	1105.5	1114.1	1032.1	953.9	1003.0	1003.0	-1.34	-1.05	-7.24	-13.78	-10.63	-8.85

Table 3.2. Raw mean numbers and changes in percent methylation compared to GM10115 control. (A) Internal cytosine (CpG) methylation of stable and unstable clones. (B) External cytosine (CpC) methylation of stable and unstable clones.

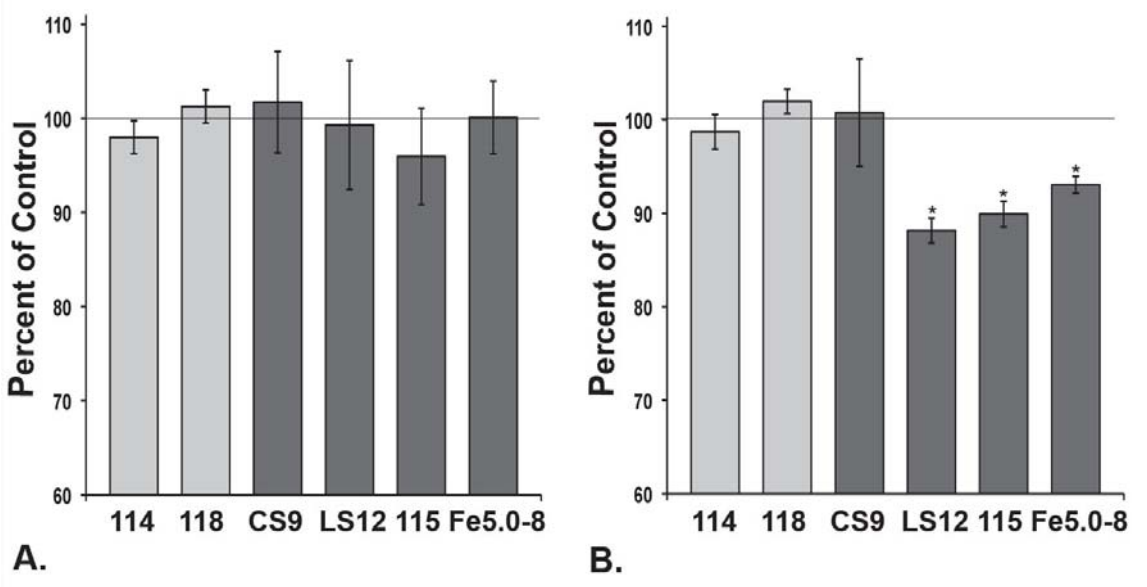

Figure 3.7. Changes in global DNA methylation in the clones. (A) Internal cytosine (CpG) percent methylation and (B) External cytosine (CpC) percent methylation of stable and unstable clones. For the internal and the external cytosine, eleven and nine bands were analyzed for each sample, respectively. The mean percent methylation for all bands from each clone was normalized to the mean percent methylation of control. Error bars indicate mean +/- SEM. * $p \leq 0.05$ versus GM10115 control, Student's t-test. Changes in percent methylation compared to control are CpG: -2.00, 1.26, 1.72, -0.72, -4.06, 0.08 and CpC: -1.29, 1.97, 0.76, -11.86, -10.07, -6.95 for CpG: 114, 118, CS9, LS12, 115, Fe5.0-8 and CpC: 114, 118, CS9, LS12, 115, Fe5.0-8, respectively. The raw mean numbers are CpG: GM10115 = 2016.3, 114 = 1973.7, 118 = 2050.0, CS9 = 2057.2, LS12 = 2009.0, 115 = 1925.4, Fe5.0-8 = 2013.6; CpC: GM10115 = 1674.6, 114 = 1659.5, 118 = 1706.6, CS9 = 1697.8, LS12 = 1493.7, 115 = 1532.2, Fe5.0-8 = 1558.3.

```
>emb|AL669824.13| Mouse DNA sequence from clone RP23-396G1 on chromosome 2 Contains
the 5' end of the gene for a novel protein containing HEAT
repeat domains, the gene for the orthologue of H. sapiens
chromosome 20 open reading frame 77 (C20orf77), the Tgm2 gene
for transglutaminase 2 C polypeptide and a CpG island, complete
sequence
Length=139077

 Score =  407 bits (450),  Expect = 3e-110
 Identities = 309/363 (86%), Gaps = 30/363 (8%)
 Strand=Plus/Plus

Query  1       TTTCTGTCCTTACTGTACCGTGTCTCAGGGCTTTGTTCCTTTTCACTGCCAAGCAATACT  60
               ||||||||||||||||| ||||| |||||||||| |||||||||||||||||| ||||||
Sbjct  102170  TTTCTGTCCTTACTGTAGCGTGTATCAGGGCTTCGTTCCTTTTCACTGCCAAGTAATACT  102229

Query  61      CCATGGTCCATACACCATAGTTTATTTGTCTC----TTAAGTTAATGGACAGGTGGGTTG  116
               ||||||||||||| |||||||||| |||||    |||||||| ||| ||||||||||||
Sbjct  102230  CCATGGTCCATACAGCATAGTTTATTGGTCTCTTAATTAAGTTAGTGGGCAGGTGGGTTG  102289

Query  117     CTTCCACTTTTTATCCAATGCGGATGACGGCACCGACAACATCATTGAACATCTTTCTGT  176
               ||| |||||||| ||    ||||||||||||||||||||||||| ||||||||||||||
Sbjct  102290  CTTTCACTTTTTCTCTCCTGCGGATGACGGCACCGACAACATCACTGAACATCTTTCTGT  102349

Query  177     GTGCACGCGTGCTTCCATTTCTCATGGATAAATATCTG---CAGGTGGAATAAGTGGGAA  233
               || |||| |||||     |||||||||||    | ||||   ||  |  |||||||  |||
Sbjct  102350  GTCCACGGGTGCT----TTTCTCATGGAT---TTTCTGGTTCA--TACAATAAGTACGAA  102400

Query  234     ATAGGGTAACTCCTTACTTATCACTCTGGTCTTCTGAGCCTTACTTTCTCAGCCCCCGGG  293
               |      |||||||||||||||| |||||||||||||| |||||||||         |
Sbjct  102401  A------AACTCCTTACTTATCACTTTGGTCTTCTGAGCCTGACTTTCTCA--------G  102446

Query  294     GCTACTAATGGGGAAACAATGTGTGGATAAACCCAAGGCTTCCAATGTCCAGGGTCCTGG  353
               |||||||||||||||||| ||||||||||||||||||||||||||||||||||||||||
Sbjct  102447  GCTACTAATGGGGAAACAGTGTGTGGATAAACCCAAGGCTTCCAATGTCCAGGGTCCTGG  102506

Query  354     AAA  356
               |||
Sbjct  102507  AAA  102509
```

```
101641 gacctgcagc tggctggaat ggacatggta ctgaacgatt aagggtttac gaaggcccca
101701 gggaccctct gactttaccc agtgggcagg agtaacccgta atcacggaca actgtctaca
101761 gaatgcaccg taccctcaaa cggacggcac cacctcctct ctgctccctc atttcacaaa
101821 acaaagaagc cggaagggaa tgggatgttt actgagcatg cccaagcaaa tcccccagac
101881 agaacccagg ctgcggctct cagctcagcc ttctcccttc ccctgctcat actaatcatt
101941 tagatggctt tattgagata gaactcacat gccgtacaag ttagttcaat ggcctccagt
102001 ccagacaact gcacccatga agacagtcta cagaattccc ataatccccct agttccaact
102061 ccccatccct ccgcatctca aggcccaggc agccacctgt ctccttcctc tctataggtg
102121 catcacacat tctgacagct ttggtttctg ttttcttcca cttagcctat ttctgtcctt
102181 actgtagcgt gtatcagggc ttcgttcctt ttcactgcca agtaatactc catggtccat
102241 acagcatagt ttattggtct cttaattaag ttagtgggca ggtgggttgc tttcactttt
102301 tctctcctgc ggatgacggc accgacaaca tcactgaaca tctttctgtg tccacgggtg
102361 cttttctcat ggattttctg gttcatacaa taagtacgaa aaactcctta cttatcactt
102421 tggtcttctg agcctgactt tctcaggcta ctaatgggga aacagtgtgt ggataaaccc
102481 aaggcttcca atgtccaggg tcctggaaac aagcctgccc ctttcctgtc ctccccacat
102541 cctctcccct cctctcttta ggccattctt cagagagcgg tgggacaact cctctctaac
```

TGATTTATTTAGTGGGTAGGAGTATATATAATTATTGATAGTTGTTATGAAAAATGTAATATGT
TTTTAAATTGATGGTATTTTTTTTTTTAGTAGTAATAATAAAGATTTAGGGAGGGGGTGAGTTTT
TTTTTGATTATGTTTAGGTAGAATATTAGATCGTTGTTTTGAGTTTAATTTTTTTTTTTTTTGTGT
TTATATTAATTATTTA**GATGGTTTTATTGAGATAGAATTTA**

Figure 3.8. The sequence of the HpaII band #4 - CpG island and bisulfite sequencing. The NCBI blast results are shown on the top. In the middle, the sequence attained from sequencing is highlighted in pink. The rest of the sequence was obtained from the NCBI. The potential enzyme cut site, CCGG, is highlighted in yellow. CpG sites are highlighted in red. The bisulfite sequencing primers' binding site is bold and underlined. On the bottom, the sequence obtained from bisulfite sequencing is shown. The hamster sequence was different from the mouse sequence shown in the middle. CCGG site could not be identified and only two CpG sites are detected.

```
>emb|AL627074.11| Mouse DNA sequence from clone RP23-465A17 on chromosome 3 Cont
a glycine cleavage system protein H (aminomethyl carrier)
(Gcsh) pseudogene, a lysosomal associated protein transmembrane
pseudogene, the 3' end of the Spata5 gene for spermatogenesis
associated 5, a px19-lie protein (PX19) pseudogene
and a CpG island, complete sequence
Length=177133

 Score =  183 bits (202),  Expect = 1e-43
 Identities = 103/104 (99%), Gaps = 0/104 (0%)
 Strand=Plus/Minus

Query  1       AGCTTTTCCAGAGAGGCATTTCCTTCCTTGAGGTCCTCACAGAAAAGTCTGCTTTATTTT  60
               ||||||||||||||||||||||||||||||||||||||||||||||||||||||||||||
Sbjct  162798  AGCTTTTCCAGAGAGGCATTTCCTTCCTTGAGGTCCTCACAGAAAAGTCTGCTTTATTTT  162739

Query  61      TAGTAATATCCTGGCTCCTGGTATTGTGTTTGTGCACATAATCC  104
               |||||||||||||||||||||||| ||||||||||||||||
Sbjct  162738  TAGTAATATCCTGGCTCCTGGTATTGTATTTGTGCACATAATCC  162695
```

```
162421 caccctcctc ttctgattca ttttactctg atttcttcct ttcctgtgga cttaatcagc
162481 cagcccggca ctgaggacga attccattcg gaaacacact ggggaagaag gcaaaagaat
162541 tttggcaaaa tcacaaaatg ggaataataa tacagagatc ggaatggaac acccacccat
162601 ctcacccggg tgctgggaga attaattaac gtctgtaaag gcctttgagt tccttggggg
162661 gacgtgccac cagacagcta gcgttattgt ggaggatta tgtgcacaaa tacaatacca
162721 ggagccagga tattactaaa aataaagcag actttctgt gaggacctca aggaaggaaa
162781 tgcctctctg gaaaagctta actctccttt aattccatcg cttgggctgc cggggacaga
162841 acagcaaagc cgagattcca ctgtgagaag aggattatgt tttctgagca ttgtcaaggt
```

TATTGGGGAAGAAGGTAAAAGAATTTTGGTAAAATTATAAAATGGGAATAATAATATAGAGA
TCGGAATGGAATTTTTATTTATTTTATTCGGGTGTTGGGAGAATTAATTAACGTTTGTGAAGGT
TTTTGAGTTTTTTGGGGGGACGTGTTATTAGATAGTTATCGTTATTGTGGAGGGATTATGTGT
ATAAATATAATATTAGGAGTTAGGATATTATTAAAAATAAAGTAGATTTTT**TTGTGAGGATTTT**
AAGGAAGG

Figure 3.9. The sequence of the HpaII band #10 - CpG island and bisulfite sequencing. The NCBI blast results are shown on the top. In the middle, the sequence attained from sequencing is highlighted in pink. The rest of the sequence was obtained from the NCBI. The potential enzyme cut site, CCGG, is highlighted in yellow. CpG sites are highlighted in red. The bisulfite sequencing primers' binding site is bold and underlined. On the bottom, the sequence obtained from bisulfite sequencing is shown. The hamster sequence was almost identical to the mouse sequence shown in the middle. CCGG site and all the CpG sites are detected.

```
>emb|AL807774.10| Mouse DNA sequence from clone RP23-198L2 on chromosome 4 Contains
the 5' end of the Ptprf gene for protein tyrosine phosphatase
receptor type F and a CpG island, complete sequence
Length=67374

 Score =  194 bits (214),  Expect = 1e-46
 Identities = 124/134 (93%), Gaps = 1/134 (0%)
 Strand=Plus/Minus

Query  1      GGAGACATCGCTTGGCCTTCACATATGAGCACAAGGACAATGCCTCCCCTCCAGGCCTAG  60
              ||||||||| ||||||||||||||||||||||||||||| ||||||||||||||||||| |
Sbjct  47636  GGAGACATCACTTGGCCTTCACATATGAGCACAAGGACA-TGCCTCCCCTCCAGGCCTCG  47578

Query  61     GAGCAGGGCAGCAGGGGCAGGTCCGCAAGGACCTTGTGCTCAGAGTTTGACAATGTGGCC  120
              |||||||||||||||||||||||| ||| |||||| |||||||||||||||||||| ||| |
Sbjct  47577  GAGCAGGGCAGCAGGGGCAGGTCTGCATGGACCCTGTGCTCAGAGTTTGACAATCTGGTC  47518

Query  121    TGAGCCCTGGCTTT  134
              |||| | ||||||| 
Sbjct  47517  TGAGACTTGGCTTT  47504
```

```
47341 gaaggctggg cagaagaaca ctgggacccc tatggtctaa tttcagaatg tatagcacct
47401 ggctgcccac aaactcaggg gaatgaaaca gaggctcagg ccctgaggcc acaggatgag
47461 agaacagtct tgggggggg gactagatgg catatgaaga aataaagcca agtctcagac
47521 cagattgtca aactctgagc acagggtcca tgcagacctg cccctgctgc cctgctccga
47581 ggcctggagg ggaggcatgt ccttgtgctc atatgtgaag gccaagtgat gtctccctggc
47641 agcagtgctg tgtctgctgt gtcccagccc cagggtgcag ggtgagggaa gcgccagatg
```

AGGGGAATGAAATAGAGGTTTAGGGTTTGAGGTTATATGATAAGAGGAAAAGAAAATTTTTA
GGTGATCGGTTTTAGATGGTATATAAAGAAAAATAAAGTTAGGGTTTAGATTA**GATTGTTAAA**
TTTTGAGTATAAGGT

Figure 3.10. The sequence of the MspI band #9 - PTPR-F promoter and bisulfite sequencing. The NCBI blast results are shown on the top. In the middle, the sequence attained from sequencing is highlighted in pink. The rest of the sequence was obtained from the NCBI. The potential enzyme cut sites CCTG and CAGG are highlighted in gray and green, respectively. CpC sites are highlighted in violet. The bisulfite sequencing primers' binding site is bold and underlined. On the bottom, the sequence obtained from bisulfite sequencing is shown. The hamster sequence was different from the mouse sequence shown in the middle. CCTG site, some CpC sites and a CpG site are detected.

MiRNA

MiRNA microarrays were used to identify the miRNA differentially expressed between the clones and the GM10115 control based on defined criteria ($p \leq 0.05$, signal ≥ 100, and fold change ≥ 1.5). A trend was observed such that CS9 and LS12, and 115 and Fe5.0-8 unstable clones had similar expression patterns to each other and different from the control and the stable clones. There were nine miRNA differentially expressed in the group CS9 & LS12 (mmu-miR-466f-3p, mmu-miR-466i, mmu-miR-467a, mmu-miR-467b, mmu-miR-467f, mmu-miR-669f, mmu-miR-1187, hsa-miR-130a, hsa-miR-574-5p) and six miRNA in the group 115 & Fe.5.0-8 (mmu-miR-466g, hsa-miR-15a, hsa-miR-30a, hsa-miR-30b, hsa-miR-191, hsa-miR-195) compared to control and stable clones. Among the candidate miRNA identified by the microarray, those with a signal equal to or above 500 and those involved in pathways of interest were validated with qRT-PCR (Table 3.3). Final validation of these miRNA requires knockdown or overexpression analysis and eventually a biological readout.

	Fold Change Microarray		Fold Change qRT-PCR	
	115	**Fe5.0-8**	**115**	**Fe5.0-8**
miRNA				
mmu-miR-466g	1.53	1.74	1.38	1.40

Table 3.3. MiRNA altered in unstable clones 115 and Fe5.0-8, identified by microarray analysis and validated by qRT-PCR.

Gene expression microarray results also showed a similar trend such that CS9 and LS12, and 115 and Fe5.0-8 unstable clones had similar expression patterns to each other and different from the control and the stable clones. In addition to the gene expression array, the gene targets for the miRNA were also identified using three different predictive databases. The common genes identified by both the three different target databases and the gene expression microarray were merged. This merged list of gene targets was used for pathway analysis using the DAVID database. Mmu-miR-466g is thought to be involved in apoptosis and chromatin remodeling (Table 3.4). However, the target genes obtained from the gene expression array were not validated.

	Apoptosis	Chromatin remodeling
miRNA		
mmu-miR-466g	ZFP91, GSPT1, MCL1	BPTF, UBN1, NCOR1, ATXN7L3

Table 3.4. Target genes of mmu-miR-466g and the functional pathways in which the genes are involved.

Discussion

NFκB has been identified as an important gene candidate potentially involved in RIGI in our GM10115 cell system [48]. The involvement of the *NFκB* gene in cellular responses to radiation exposure and in cancer has also been shown [153, 154]. *TSLC1* and *CDH1* gene promoter regions are hypermethylated in cancer cells and these genes also play a role in cancer progression [155, 156]. However, neither stable nor unstable clones had changes in DNA methylation at these promoter regions. To date, studies have

not looked into specific locus promoter methylation in cells with RIGI. Methylation changes in promoter regions of certain genes may be affected in cells with RIGI, however, *NFκB, TSLC1 and CDH1* may not be those genes. It is possible that our current study may be limited in observing such changes since it uses an *in vitro* cell culture model. Endpoints observed in complex tissue systems or whole organisms could be different than those observed in cells *in vitro*.

For the unstable clones LS12 and 115, the PCR of the *NFκB* promoter region showed a faint band and no band suggesting potential mono- and bi-allelic deletion of this region, respectively. This might also suggest that LS12 clone is heterogeneous and the *NFκB* promoter is deleted in subpopulations of cells. FISH analysis for chromosome 4 also shows a heterogeneous LS12 clone with 5 different subpopulations, therefore, some of these subpopulations may have lost a piece of chromosome 4 that includes the *NFκB* promoter. These deletions may be important in genomic instability. Previous studies from our lab have identified *NFκB* to be down-regulated [48]. The loss of the promoter region may offer an explanation for the down-regulation of *NFκB* mRNA.

Approximately thirty percent of the human genome is comprised of LINE-1 and Alu repeat elements that are hypermethylated to prevent reactivation of transposable DNA sequences [162, 163]. Hypomethylation of these repeat elements can lead to genomic instability and cancer [164-166]. In the unstable clones CS9 and LS12, hypermethylation of LINE-1 and in the unstable clones 115 and Fe5.0-8 hypomethylation of Alu was observed relative to control. No change in methylation was observed in the stable clones. Even though hypomethylation of repeat elements is known to lead to genomic instability, a study by Kaup et al. observed hypermethylation of repeat elements

in cells with RIGI [104]. In addition, since any aberration in DNA methylation is considered detrimental to the cell, the change itself may be more important than the direction of the change. Even though the changes in repeat element methylation observed in this assay are not large percent changes, the LINE-1 assay evaluates just two CpG sites and the Alu assay evaluates one CpG site. Therefore, the changes in this assay may represent a broader global change in methylation. The results from this assay suggest that aberrant repeat element DNA methylation is associated with RIGI. It can be extrapolated that the aberrant methylation observed in the repeat elements could be perpetuating the instability.

Cancer cells generally go through genome-wide hypomethylation [168]. This is in reference to CpG methylation as studies have predominantly looked into methylation at these sites. Methylation at non-CpG sites has been identified by numerous studies in the past and also more recently [51-53, 55, 56]. In embryonic stem cells, non-CpG methylation is prevalent and thought to be mediated by DNMT3a [55]. Non-CpG methylation of *proliferator-activated receptor γ (PPARγ) coactivator-1 α* (*PGC-1α*) promoter has been shown to occur in somatic cells by DNMT3b [56]. Similar to CpG methylation, hypermethylation of non-CpG sites in *PGC-1α* promoter resulted in repression of its expression. However, only limited studies have described non-CpG methylation and it is controversial as to whether or not it exists in mammalian somatic cells [134]. For example, Rein et al. [135] have stated that non-CpG methylation does not occur and those reported by Woodcock et al. may be an experimental artifact [54].

In our global DNA methylation assay, we measured both the CpG methylation (internal cytosine methylation) and non-CpG methylation (external cytosine

methylation). Non-CpG methylation can occur at cytosine-phosphate-adenine (CpA), cytosine-phosphate-thymine (CpT), and CpC sites but with this assay we only measured CpC methylation. At the CpG site, no change in global methylation was observed. Individual band measurements showed hypomethylation of bands #8 and 9 more significantly in unstable clones 115 and Fe. There was no change in methylation in bands #4 and 10 and bisulfite sequencing validated this observation. At the CpC site, global hypomethylation in the unstable clones LS12, 115, and Fe5.0-8 was shown. Individual band measurements showed that all the bands except for #4, 5 and 7 were hypomethylated. Despite this observation, bisulfite sequencing of band #9 showed no change in methylation between the stable clone 118 and unstable clone 115. Additionally, there was no CpC methylation observed. Therefore, there is no direct evidence of CpC methylation and more bands need to be analyzed to figure out whether CpC methylation exists in these cell lines. A study by Kaup et al. have observed both global hypomethylation and hypermethylation in cells with RIGI [104]. In terms of global non-CpG methylation, the literature provides no comparisons since non-CpG methylation in cells with RIGI has not been evaluated previously. The results from this assay suggest that aberrant global DNA methylation is mostly associated with RIGI. It could be extrapolated that the observed aberrant global methylation could be perpetuating the instability.

MiRNA regulate a number of cellular pathways and deregulation of miRNA expression levels can lead to cancer [81, 82]. In terms of validated miRNA, only mmu-miR-466g was differentially expressed in the unstable clones 115 and Fe.5.0-8 relative to control. These miRNA were not differentially expressed in the stable clones compared to

control. Changes in miRNA expression in cells with RIGI have not been studied previously. The potential functional targets of this miRNA suggest that it could play a role in apoptosis and chromatin remodeling. The genes in these pathways have been identified by mRNA expression aray, however, they are yet to be validated. Therefore, conclusions regarding pathways are limited at this point. That being said, the changes in these pathways, apoptosis and chromatin remodeling, are observed in cells with RIGI [132]. Alterations in the expression of miRNA and especially those involved in the pathways mentioned above have also been shown to be present in cancer cells [81]. The results from this assay may suggest that some aberrant miRNA expression may be observed in cells with RIGI. The aberrant miRNA expression and the resulting altered function of the targeted cellular pathways could potentially be perpetuating the instability. However, further examination will help better determine the relationship between miRNA changes and RIGI.

It is interesting to note that different unstable clones may be perpetuating RIGI through epigenetics but with slightly different mechanisms. CS9 and LS12 unstable clones were hypermethylated in LINE-1 repeat element and had different miRNA expression, while unstable clones 115 and Fe5.0-8 were hypomethylated in Alu repeat element and another set of miRNA were differentially expressed. This observation is in agreement with the mRNA microarray results of Snyder and Morgan, who observed differences between unstable clones in terms of gene expression and could not find a commonly altered gene to all unstable clones that could be the causative factor of RIGI [8]. This shows the heterogeneous nature of RIGI. The observed heterogeneity is similar to that seen in carcinogenesis in which the mechanism of initiation could vary based on

genes inactivated and the method of inactivation. DNA hypomethylation has been shown to arise later than DNA hypermethylation in prostate cancer progression that results in metastatic tumor heterogeneity [174]. Even though the exact mechanism of RIGI may vary from one clone to another, this study suggests that epigenetics might play a role in the perpetuation of RIGI.

This study is one of the few that has characterized DNA methylation changes in cells with RIGI and first to examine changes in miRNA expression in radiation-induced genomically unstable cells. Our findings suggest that epigenetic changes including subtle alterations in DNA methylation and change in a miRNA expression are associated with the unstable phenotype. Finally, this study demonstrated DNA methylation and miRNA expression changes in chromosomally unstable clones suggesting that epigenetic aberrations may be involved in perpetuating RIGI.

Chapter 4: CONCLUSIONS

Deciphering the mechanisms behind the phenomenon of radiation-induced genomic instability (RIGI) is critical in understanding radiation-induced carcinogenesis. This work is devoted to discovering epigenetic alterations that could elucidate the initiating and perpetuating mechanisms of RIGI. I hypothesized that radiation-induced epigenetic changes could be an initiating factor of the instability. These alterations may be heritable and persist at delayed times post-irradiation in the progeny of the irradiated cells. Alternatively or additionally, epigenetic alterations could be a late arising delayed effect of irradiation driving the perpetuation of the instability.

This work shows epigenetic alterations, including aberrant methylation and changes in microRNA (miRNA) expression, induced by irradiation. There were differing outcomes in the epigenetic alterations between low and high LET radiations. Even though the validation is yet to be performed, the predicted functional targets of the miRNA are involved in pathways including chromatin remodeling and DNA methylation. However, FISH analysis suggested chromosomal stability in these clones, therefore, the epigenetic alterations might arise in the cell without initiating RIGI.

Radiation-induced epigenetic aberrations are observed in irradiated cells without RIGI but the progeny of irradiated cells at later times show only a few epigenetic changes in the stable clones 114 and 118. Aberrant epigenetic mechanisms may be repaired at later times after irradiation without leading to instability and those cells stay stable. RIGI might arise in cells that are unable to recover from radiation-induced epigenetic aberrations and/or those that also acquire other epigenetic alterations.

In the unstable clones, CS9, LS12, 115 and Fe5.0-8, I demonstrate that epigenetic changes are associated with RIGI. Even though this is yet to be validated, aberrantly expressed miRNA is predicted to play a role in apoptosis and chromatin remodeling. Thus, DNA methylation and miRNA expression changes in chromosomally unstable clones could suggest that epigenetic aberrations may be perpetuating RIGI.

Low and high LET radiation-induced epigenetic alterations are shown to be different post-irradiation since fewer incidences of both DNA methylation and miRNA expression were observed after Fe ion irradiations than x-rays. However, at delayed times the epigenetic aberrations perpetuated in unstable clones are not distinct based on the irradiation history but the status of instability. Unstable clones 115 and Fe5.0-8 showed similar epigenetic aberrations even though they were obtained after low LET and high LET irradiation, respectively. This observation might suggest that late arising epigenetic aberrations could be involved, or that instability is perpetuated by specific types of epigenetic alterations.

Even though epigenetics may be involved in initiating and perpetuating RIGI, distinct epigenetic alterations are observed. Different epigenetic aberrations are shown in unstable clones such as CS9 and LS12 vs. 115 and Fe5.0-8. While CS9 and LS12 were

hypermethylated in LINE-1 repeat element and had distinctive miRNA expression, 115 and Fe5.0-8 were hypomethylated in Alu repeat element and another set of miRNA were differentially expressed. This demonstrates the heterogeneous nature of RIGI. This is similar to carcinogenesis in which the mechanism of initiation could vary based on genes inactivated and the method of inactivation. There may not be one specific mechanism for RIGI but many different ones that lead to this phenotype. Further investigation needs to be performed to pinpoint the exact epigenetic mechanisms involved in RIGI. RIGI, in unstable clones, is likely due to a combination of events that ultimately lead to a common outcome and may not follow an identical pathway for each clone.

REFERENCES

1. Ullrich, R.L. and B. Ponnaiya, *Radiation-induced instability and its relation to radiation carcinogenesis.* Int J Radiat Biol 1998. 74: p. 747-54.
2. Little, J.B., *Radiation carcinogenesis.* Carcinogenesis, 2000. 21: p. 397-404.
3. Morgan, W.F., *Non-targeted and Delayed effects of exposure to ionizing radiation: I. Radiation-induced genomic instability and bystander effects in vitro.* Radiat Res, 2003. 159: p. 567-80.
4. Wright, E.G., *Manifestations and mechanisms of non-targeted effects of ionizing radiation.* Mutat Res, 2010. 687: p. 28-33.
5. Marder, B.A. and W.F. Morgan, *Delayed chromosomal instability induced by DNA damage.* Mol Cell Biol, 1993. 13: p. 6667-77.
6. Limoli, C.L., M.I. Kaplan, J. Corcoran, M. Meyers, D.A. Boothman, and W.F. Morgan, *Chromosomal instability and its relationship to other end points of genomic instability.* Cancer Res, 1997. 57: p. 5557-63.
7. Morgan, W.F., J. Corcoran, A. Hartmann, M.I. Kaplan, C.L. Limoli, and B. Ponnaiya, *DNA double-strand breaks, chromosomal rerrangements, and genomic instability.* Mutat Res, 1998. 404: p. 125-8.
8. Snyder, A.R. and W.F. Morgan, *Lack of consensus gene expression changes associated with radiation-induced chromosomal instability.* DNA Repair (Amst.), 2005. 4: p. 958-70.
9. Jones, P.A. and S.B. Baylin, *The epigenomics of cancer.* Cell, 2007. 128: p. 683-92.
10. Kovalchuk, O. and J.E. Baulch, *Epigenetic changes and nontargeted radiation effects—is there a link?* Environ Mol Mutagen, 2008. 49: p. 16-25.
11. Tawa, R., Y. Kimura, J. Komura, Y. Miyamura, A. Kurishita, M.S. Sasaki, H. Sakurai, and T. Ono, *Effects of X-ray irradiation on genomic DNA methylation levels in mouse tissues.* J Radiat Res, 1998. 39: p. 271-8.
12. Pogribny, I., J. Raiche, M. Slovack, and O. Kovalchuk, *Dose-dependence, sex- and tissue-specificity and persistence of radiation-induced genomic DNA methylation changes.* Biochem Biophys Res Commun, 2004. 320: p. 1253-61.
13. Upton, A.C., *Historical perspectives on radiation carcinogenesis.* Radiation Carcinogenesis, 1986. : p. 1-10.
14. Ward, J.F., *DNA damage produced by ionizing radiation in mammalian cells: identities, mechanisms of formation, and reparability.* Prog Nucleic Acid Res Mol Biol, 1988. 35: p. 95-125.
15. Snyder, A.R. and W.F. Morgan, *Radiation-induced chromosomal instability and gene expression profiling: searching for clues to initiation and perpetuation.* Mutat Res, 2004. 568: p. 89-96.
16. Waldren, C.A., *Classical radiation biology dogma, bystander effects and paradigm shifts.* Hum Exp Toxicol 2004. 23: p. 95-100.
17. Spitz, D.R., E.I. Azzam, J.J. Li, and D. Gius, *Metabolic oxidation/reduction reactions and cellular responses to ionizing radiation: a unifying concept in stress response biology.* Cancer Metastasis Rev, 2004. 23: p. 311-22.

18. Lorimore, S.A., P.J. Coates, and E.G. Wright, *Radiation-induced genomic instability and bystander effects: inter-related nontargeted effects of exposire to ionizing radiation.* Oncogene, 2003. 22: p. 7058-69.
19. Sowa Resat, M.B. and W.F. Morgan, *Radiation-induced genomic instability: a role for secreted soluble factors in communicating the radiation response to non-irradiated cells.* J Cell Biochem, 2004. 92: p. 1013-9.
20. Morgan, W.F., J.P. Day, M.I. Kaplan, E.M. McGhee, and C.L. Limoli, *Genomic instability induced by ionizing radiation.* Radiat Res, 1996. 146: p. 247-58.
21. Morgan, W.F., *Non-targeted and delayed effects of exposure to ionizing radiation. II. Radiation-induced genomic instability and bystander effects in vivo, clastogenic factors and transgenerational effects.* Radiat Res, 2003. 159: p. 581-96.
22. Kadhim, M.A., D.A. Macdonald, D.T. Goodhead, S.A. Lorimore, S.J. Marsden, and E.G. Wright, *Transmission of chromosomal instability after plutonium alpha-particle irradiation.* Nature, 1992. 355: p. 738-740.
23. Watson, G.E., S.A. Lorimore, D.A. Macdonald, and E.G. Wright, *Chromosomal instability in unirradiated cells induced in vivo by a bystander effect of ionizing radiation.* Cancer Res, 2000. 60: p. 5608-11.
24. Lorimore, S.A., P.J. Coates, G.E. Scobie, G. Milne, and E.G. Wright, *Inflammatory-type responses after exposure to ionizing radiation in vivo: a mechanism for radiation-induced bystander effects?* Oncogene, 2001. 20: p. 7085-7095.
25. Lorimore, S.A. and E.G. Wright, *Radiation-induced genomic instability and bystander effects: related inflammatory-type responses to radiation-induced stress and injury? A review.* Int J Radiat Biol, 2003. 79: p. 15-25.
26. Kadhim, M.A., S.A. Lorimore, M.D. Hepburn, D.T. Goodhead, V.J. Buckle, and E.G. Wright, *Alpha-particle-induced chromosomal instability in human bone marrow cells.* Lancet, 1994. 344: p. 987-988.
27. Holmberg, K., S. Falt, A. Johansson, and B. Lambert, *Clonal chromosome aberrations and genomic instability in X-irradiated human T-lymphocyte cultures.* Mutat Res, 1993. 286: p. 321-30.
28. Holmberg, K., A.E. Meijer, G. Auer, and B.O. Lambert, *Delayed chromosomal instability in human T-lymphocyte clones exposed to ionizing radiation.* Int J Radiat Biol, 1995. 68: p. 245-55.
29. Pommier, J.P., J. Lebeau, C. Ducray, and L. Sabatier, *Chromosomal instability and alteration of telomere repeat sequences.* Biochimie, 1995. 77: p. 817-825.
30. Lambert, B., K. Holmberg, P. Hackman, and A. Wennborg, *Radiation induced chromosomal instability in human T-lymphocytes.* Mutat Res, 1998. 405: p. 161-70.
31. Romney, C.A., J.D. Paulauskis, H. Nagasawa, and J.B. Little, *Multiple manifestations of X-ray-induced genomic instability in Chinese hamster ovary (CHO) cells.* Mol Carcinog, 2001. 32: p. 118-27.
32. Limoli, C.L., B. Ponnaiya, J.J. Corcoran, E. Giedzinski, and W.F. Morgan, *Chromosomal instability induced by heavy ion irradiation.* Int J Radiat Biol, 2000. 76: p. 1599-606.
33. Limoli, C.L., M.I. Kaplan, J.W. Phillips, G.M. Adair, and W.F. Morgan, *Differential induction of chromosomal instability by DNA strand-breaking agents.* Cancer Res, 1997. 57: p. 4048-56.
34. Ponnaiya, B., C.L. Limoli, J. Corcoran, M.I. Kaplan, A. Hartmann, and W.F. Morgan, *The evolution of chromosomal instability in Chinese hamster cells: a changing picture?* Int J Radiat Biol, 1998. 74: p. 765-70.
35. Clutton, S.M., K.M. Townsend, C. Walker, J.D. Ansell, and E.G. Wright, *Radiation-induced genomic instability and persisting oxidative stress in primary bone marrow cultures.* Carcinogenesis, 1996. 17: p. 1633-1639.
36. Limoli, C.L., A. Hartmann, L. Shephard, C. Yang, D.A. Boothman, J. Bartholomew, and W.F. Morgan, *Apoptosis, reproductive failure, and oxidative stress in Chinese hamster ovary cells with compromised genomic integrity.* Cancer Res, 1998. 58: p. 3712-8.
37. Limoli, C.L., E. Giedzinski, W.F. Morgan, S.G. Swarts, G.D. Jones, and W. Hyun, *Persistent oxidative stress in chromosomally unstable cells.* Cancer Res, 2003. 63: p. 3107-11.
38. Kim, G.J., G.M. Fiskum, and W.F. Morgan, *A role for mitochondrial dysfunction in perpetuating radiation-induced genomic instability.* Cancer Res, 2006. 66: p. 10377-83.

39. Kim, G.J., K. Chandrasekaran, and W.F. Morgan, *Mitochondrial dysfunction, persistently elevated levels of reactive oxygen species and radiation-induced genomic instability: a review.* Mutagenesis, 2006. 21: p. 361-367.
40. Miller, J.H., S. Jin, W.F. Morgan, A. Yang, Y. Wan, U. Aypar, J.S. Peters, and D.L. Springer, *Profiling mitochondrial proteins in radiation-induced genome-unstable cell lines with persistent oxidative stress by mass spectrometry.* Radiat Res, 2008. 169: p. 700-6.
41. Dayal, D., S.M. Martin, C.L. Limoli, and D.R. Spitz, *Hydrogen peroxide mediates the radiation-induced mutator phenotype in mammalian cells.* Biochem J, 2008. 413: p. 185-91.
42. Dayal, D., S.M. Martin, K.M. Owens, N. Aykin-Burns, Y. Zhu, A. Boominathan, D. Pain, C.L. Limoli, P.C. Goswami, F.E. Domann, and D.R. Spitz, *Mitochondrial complex II dysfunction can contribute significantly to genomic instability after exposure to ionizing radiation.* Radiat Res, 2009. 172: p. 737-45.
43. Nagar, S., L.E. Smith, and W.F. Morgan, *Characterization of a novel epigenetic effect of ionizing radiation: The death-inducing effect.* Cancer Res 2003. 63: p. 324-8.
44. Nagar, S. and W.F. Morgan, *The death-inducing effect and genomic instability.* Radiat Res, 2005. 163: p. 316-23.
45. Morgan, W.F., A. Hartmann, C.L. Limoli, S. Nagar, and B. Ponnaiya, *Bystander effects in radiation-induced genomic instability.* Mutat Res, 2002. 504: p. 91-100.
46. Laiakis, E.C., J.E. Baulch, and W.F. Morgan, *Interleukin 8 exhibits a pro-mitogenic and pro-survival role in radiation induced genomically unstable cells.* Mutat Res, 2008. 640: p. 74-81.
47. Snyder, A.R. and W.F. Morgan, *Persistent oxidative stress and gene expression changes in radiation-induced genomic instability.* Int Congr Ser, 2003. 1258: p. 199-206.
48. Snyder, A.R. and W.F. Morgan, *Differential induction and activation of NF-kB transcription complexes in radiation-induced chromosomally unstable cell lines.* Environ Mol Mutagen, 2005. 45: p. 177-87.
49. Jirtle, R.L. and M.K. Skinner, *Environmental epigenomics and disease susceptibility.* Nat Rev Genet, 2007. 8: p. 253-62.
50. Gronbaek, K., C. Hother, and P.A. Jones, *Epigenetic changes in cancer.* APMIS, 2007. 115: p. 1039-59.
51. Salomon, R. and A.M. Kaye, *Methylation of mouse DNA in vivo: di- and tripyrimidine sequences containing 5-methylcytosine.* Biochim Biophys Acta, 1970. 204: p. 340-51.
52. Grafstrom, R.H., R. Yuan, and D.L. Hamilton, *The characteristics of DNA methylation in an in vitro DNA synthesizing system from mouse fibroblasts.* Nucleic Acids Res, 1985. 13: p. 2827-42.
53. Nyce, J., L. Liu, and P.A. Jones, *Variable effects of DNA-synthesis inhibitors upon DNA methylation in mammalian cells.* Nucleic Acids Res, 1986. 14: p. 4353-67.
54. Woodcock, D.M., P.J. Crowther, and W.P. Diver, *The majority of methylated deoxycytidines in human DNA are not in the CpG dinucleotide.* Biochem Biophys Res Commun, 1987. 145: p. 888-94.
55. Ramsahoye, B.H., D. Biniszkiewicz, F. Lyko, V. Clark, A.P. Bird, and R. Jaenisch, *Non-CpG methylation is prevalent in embryonic stem cells and may be mediated by DNA methyltransferase 3a.* Proc Natl Acad Sci U S A, 2000. 97: p. 5237-42.
56. Barres, R., M.E. Osler, J. Yan, A. Rune, T. Fritz, K. Caidahl, A. Krook, and J.R. Zierath, *Non-CpG methylation of the PGC-1alpha promoter through DNMT3B controls mitochondrial density.* Cell Metab, 2009. 10: p. 189-98.
57. Bestor, T.H., *The DNA methyltransferases of mammals.* Hum Mol Genet, 2009. 9: p. 2395-402.
58. Okano, M., D.W. Bell, D.A. Haber, and E. Li, *DNA methyltransferases Dnmt3a and Dnmt3b are essential for de novo methylation and mammalian development.* Cell, 1999. 99: p. 247-57.
59. Goll, M.G., F. Kirpekar, K.A. Maggert, J.A. Yoder, C.L. Hsieh, X. Zhang, K.G. Golic, S.E. Jacobsen, and T.H. Bestor, *Methylation of tRNAAsp by the DNA methyltransferase homolog Dnmt2.* Science, 2006. 311: p. 395-8.
60. Herman, J.G. and S.B. Baylin, *Gene silencing in cancer in association with promoter hypermethylation.* N Engl J Med, 2003. 349: p. 2042-54.
61. Feinberg, A.P., H. Cui, and R. Ohlsson, *DNA methylation and genomic imprinting: insights from cancer into epigenetic mechanisms.* Semin Cancer Biol, 2002. 12: p. 389-98.
62. Reik, W. and A. Lewis, *Co-evolution of X-chromosome inactivation and imprinting in mammals.* Nat Rev Genet, 2005. 6: p. 403-10.

63. Bestor, T.H., *Transposons reanimated in mice.* Cell, 2005. 122: p. 322-5.
64. Xu, G.L., T.H. Bestor, D. Bourc'his, C.L. Hsieh, N. Tommerup, M. Bugge, M. Hulten, X. Qu, J.J. Russo, and E. Viegas-Péquignot, *Chromosome instability and immunodeficiency syndrome caused by mutations in a DNA methyltransferase gene.* Nature, 1999. 402: p. 187-91.
65. Wang, G.G., C.D. Allis, and P. Chi, *Chromatin remodeling and cancer, Part I: Covalent histone modifications.* Trends Mol Med, 2007. 13: p. 363-72.
66. Zhou, W., X. Wang, and M.G. Rosenfeld, *Histone H2A ubiquitination in transcriptional regulation and DNA damage repair.* Int J Biochem Cell Biol, 2009. 41: p. 12-5.
67. Rogakou, E.P., D.R. Pilch, A.H. Orr, V.S. Ivanova, and W.M. Bonner, *DNA double-stranded breaks induce histone H2AX phosphorylation on serine 139.* J Biol Chem, 1998. 273: p. 5858-68.
68. Fernandez-Capetillo, O., A. Lee, M. Nussenzweig, and A. Nussenzweig, *H2AX: the histone guardian of the genome.* DNA Repair, 2004. 3: p. 959-67.
69. Fillingham, J., M.C. Keogh, and N.J. Krogan, *GammaH2AX and its role in DNA double-strand break repair.* Biochem Cell Biol, 2006. 84: p. 568-77.
70. Yin, B. and C.H. Bassing, *The sticky business of histone H2AX in V(D)J recombination, maintenance of genomic stability, and suppression of lymphoma.* Immunol Res, 2008. 42: p. 29-40.
71. Srivastava, N., S. Gochhait, P. de Boer, and R.N. Bamezai, *Role of H2AX in DNA damage response and human cancers.* Mutat Res, 2009. 681: p. 180-8.
72. Cai, X., C.H. Hagedorn, and B.R. Cullen, *Human microRNAs are processed from capped, polyadenylated transcripts that can also function as mRNAs.* RNA, 2004. 10: p. 1957-66.
73. Lee, Y., M. Kim, J. Han, K.H. Yeom, S. Lee, S.H. Baek, and V.N. Kim, *MicroRNA genes are transcribed by RNA polymerase II.* EMBO J, 2004. 23: p. 4051-60.
74. Lee, Y., C. Ahn, J. Han, H. Choi, J. Kim, J. Yim, J. Lee, P. Provost, O. Rådmark, S. Kim, and V.N. Kim, *The nuclear RNase III Drosha initiates microRNA processing.* Nature, 2003. 425: p. 415-9.
75. Landthaler, M., A. Yalcin, and T. Tuschl, *The human DiGeorge syndrome critical region gene 8 and its D. melanogaster homolog are required for miRNA biogenesis.* Curr Biol, 2004. 14: p. 2162-7.
76. Yi, R., Y. Qin, I.G. Macara, and B.R. Cullen, *Exportin-5 mediates the nuclear export of pre-microRNAs and short hairpin RNAs.* Genes Dev, 2003. 17: p. 3011-6.
77. Lee, Y., K. Jeon, J.T. Lee, S. Kim, and V.N. Kim, *MicroRNA maturation: stepwise processing and subcellular localization.* EMBO J, 2002. 21: p. 4663-70.
78. Meister, G., M. Landthaler, A. Patkaniowska, Y. Dorsett, G. Teng, and T. Tuschl, *Human Argonaute2 mediates RNA cleavage targeted by miRNAs and siRNAs.* Mol Cell, 2004. 15: p. 185-97.
79. Schwarz, D.S., G. Hutvágner, T. Du, Z. Xu, N. Aronin, and P.D. Zamore, *Asymmetry in the assembly of the RNAi enzyme complex.* Cell, 2003. 115: p. 199-208.
80. Stark, A., J. Brennecke, N. Bushati, R.B. Russell, and S.M. Cohen, *Animal MicroRNAs confer robustness to gene expression and have a significant impact on 3' UTR evolution.* Cell, 2005. 123: p. 1133-46.
81. Cowland, J.B., C. Hother, and K. Gronbaek, *MicroRNAs and cancer.* APMIS, 2007. 115: p. 1090-106.
82. Schickel, R., B. Boyerinas, S.M. Park, and M.E. Peter, *MicroRNAs: key players in the immune system, differentiation, tumorigenesis and cell death.* Oncogene, 2008. 27: p. 5959-74.
83. Jones, P.A. and S.B. Baylin, *The fundamental role of epigenetic events in cancer.* Nat Rev Genet, 2002. 3: p. 415-28.
84. Nakayama, M., H. Wada, T. Harada, J. Nagayama, H. Kusaba, K. Ohshima, M. Kozuru, H. Komatsu, R. Ueda, and M. Kuwano, *Hypomethylation status of CpG sites at the promoter region and overexpression of the human MDR1 gene in acute myeloid leukemias.* Blood, 1998. 92: p. 4296-307.
85. Brock, M.V., J.G. Herman, and S.B. Baylin, *Cancer as a manifestation of aberrant chromatin structure.* Cancer J, 2007. 13: p. 3-8.
86. Wang, G.G., C.D. Allis, and P. Chi, *Chromatin remodeling and cancer, Part II: ATP-dependent chromatin remodeling.* Trends Mol Med, 2007. 13: p. 373-80.

87. Lafon-Hughes, L., M.V. Di Tomaso, L. Méndez-Acuña, and W. Martínez-López, *Chromatin-remodelling mechanisms in cancer.* Mutat Res, 2008. 658: p. 191-214.
88. Guil, S. and M. Esteller, *DNA methylomes, histone codes and miRNAs: Tying it all together.* Int J Biochem Cell Biol, 2009. 41: p. 87-95.
89. Wilkins, J.A. and O.J. Sansom, *C-Myc is a critical mediator of the phenotypes of Apc loss in the intestine.* Cancer Res, 2008. 68: p. 4963-6.
90. Trani, D., K. Datta, K. Doiron, B. Kallakury, and A.J. Fornace, Jr., *Enhanced intestinal tumor multiplicity and grade in vivo after HZE exposure: mouse models for space radiation risk estimates.* Radiat Environ Biophys, 2010. 49: p. 389-96.
91. Taniguchi, H., H. Yamamoto, T. Hirata, N. Miyamoto, M. Oki, K. Nosho, Y. Adachi, T. Endo, K. Imai, and Y. Shinomura, *Frequent epigenetic inactivation of Wnt inhibitory factor-1 in human gastrointestinal cancers.* Oncogene, 2005. 24: p. 7946-7952.
92. Prochownik, E.V. and Y. Li, *The ever expanding role for c-Myc in promoting genomic instability.* Cell Cycle, 2007. 6: p. 1024-9.
93. Pendas-Franco, N., O. Aguilera, F. Pereira, J.M. Gonzalez-Sancho, and A. Munoz, *Vitamin D and Wnt/beta-catenin pathway in colon cancer: role and regulation of DICKKOPF genes.* Anticancer Res, 2008. 28: p. 2613-23.
94. Klarmann, G.J., A. Decker, and W.L. Farrar, *Epigenetic gene silencing in the Wnt pathway in breast cancer.* Epigenetics, 2008. 3: p. 59-63.
95. Hu, H., L. Du, G. Nagabayashi, R.C. Seeger, and R.A. Gatti, *ATM is down-regulated by N-Myc-regulated microRNA-421.* Proc Natl Acad Sci U S A, 2010. 107: p. 1506-11.
96. Raiche, J., R. Rodriguez-Juarez, I. Pogribny, and O. Kovalchuk, *Sex and tissue specific expression of maintenance and de novo DNA methyltransferases upon low dose X-irradiation in mice.* Biochem Biophys Res Commun, 2004. 325: p. 39-47.
97. Kalinich, J.F., G.N. Catravas, and S.L. Snyder, *The effect of γ irradiation on DNA methylation.* Radiat Res, 1989. 117: p. 185-97.
98. Koturbash, I., M. Baker, J. Loree, K. Kutanzi, D. Hudson, I. Pogribny, O. Sedelnikova, W. Bonner, and O. Kovalchuk, *Epigenetic dysregulation underlies radiation-induced transgenerational genome instability in vivo.* Int J Radiat Oncol Biol Phys, 2006. 66: p. 327-30.
99. Kovalchuk, O., P. Burke, A. Arkhipov, N. Kuchma, S.J. James, I. Kovalchuk, and I. Pogribny, *Genome hypermethylation in Pinus silvestris of Chernobyl—a mechanism for radiation adaptation?* Mutat Res, 2003. 529: p. 13-20.
100. Koturbash, I., I. Pogribny, and O. Kovalchuk, *Stable loss of global DNA methylation in the radiation –target tissue—A possible mechanism contributing to radiation carcinogenesis?* Biochem Biophys Res Commun, 2005. 337: p. 526-33.
101. Loree, J., I. Koturbash, K. Kutanzi, M. Baker, I. Pogribny, and O. Kovalchuk, *Radiation-induced molecular changes in rat mammary tissue: Possible implications for radiation-induced carcinogenesis.* Int J Radiat Biol, 2006. 82: p. 805-15.
102. Pogribny, I., I. Koturbash, V. Tryndyak, D. Hudson, S.M. Stevenson, O. Sedelnikova, W. Bonner, and O. Kovalchuk, *Fractionated low-dose radiation exposure leads to accumulation of DNA damage and profound alterations in DNA and histone methylation in the murine thymus.* Mol Cancer Res, 2005. 3: p. 553-61.
103. Kovalchuk, O., P. Burke, J. Besplug, M. Slovack, J. Filkowski, and I. Pogribny, *Methylation changes in muscle and liver tissues of male and female mice exposed to acute and chronic low-dose X-ray-irradiation.* Mutat Res, 2004. 548: p. 75-84.
104. Kaup, S., V. Grandjean, R. Mukherjee, A. Kapoor, E. Keyes, C.B. Seymour, C.E. Mothersill, and P.N. Schofield, *Radiation-induced genomic instability is associated with DNA methylation changes in cultured human keratinocytes.* Mutat Res, 2006. 597: p. 87-97.
105. Schuffenhauer, S., O. Bartsch, M. Stumm, T. Buchholz, T. Petropoulou, S. Kraft, B. Belohradsky, G.K. Hinkel, T. Meitinger, and R.D. Wegner, *DNA, FISH and complementation studies in ICF syndrome: DNA hypomethylation of repetitive and single copy loci and evidence for a trans acting factor.* Hum Genet, 1995. 96: p. 562-71.
106. Cerda, S. and S.A. Weitzman, *Influence of oxygen radical injury on DNA methylation.* Mutat Res, 1997. 386: p. 141-52.
107. Franco, R., O. Schoneveld, A.G. Georgakilas, and M.I. Panayiotidis, *Oxidative stress, DNA methylation and carcinogenesis.* Cancer Lett, 2008. 266: p. 6-11.

108. Zawia, N.H., D.K. Lahiri, and F. Cardozo-Pelaez, *Epigenetics, oxidative stress, and Alzheimer disease.* Free Radic Biol Med, 2009. 46: p. 1241-9.
109. Roy, K., S. Kodama, K. Suzuki, K. Fukase, and M. Watanabe, *Hypoxia relieves X-ray-induced delayed effects in normal human embryo cells.* Radiat Res, 2000. 154: p. 659-66.
110. Limoli, C.L., M.I. Kaplan, E. Giedzinski, and W.F. Morgan, *Attenuation of radiation-induced genomic instability by free radical scavengers and cellular proliferation.* Free Radic Biol Med, 2001. 31: p. 10-9.
111. Kuo, L.J. and L.X. Yang, *Gamma-H2AX - a novel biomarker for DNA double-strand breaks.* In Vivo, 2008. 22: p. 305-9.
112. Karagiannis, T.C., K.N. Harikrishnan, and A. El-Osta, *Disparity of histone deacetylase inhibition on repair of radiation-induced DNA damage on euchromatin and constitutive heterochromatin compartments.* Oncogene, 2007. 26: p. 3963-71.
113. Vasireddy, R.S., T.C. Karagiannis, and A. El-Osta, *γ–radiation-induced γH2AX formation occurs preferentially in actively transcribing euchromatic loci.* Cell Mol Life Sci, 2010. 67: p. 291-4.
114. Falk, M., E. Lukasova, and S. Kozubek, *Chromatin structure influences the sensitivity of DNA to γ–radiation.* Biochim Biophys Acta, 2008. 1783: p. 2398-414.
115. Falk, M., E. Lukasova, B. Gabrielova, V. Ondrej, and S. Kozubek, *Chromatin dynamics during DSB repair.* Biochim Biophys Acta, 2007. 1773: p. 1534-45.
116. Park, J.H., E.J. Park, H.S. Lee, S.J. Kim, S.K. Hur, A.N. Imbalzano, and J. Kwon, *Mammalian SWI/SNF complexes facilitate DNA double-strand break repair by promoting gamma-H2AX induction.* EMBO J, 2006. 25: p. 3986-97.
117. Ziv, Y., D. Bielopolski, Y. Galanty, C. Lukas, Y. Taya, D.C. Schultz, J. Lukas, S. Bekker-Jensen, J. Bartek, and Y. Shiloh, *Chromatin relaxation in response to DNA double-strand breaks is modulated by a novel ATM- and KAP-1 dependent pathway.* Nat Cell Biol, 2006. 8: p. 870-6.
118. Goodarzi, A.A., A.T. Noon, D. Deckbar, Y. Ziv, Y. Shiloh, M. Lobrich, and P.A. Jeggo, *ATM signaling facilitates repair of DNA double-strand breaks associated with heterochromatin.* Mol Cell, 2008. 31: p. 167-77.
119. Ayoub, N., A.D. Jeyasekharan, J.A. Bernal, and A.R. Venkitaraman, *HP1-beta mobilization promotes chromatin changes that initiate the DNA damage response.* Nature, 2008. 453: p. 682-686.
120. Ishii, H. and T. Saito, *Radiation-induced response of micro RNA expression in murine embryonic stem cells.* Med Chem, 2006. 2: p. 555-63.
121. Maes, O.C., J. An, H. Sarojini, H. Wu, and E. Wang, *Changes in microRNA expression patterns in human fibroblasts after low-LET radiation.* J Cell Biochem, 2008. 105: p. 824-34.
122. Jaklevic, B., L. Uyetake, A. Wichmann, A. Bilak, C.N. English, and T.T. Su, *Modulation of ionizing radiation-induced apoptosis by bantam microRNA in Drosophila.* Dev Biol, 2008. 320: p. 122-30.
123. Ilnytskyy, Y., I. Koturbash, and O. Kovalchuk, *Radiation-induced bystander effects in vivo are epigenetically regulation in a tissue-specific manner.* Environ Mol Mutagen, 2009. 50: p. 105-13.
124. Tamminga, J., P. Kathiria, I. Koturbash, and O. Kovalchuk, *DNA damage-induced upregulation of miR-709 in the germline downregulates BORIS to counteract aberrant DNA hypomethylation.* Cell Cycle, 2008. 7: p. 3731-6.
125. Shin, S., H.J. Cha, E.M. Lee, S.J. Lee, S.K. Seo, H.O. Jin, I.C. Park, Y.W. Jin, and S. An, *Alteration of miRNA profiles by ionizing radiation in A549 human non-small cell lung cancer cells.* Int J Oncol, 2009. 35: p. 81-6.
126. Cha, H.J., S. Shin, H. Yoo, E.M. Lee, S. Bae, K.H. Yang, S.J. Lee, I.C. Park, Y.W. Jin, and S. An, *Identification of ionizing radiation-responsive microRNAs in the IM9 human B lymphoblastic cell line.* Int J Oncol, 2009. 34: p. 1661-8.
127. Cha, H.J., K.M. Seong, S. Bae, J.H. Jung, C.S. Kim, K.H. Yang, Y.W. Jin, and S. An, *Identification of specific microRNAs responding to low and high dose gamma-irradiation in the human lymphoblast line IM9.* Oncol Rep, 2009. 22: p. 863-8.
128. Shin, S., H.J. Cha, E.M. Lee, J.H. Jung, S.J. Lee, I.C. Park, Y.W. Jin, and S. An, *MicroRNAs are significantly influenced by p53 and radiation in HCT116 human colon carcinoma cells.* Int J Oncol, 2009. 34: p. 1645-52.

129. Simone, N.L., B.P. Soule, D. Ly, A.D. Saleh, J.E. Savage, W. Degraff, J. Cook, C.C. Harris, D. Gius, and J.B. Mitchell, *Ionizing radiation-induced oxidative stress alters miRNA expression.* PLoS One, 2009. 4: p. e6377.
130. Sonkoly, E. and A. Pivarcsi, *microRNAs in inflammation.* Int Rev Immunol, 2009. 28: p. 535-61.
131. Davidson-Moncada, J., F.N. Papavasiliou, and W. Tam, *MicroRNAs of the immune system: roles in inflammation and cancer.* Ann N Y Acad Sci, 2010. 1183: p. 183-94.
132. Aypar, U., W.F. Morgan, and J.E. Baulch, *Radiation-induced genomic instability: Are epigenetic mechanisms the missing link?* Int J Radiat Biol, 2010.
133. Herman, J.G. and S.B. Baylin, *Gene silencing in cancer in association with promoter hypermethylation.* N Engl J Med, 2003. 349: p. 2042-54.
134. Denisova, O.V., A.V. Chernov, T.Y. Koledachkina, and N.I. Matvienko, *A tag-based approach for high-throughput analysis of CCWGG methylation.* Anal Biochem, 2007. 369: p. 154-60.
135. Rein, T., H. Zorbas, and M.L. DePamphilis, *Active mammalian replication origins are associated with a high-density cluster of mCpG dinucleotides.* Mol Cell Biol, 1997. 17: p. 416-26.
136. Zeitlin, C., L. Heilbronn, and J. Miller, *Detailed characterization of the 1087 MeV/nucleon iron-56 beam used for radiobiology at the alternating gradient synchrotron.* Radiat Res, 1998. 149: p. 560-9.
137. Fenech, M., *The in vitro micronucleus technique.* Mutat Res, 2000. 455: p. 81-95.
138. Clark, S.J., J. Harrison, C.L. Paul, and M. Frommer, *High sensitivity mapping of methylated cytosines.* Nucleic Acids Res, 1994. 22: p. 2990-7.
139. Brandes, J.C., H. Carraway, and J.G. Herman, *Optimal primer design using the novel primer design program: MSPprimer provides accurate methylation analysis of the ATM promoter.* Oncogene, 2007. 26: p. 6229-37.
140. Ten, R.M., C.V. Paya, N. Israel, O. Le Bail, M.G. Mattei, J.L. Virelizier, P. Kourilsky, and A. Israel, *The characterization of the promoter of the gene encoding the p50 subunit of NF-kappa B indicates that it participates in its own regulation.* EMBO J, 1992. 11: p. 195-203.
141. Shimizu, K., M. Onishi, E. Sugata, H. Fujii, K. Honoki, and T. Tsujiuchi, *Aberrant DNA methylation of the 5′ upstream region of Tslc1 gene in hamster pancreatic tumors.* Biochem Biophys Res Commun, 2007. 353: p. 522-6.
142. Shimizu, K., M. Hanaoka, A. Kato, H. Fujii, K. Honoki, and T. Tsujiuchi, *Reduced expression of the E-cadherin gene and its aberrant DNA methylation in hamster pancreatic tumors.* Biochem Biophys Res Commun, 2005. 336: p. 49-53.
143. Yang, A.S., M.R. Estecio, K. Doshi, Y. Kondo, E.H. Tajara, and J.P. Issa, *A simple method for estimating global DNA methylation using bisulfite PCR of repetitive DNA elements.* Nucleic Acids Res, 2004. 32: p. e38.
144. Gonzalgo, M.L., G. Liang, C.H. Spruck, 3rd, J.M. Zingg, W.M. Rideout, 3rd, and P.A. Jones, *Identification and characterization of differentially methylated regions of genomic DNA by methylation-sensitive arbitrarily primed PCR.* Cancer Res, 1997. 57: p. 594-9.
145. Lewis, B.P., C.B. Burge, and D.P. Bartel, *Conserved seed pairing, often flanked by adenosines, indicates that thousands of human genes are microRNA targets.* Cell, 2005. 120: p. 15-20.
146. Krek, A., D. Grun, M.N. Poy, R. Wolf, L. Rosenberg, E.J. Epstein, P. MacMenamin, I. da Piedade, K.C. Gunsalus, M. Stoffel, and N. Rajewsky, *Combinatorial microRNA target predictions.* Nat Genet, 2005. 37: p. 495-500.
147. Betel, D., M. Wilson, A. Gabow, D.S. Marks, and C. Sander, *The microRNA.org resource: targets and expression.* Nucleic Acids Res, 2008. 36: p. D149-53.
148. Griffiths-Jones, S., H.K. Saini, S. van Dongen, and A.J. Enright, *miRBase: tools for microRNA genomics.* Nucleic Acids Res, 2008. 36: p. D154-8.
149. Griffiths-Jones, S., R.J. Grocock, S. van Dongen, A. Bateman, and A.J. Enright, *miRBase: microRNA sequences, targets and gene nomenclature.* Nucleic Acids Res, 2006. 34: p. D140-4.
150. Griffiths-Jones, S., *The microRNA Registry.* Nucleic Acids Res, 2004. 32: p. D109-11.
151. Dennis, G., Jr., B.T. Sherman, D.A. Hosack, J. Yang, W. Gao, H.C. Lane, and R.A. Lempicki, *DAVID: Database for Annotation, Visualization, and Integrated Discovery.* Genome Biol, 2003. 4: p. P3.
152. Huang da, W., B.T. Sherman, and R.A. Lempicki, *Systematic and integrative analysis of large gene lists using DAVID bioinformatics resources.* Nat Protoc, 2009. 4: p. 44-57.

153. Mantovani, A., *Molecular pathways linking inflammation and cancer.* Curr Mol Med, 2010. 10: p. 369-73.
154. Wang, T., X. Zhang, and J.J. Li, *The role of NF-kappaB in the regulation of cell stress responses.* Int Immunopharmacol, 2002. 2: p. 1509-20.
155. Fukami, T., H. Fukuhara, M. Kuramochi, T. Maruyama, K. Isogai, M. Sakamoto, S. Takamoto, and Y. Murakami, *Promoter methylation of the TSLC1 gene in advanced lung tumors and various cancer cell lines.* Int J Cancer, 2003. 107: p. 53-9.
156. Celebiler Cavusoglu, A., A.I. Sevinc, S. Saydam, T. Canda, Z. Baskan, Y. Kilic, and M. Sakizli, *Promoter methylation and expression changes of CDH1 and P16 genes in invasive breast cancer and adjacent normal breast tissue.* Neoplasma, 2010. 57: p. 465-72.
157. Belyakov, O.V., K.M. Prise, K.R. Trott, and B.D. Michael, *Delayed lethality, apoptosis and micronucleus formation in human fibroblasts irradiated with X-rays or alpha-particles.* Int J Radiat Biol, 1999. 75: p. 985-93.
158. Manti, L., M. Jamali, K.M. Prise, B.D. Michael, and K.R. Trott, *Genomic instability in Chinese hamster cells after exposure to X rays or alpha particles of different mean linear energy transfer.* Radiat Res, 1997. 147: p. 22-8.
159. Limoli, C.L., B. Ponnaiya, J.J. Corcoran, E. Giedzinski, M.I. Kaplan, A. Hartmann, and W.F. Morgan, *Genomic instability induced by high and low LET ionizing radiation.* Adv Space Res, 2000. 25: p. 2107-17.
160. Smith, L.E., S. Nagar, G.J. Kim, and W.F. Morgan, *Radiation-induced genomic instability: radiation quality and dose response.* Health Phys, 2003. 85: p. 23-9.
161. Kadhim, M.A., M.A. Hill, and S.R. Moore, *Genomic instability and the role of radiation quality.* Radiat Prot Dosimetry, 2006. 122: p. 221-7.
162. Lander, E.S., L.M. Linton, B. Birren, C. Nusbaum, M.C. Zody, J. Baldwin, K. Devon, K. Dewar, M. Doyle, W. FitzHugh, R. Funke, D. Gage, K. Harris, A. Heaford, J. Howland, L. Kann, J. Lehoczky, R. LeVine, P. McEwan, K. McKernan, J. Meldrim, J.P. Mesirov, C. Miranda, W. Morris, J. Naylor, C. Raymond, M. Rosetti, R. Santos, A. Sheridan, C. Sougnez, N. Stange-Thomann, N. Stojanovic, A. Subramanian, D. Wyman, J. Rogers, J. Sulston, R. Ainscough, S. Beck, D. Bentley, J. Burton, C. Clee, N. Carter, A. Coulson, R. Deadman, P. Deloukas, A. Dunham, I. Dunham, R. Durbin, L. French, D. Grafham, S. Gregory, T. Hubbard, S. Humphray, A. Hunt, M. Jones, C. Lloyd, A. McMurray, L. Matthews, S. Mercer, S. Milne, J.C. Mullikin, A. Mungall, R. Plumb, M. Ross, R. Shownkeen, S. Sims, R.H. Waterston, R.K. Wilson, L.W. Hillier, J.D. McPherson, M.A. Marra, E.R. Mardis, L.A. Fulton, A.T. Chinwalla, K.H. Pepin, W.R. Gish, S.L. Chissoe, M.C. Wendl, K.D. Delehaunty, T.L. Miner, A. Delehaunty, J.B. Kramer, L.L. Cook, R.S. Fulton, D.L. Johnson, P.J. Minx, S.W. Clifton, T. Hawkins, E. Branscomb, P. Predki, P. Richardson, S. Wenning, T. Slezak, N. Doggett, J.F. Cheng, A. Olsen, S. Lucas, C. Elkin, E. Uberbacher, M. Frazier, R.A. Gibbs, D.M. Muzny, S.E. Scherer, J.B. Bouck, E.J. Sodergren, K.C. Worley, C.M. Rives, J.H. Gorrell, M.L. Metzker, S.L. Naylor, R.S. Kucherlapati, D.L. Nelson, G.M. Weinstock, Y. Sakaki, A. Fujiyama, M. Hattori, T. Yada, A. Toyoda, T. Itoh, C. Kawagoe, H. Watanabe, Y. Totoki, T. Taylor, J. Weissenbach, R. Heilig, W. Saurin, F. Artiguenave, P. Brottier, T. Bruls, E. Pelletier, C. Robert, P. Wincker, D.R. Smith, L. Doucette-Stamm, M. Rubenfield, K. Weinstock, H.M. Lee, J. Dubois, A. Rosenthal, M. Platzer, G. Nyakatura, S. Taudien, A. Rump, H. Yang, J. Yu, J. Wang, G. Huang, J. Gu, L. Hood, L. Rowen, A. Madan, S. Qin, R.W. Davis, N.A. Federspiel, A.P. Abola, M.J. Proctor, R.M. Myers, J. Schmutz, M. Dickson, J. Grimwood, D.R. Cox, M.V. Olson, R. Kaul, N. Shimizu, K. Kawasaki, S. Minoshima, G.A. Evans, M. Athanasiou, R. Schultz, B.A. Roe, F. Chen, H. Pan, J. Ramser, H. Lehrach, R. Reinhardt, W.R. McCombie, M. de la Bastide, N. Dedhia, H. Blocker, K. Hornischer, G. Nordsiek, R. Agarwala, L. Aravind, J.A. Bailey, A. Bateman, S. Batzoglou, E. Birney, P. Bork, D.G. Brown, C.B. Burge, L. Cerutti, H.C. Chen, D. Church, M. Clamp, R.R. Copley, T. Doerks, S.R. Eddy, E.E. Eichler, T.S. Furey, J. Galagan, J.G. Gilbert, C. Harmon, Y. Hayashizaki, D. Haussler, H. Hermjakob, K. Hokamp, W. Jang, L.S. Johnson, T.A. Jones, S. Kasif, A. Kaspryzk, S. Kennedy, W.J. Kent, P. Kitts, E.V. Koonin, I. Korf, D. Kulp, D. Lancet, T.M. Lowe, A. McLysaght, T. Mikkelsen, J.V. Moran, N. Mulder, V.J. Pollara, C.P. Ponting, G. Schuler, J. Schultz, G. Slater, A.F. Smit, E. Stupka, J. Szustakowski, D. Thierry-Mieg, J. Thierry-Mieg, L. Wagner, J. Wallis, R. Wheeler, A. Williams, Y.I. Wolf, K.H. Wolfe, S.P. Yang, R.F. Yeh, F. Collins, M.S. Guyer, J. Peterson, A. Felsenfeld, K.A. Wetterstrand, A. Patrinos, M.J. Morgan, P.

de Jong, J.J. Catanese, K. Osoegawa, H. Shizuya, S. Choi and Y.J. Chen, *Initial sequencing and analysis of the human genome.* Nature, 2001. 409: p. 860-921.
163. Kimmel, M. and M. Mathaes, *Modeling neutral evolution of Alu elements using a branching process.* BMC Genomics, 2010. 11 Suppl 1: p. S11.
164. Chalitchagorn, K., S. Shuangshoti, N. Hourpai, N. Kongruttanachok, P. Tangkijvanich, D. Thong-ngam, N. Voravud, V. Sriuranpong, and A. Mutirangura, *Distinctive pattern of LINE-1 methylation level in normal tissues and the association with carcinogenesis.* Oncogene, 2004. 23: p. 8841-6.
165. Estecio, M.R., V. Gharibyan, L. Shen, A.E. Ibrahim, K. Doshi, R. He, J. Jelinek, A.S. Yang, P.S. Yan, T.H. Huang, E.H. Tajara, and J.P. Issa, *LINE-1 hypomethylation in cancer is highly variable and inversely correlated with microsatellite instability.* PLoS One, 2007. 2: p. e399.
166. Kazazian, H.H., Jr. and J.L. Goodier, *LINE drive. retrotransposition and genome instability.* Cell, 2002. 110: p. 277-80.
167. Koturbash, I., A. Boyko, R. Rodriguez-Juarez, R.J. McDonald, V.P. Tryndyak, I. Kovalchuk, I.P. Pogribny, and O. Kovalchuk, *Role of epigenetic effectors in maintenance of the long-term persistent bystander effect in spleen in vivo.* Carcinogenesis, 2007. 28: p. 1831-8.
168. Baylin, S.B., J.G. Herman, J.R. Graff, P.M. Vertino, and J.P. Issa, *Alterations in DNA methylation: a fundamental aspect of neoplasia.* Adv Cancer Res, 1998. 72: p. 141-96.
169. Goodhead, D.T., *Initial events in the cellular effects of ionizing radiations: clustered damage in DNA.* Int J Radiat Biol, 1994. 65: p. 7-17.
170. Held, K.D., *Effects of low fluences of radiations found in space on cellular systems.* Int J Radiat Biol, 2009. 85: p. 379-90.
171. Baumstark-Khan, C., J. Heilmann, and H. Rink, *Induction and repair of DNA strand breaks in bovine lens epithelial cells after high LET irradiation.* Adv Space Res, 2003. 31: p. 1583-91.
172. Wan, X.S., P. Bloch, J.H. Ware, Z. Zhou, J.J. Donahue, J. Guan, J. Stewart, and A.R. Kennedy, *Detection of oxidative stress induced by low- and high-linear energy transfer radiation in cultured human epithelial cells.* Radiat Res, 2005. 163: p. 364-8.
173. Cannell, I.G. and M. Bushell, *Regulation of Myc by miR-34c: A mechanism to prevent genomic instability?* Cell Cycle, 2010. 9: p. 2726-30.
174. Yegnasubramanian, S., M.C. Haffner, Y. Zhang, B. Gurel, T.C. Cornish, Z. Wu, R.A. Irizarry, J. Morgan, J. Hicks, T.L. DeWeese, W.B. Isaacs, G.S. Bova, A.M. De Marzo, and W.G. Nelson, *DNA hypomethylation arises later in prostate cancer progression than CpG island hypermethylation and contributes to metastatic tumor heterogeneity.* Cancer Res, 2008. 68: p. 8954-67.